

Nourishment strategies for the Ameland Inlet

M.Sc. Thesis Report

September 1, 2017

Nourishment strategies for the Ameland Inlet

by

Jasper Bak

in partial fulfillment of the requirements for the degree of

Master of Science

in Hydraulic Engineering

at the Delft University of Technology,
to be defended publicly on October 6, 2017 at 16:00 PM
in instruction room 1.98 of the CITG building.

Thesis committee:	Prof.dr.ir. Z.B. Wang,	TU Delft & Deltares
	Ir. S.G. Pearson,	TU Delft & Deltares
	Dr.ir. D.J.R. Walstra,	TU Delft & Deltares
	Dr.ir. B.C. van Prooijen,	TU Delft
	Dr.ir. J.S.M. van Thiel de Vries,	Boskalis
	Ir. A.P. de Looff,	Rijkswaterstaat

An electronic version of this thesis is available at <http://repository.tudelft.nl/>.

Sea level rise poses challenges to the tidal inlet systems of the Wadden Sea, including the barrier islands. If no measures are taken, the shorelines of the islands will retreat and the basins may drown. In the Ameland Inlet, the Boschplaat at the eastern tip of Ameland and Bornrif at the western tip of Terschelling are currently shrinking.

This thesis evaluates different nourishment strategies to counteract the coastal retreat, with the ultimate goal of improving our understanding of how nourishment sand of different grain sizes is shared between the different morphological units of the Ameland Inlet.

The process-based model Delft3D is used as a means of predicting the transport pathways of nourishment sand on a time scale of 10 years. The model was set up by DE FOCKERT [2008] and improved by JIAO [2014] and WANG [2015]; WANG *et al.* [2016]. In this thesis, further model advancements are made, in order to make it suitable for medium term nourishment calculations. The Mormerge (parallel online) approach is applied in combination with a phase shift in the tidal signal for the different wave conditions. As a result the computational time is significantly reduced. The bathymetry is updated based on the 2016 Vaklodingen and Bed Composition Generation is used to create a suitable bottom composition. The composition of the nourishments is based on the particle size distribution of the borrow area.

The model results suggest that different objectives, such as feeding the Terschelling or Ameland coast, feeding the basin, or reinforcing the ebb tidal delta, can be met by varying the nourishment location and composition.

Figure 1 summarizes the main findings regarding the transport pathways within the inlet system. Near the Terschelling beach import via Boschgat is dominant. Further offshore, bypassing via the ebb tidal delta is the most important transport pathway. Boschgat feeds the western part of the basin and Borndiep feeds the eastern part, but interaction between the two is limited. The model predicts some transport from Boschgat to Borndiep via Westgat under the influence of the tide, or driven by waves over the shallow area in between the channels. There is no connection in the other direction. Borndiep connects the basin to the ebb tidal delta, resulting in transport in and out of the system. Bornrif is the only location where a net westward transport into the inlet is observed.

Finer fractions are imported further into the basin by the tidal flow. When bypassing the inlet, they are transported further offshore, since they are more influenced by the tidal currents flowing out of the inlet. As a result coarser nourishment fractions end up closer to the Ameland shoreline.

The model has several limitations, mainly since insufficient data is currently available for a

sound calibration and validation. However important phenomena observed in the field are reproduced by the model, such as the coastal retreat at Boschplaat and the bar migration at Bornrif. This gives confidence in the model performance regarding the predictions of the sediment transport patterns.

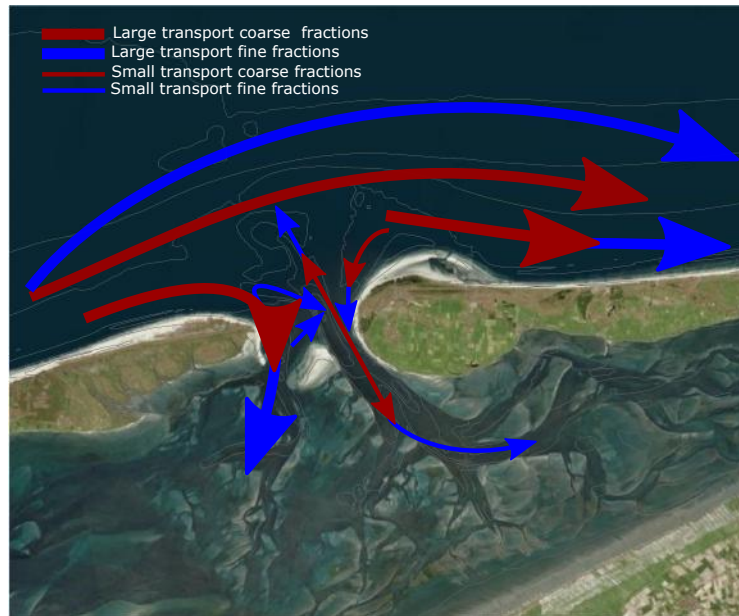


Figure 1: The main pathways of coarse and fine nourishment fractions, based on a qualitative interpretation of the model results

Acknowledgments

This thesis forms the final part of my Master study, the Master of Science Hydraulic Engineering at the Faculty of Civil Engineering and Geosciences, Delft University of Technology, The Netherlands. The project has been performed as a cooperation between Boskalis, Deltares and the TU Delft. It has been conducted at the office of Boskalis in Papendrecht and the office of Deltares in Delft. Rijkswaterstaat has also been involved, by participating in my graduation committee.

I would like to thank my graduation committee for their supervision. I really enjoyed working on this thesis with all of you, it has been an interesting and challenging project. Thank you Jaap van Thiel de Vries, for providing me the opportunity to graduate at Boskalis, initiating the cooperation with Deltares, providing me with new ideas and for helping to get a clear structure in my report. Thank you Dirk Jan Walstra, for providing me the opportunity to work on this thesis at Deltares and for guiding me through this project. Moreover, my expressions of gratitude go to Professor Zheng Bing Wang for assisting in defining the scope of my research and for critically looking at my modeling work. Thank you Bram van Prooijen, for helping me to define the scope of my work within the SEAWAD project and for helping to set up my modeling approach. Thank you Harry de Looff, for reminding me to keep an eye on the practical application of my research and for providing me with the data I needed. Furthermore I would like to give a special thanks to Stuart Pearson. Thank you for your close involvement and devotion to the project, for critically reading and providing comments to every version of the report that I handed in, for all the weekly coffee meetings, during which we had serious discussions, or just an informal chat. It has been a great pleasure to work with you on this project and I hope I can stay involved in the future. I am happy that after all your help during my work, my results are useful for your PhD work.

Moreover, I would like to give thanks to my colleagues and fellow students at Deltares, I had a great time. In particular I would like to thank Pieter Koen Tonnon, for assisting me in setting up the Delft3D model.

I am grateful to my colleagues at Boskalis, for their help and all the fun we had. Besides work, we entered canoes, barbecued on the campus and participated in the football tournament. I am glad I have been selected for the traineeship, so I can stay working at this company.

Finally I would like to thank my family and friends for their interest in my work and their support. In particular I would like to say thanks to my dad Nico Bak, who has always motivated and supported me during my studies.

Papendrecht, September 1, 2017,

Jasper Bak

Abstract	iii
Acknowledgments	v
1 Introduction	1
1.1 Functions of the Wadden Sea	1
1.2 Problem description	2
1.3 Research objective	4
1.4 Research questions	4
2 Background	5
2.1 Characteristics of the Wadden Sea	5
2.2 Study area	5
2.3 Sediment transport	8
2.4 Sediment sorting	9
3 Model set up	13
3.1 Domain and parameter settings	13
3.2 Sediment transport	14
3.3 Forcing	14
3.4 Bed composition	15
3.5 Morphological acceleration factor	26
3.6 Sensitivity to transport calibration factors	29
3.7 Morphological performance	30
3.8 Particle tracking	31
4 Nourishment design	35
4.1 Nourishment requirements	35
4.2 Nourishment composition	40
4.3 Sediment transport at the Ameland tidal inlet system	42
4.4 Proposed locations	52
4.5 Nourishment location evaluation	53
4.6 Model implementation	54
4.7 Hypotheses	55
5 Results and Analyses	61
5.1 Effect of the nourishment location	61
5.2 Effect of the nourishment compositions	66

6 Discussion of nourishment strategies in inlet systems	85
6.1 Nourishment evaluation for the Ameland Inlet	85
6.2 Other inlet systems	90
7 Conclusions and Recommendations	93
7.1 Conclusions	93
7.2 Recommendations	95
Appendix A Bottom Composition Generation	97
A.1 Tide only scenario	97
A.2 Tide, wind and waves	100
Appendix B Map of the borrow areas	105
Appendix C Total transports	107
Appendix D Vaklodingen 2014 and 2016	113
Bibliography	115

Sea level rise poses challenges to many coastal areas all over the world. If no proper measures are taken, these areas will suffer from floods and eventually the shoreline will retreat [NICHOLLS AND CAZENAVE, 2010]. In The Netherlands, beach and foreshore nourishments are carried out regularly in order to combat this [ROELSE, 2002]. In 2011 a local mega nourishment called the Sand Engine was constructed along the Dutch coast [STIVE *et al.*, 2013]. The aim is that the nourished sand is redistributed along the coast through natural processes, building its resilience to sea level rise.

In the present thesis, various nourishment strategies will be developed for the Ameland Inlet, one of the tidal inlet systems in the Dutch Wadden Sea. With the aid of the process-based model Delft3D [LESSER *et al.*, 2004] the effectiveness of these nourishments is evaluated. The focus is on determining the effect of the grain size on the fate of a nourishment.

The research presented in this thesis is part of the SEAWAD (SEdiment supply At the Wadden Sea ebb-tidal Delta) research project, a program aimed at developing system knowledge and tools to predict the hydrodynamic, morphologic and ecologic effects of nourishments at the Wadden Sea ebb tidal deltas [TUDELFT, 2016]. SEAWAD runs parallel to Kustgenese 2.0, a research program managed by Rijkswaterstaat, aimed at generating knowledge for the long term maintenance strategy of the Dutch coastal system.

1.1 Functions of the Wadden Sea

The Wadden Sea, see Figure 1.1 is Europe's largest marine wetland [ENEMARK, 2005] and the world's largest coherent area of intertidal flats [KABAT *et al.*, 2012]. It provides a habitat for many animals. It is a very important staging, wintering and breeding area for migratory waterbirds [H. MELTOFTE, J. BLEW, J. FRIKKE, H. U. ROSNER, 1994; KOFFIJBERG *et al.*, 2006], with over 10 million water birds utilizing the Wadden Sea during some part of the year [H. MELTOFTE, J. BLEW, J. FRIKKE, H. U. ROSNER, 1994]. Besides birds, large amounts of mussels are living on the intertidal flats and in the subtidal zone [DANKER AND ZUIDEMA, 1995] and the tidal channels and the basin area are important nursery and feeding areas for many fish species [LOTZE, 2005]. In total about 10,000 animal, fungi and plant species live in the Wadden Sea [REISE *et al.*, 2010]. The Dutch Wadden Islands are also home to approximately 24.000 people [CBS, 2017].

Furthermore, the Wadden Sea has a great cultural historical value, as an old and very complex landscape which has been inhabited for over 5000 years [KABAT *et al.*, 2012].

Because of these properties UNESCO declared the Wadden Sea a World Heritage Site [REISE *et al.*, 2010]. These sites should be conserved and are legally protected under the law of war of the Geneva Convention, which prohibits any acts of hostility against the historic monuments, using them in support of military effort and taking reprisals against them [JOHNSON, 2006].

Moreover, the Wadden Sea is a recreational and touristic area, many people visit the islands, take guided tours over the mud flats, or go bird or seal watching. In 2016 the Wadden Sea was voted most beautiful natural reserve of The Netherlands by the Dutch public [VERSCHUREN, 2016]. Additionally, the area is of economical and industrial importance. The basins provide a sheltered place for among others, the Dutch Eemshaven, the German Wilhelmshaven and the Danish Esbjerg harbor [KABAT *et al.*, 2012].

Besides its ecological, cultural and recreational functions, the Wadden Sea system is also an important sea defense. Wave energy is dissipated on the barrier island coasts, ebb tidal deltas, the intertidal flats and the salt marches. In this way the mainland is for the most part sheltered from wave attack. Research at the Norfolk coast of the UK has for instance shown that (depending on factors like the width, water depth, vegetation and bottom friction) a salt marsh can be so effective that almost all wave energy is dissipated before it reaches the landward shoreline [KING AND LESTERT, 1995; MOLLER, 1999; MÖLLER *et al.*, 2001; COOPER *et al.*, 2001]. For instance a sand marsh with a width of 180m reduces the significant wave height (H_s) on average by 61%, in some extreme cases the reduction was more than 98% [MÖLLER *et al.*, 2001; MOLLER, 1999]. Intertidal flats also dissipate wave energy, but at a smaller rate than salt marshes, this is mainly attributed to their smaller bottom friction [MÖLLER *et al.*, 2001; MOLLER, 1999]. Even under storm surge conditions salt marshes can significantly reduce the wave height, especially when vegetation is present [MÖLLER *et al.*, 2014]. In this way intertidal flats and salt marshes can diminish wave attack and run-up at the shoreline and contribute to flood safety.

1.2 Problem description

At the Wadden Sea the combined effects of sea level rise and bottom subsidence due to isostatic adjustment, compaction and gas and salt mining have resulted in a significant increase of the relative sea level in the past years and this process is expected to continue [ELIAS *et al.*, 2012]. According to the latest research of the Royal Netherlands Meteorological Institute (KNMI), based on the IPCC climate change models [KLEIN TANK *et al.*, 2015], sea level will rise with 0.15m to 0.40m by 2050 and with 0.25m to 0.85m by 2085, in the Wadden Sea area. Bottom subsidence due to glacial isostatic adjustment and compaction adds 0.10m by 2100 [ELIAS *et al.*, 2012]. Locally gas extraction and salt mining may reduce the bottom levels even further. At the Ameland Inlet an extra accommodation space of $15 \cdot 10^6 m^3$ is expected as a result from gas extraction by 2050 [HOEKSEMA *et al.*, 2004], equivalent to an average bottom subsidence of 0.05m.

Until now the accommodation space created through this has been naturally filled in with sediment from outside the basin and the Wadden Sea has been able to rise with the sea level [ELIAS, 2006; VAN WIJNEN AND BAKKER, 2001; REISE *et al.*, 2010]. However, there is wide agreement that there is a critical level of sea level rise above which the Wadden Sea and the Wadden Sea islands will not be able to keep up and will drown [VAN DER SPEK AND BEETS, 1992; VAN GOOR *et al.*, 2003; DE FOCKERT, 2008; DISSANAYAKE *et al.*, 2012a; HOFSTEDE *et al.*, 2016].

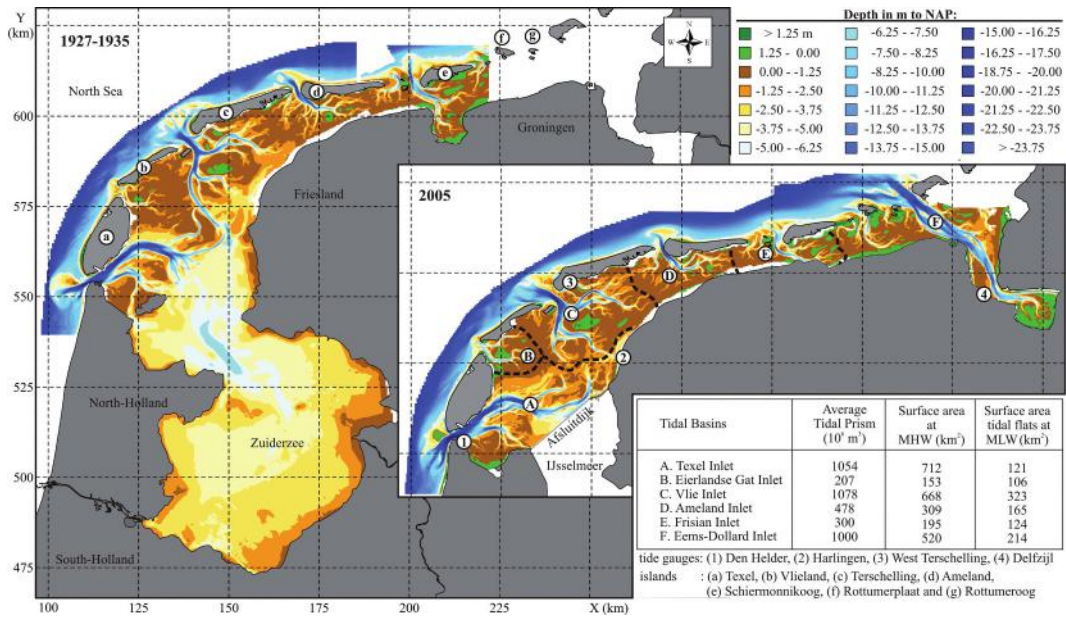


Figure 1.1: The Wadden Sea and its tidal inlet systems, obtained from ELIAS *et al.* [2012]

This drowning would have several severe consequences. First of all, an important sea defense will disappear. Wave energy dissipation by the Wadden Sea islands, ebb tidal deltas and the tidal flats will be reduced. Therefore the sea dikes along the Wadden Sea will be exposed more frequently and by higher waves. As a result, it is highly likely that the dikes would need to be adjusted. Among others a different type of revetment may be needed, since grass cannot withstand prolonged water and wave exposure [SCHIERECK AND VERHAGEN, 2012]. Changing these dikes will result in high construction and maintenance costs, although it will be necessary to prevent flooding. Moreover, harbors will not be sheltered from waves anymore, which gives rise to a nuisance for navigation and increased downtime, as a response hydraulic structures such as breakwaters may need to be build. Second, the inhabitants of the islands will lose their living environment. Third, animal and plant species will lose an important habitat. Finally, a UNESCO World Heritage site, with great cultural, recreational and touristic value will be lost.

In the past many studies have been carried out related to sediment transport processes in a tidal inlet system. ELIAS *et al.* [2006] researched sediment transport patterns at the Texel Inlet, using a numerical model including a bottom consisting of only a single sand fraction. HERRLING AND WINTER [2014] also did a numerical sediment transport study at the Otzum Balje Inlet, where they accounted for different sediment grain sizes. SON *et al.* [2011] have researched the same inlet by means of analyzing bottom samples and sand bar orientation. Furthermore, multiple studies have evaluated the effect of graded sediments in numerical models on inlet stability [ELIAS *et al.*, 2015; WANG *et al.*, 2016]. JIAO [2014] studied the morphodynamics of the Ameland Inlet by means of a medium term process-based model, including a spatial varying bed composition. The effect of nourishments on a tidal inlet system have also been studied previously. KLUYVER [2006] studied the effect of a nourishment at the Frisian Inlet and modeled the morphological response for a period of 1 year. However, studies regarding the behavior of nourishment fractions with different grain

sizes in tidal inlet systems have not yet been performed.

1.3 Research objective

The practical objective of this research is to develop different nourishment strategies with three main goals: feeding the coastal foundation, including the barrier island coasts; feeding the tidal basin to prevent the Wadden Sea from drowning; and maintaining the wave sheltering function of the ebb tidal delta.

The scientific objective is to determine effect of grain size on the fate of a nourishment, for different nourishment locations, with the aim of gaining insight into the different transport patterns of nourished sand fractions.

In this study, the focus is on the Wadden Sea and specifically the Ameland Inlet. The specific results for this inlet will be generalized and subsequently translated to other tidal inlet systems, such as the east coast of the United States, the south coast of Portugal and the coast near Venice. Furthermore, attention will be paid to the practical aspects of the execution of the nourishment.

The novelty of the present study is that it includes the bottom composition of the model domain (spatially varying bed grain size), while also accounting for different grain sizes in the nourishment.

1.4 Research questions

The thesis process will be guided by the following research question: How is nourishment sand of different grain sizes shared between the different morphological units of the Ameland Inlet system? Several sub questions are formulated:

- (a) What type of sediment is available for a nourishment? Whether sediment with certain grain sizes will be used in the nourishment depends on the availability and accessibility of sediment.
- (b) Depending on the goal of the nourishment, which locations are suitable?
- (c) What is the effect of composition on the fate of a nourishment? Different nourishment grain size distributions will be modeled to evaluate this effect

In this chapter, an overview of the most important characteristics of the Ameland Inlet system is provided. Furthermore, sediment transport and sorting in tidal inlets is discussed, needed for understanding of the processes that drive the movement of different nourishment sediment fractions.

2.1 Characteristics of the Wadden Sea

The Dutch Wadden Sea consists of six tidal inlet systems, from west to east: Texel Inlet, Eierlandse Gat Inlet, Vlie Inlet, Ameland Inlet, Frisian Inlet and the Eems-Dollard Inlet, see Figure 1.1. The total surface area of the basins is about 4000km^2 . The basins of the eastern part (Ameland Inlet, Frisian Inlet, Eems-Dollard Inlet) are relatively narrow and shallow, the tidal channels are relatively small and the intertidal flats large, the ratios of intertidal flat over total surface area are 0.7 to 0.8 [STIVE AND EYSINK, 1989; ELIAS *et al.*, 2012]. The basins in the west are wider and the ratios of intertidal flat over total surface area is 0.3 to 0.4 [ELIAS *et al.*, 2012].

The tidal wave travels from west to east along the Wadden Sea Islands, resulting in maximum shore parallel velocities of 0.5m/s to 1.0m/s . The mean tidal range increases from 1.4m at Den Helder to 2.5m in the Eems-Dollard Inlet [ELIAS *et al.*, 2012]. The significant wave height is 1.3m with a mean period of 5 seconds [ELIAS *et al.*, 2012]. Most waves come in from the north-west (see Figure 2.2), resulting in a net littoral drift to the east. Storm surges can increase the water level by more than 2 meters, which can result in large water level gradients between inside and outside the basin.

Based on the mean tidal range and significant wave height the Wadden Sea inlets can be classified as a mixed energy wave, dominant environment [HAYES, 1979; DAVIS AND HAYES, 1984].

2.2 Study area

The focus of this thesis is on the Ameland Inlet system. This inlet is chosen because it is believed to be the least disturbed one, showing the most natural behaviors [WANG *et al.*, 2016; ELIAS *et al.*, 2015]. Furthermore, the basin has minimal connectivity to other basins, so it can be numerically modeled as a closed system [RIDDERINKHOF, 1988; DISSANAYAKE *et al.*, 2012b].

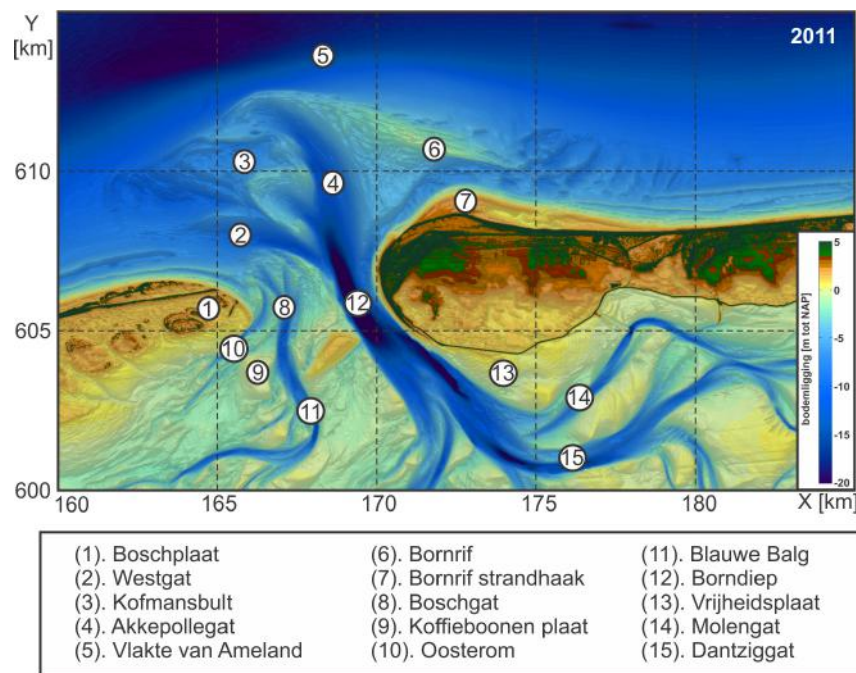


Figure 2.1: Overview of the Ameland Inlet system, obtained from Deltares Beheerbibliotheek 2013

This inlet channel is located in between the Wadden islands of Terschelling and Ameland. The inlet is about 4km wide and consists of two channels, the 25m deep channel in the east is called Borndiep and the small 10m deep channel in the west [SWINKELS AND BIJLSMA, 2012] is called Boschgat (Figure 2.1). The ebb-tidal delta has a volume of $130 \cdot 10^6\text{m}^3$ [CHEUNG *et al.*, 2007]. The surface area of the basin is 309km^2 at Mean High Water, the surface area of the tidal flats is 165km^2 at Mean Low Water and the average tidal prism is $478 \cdot 10^6\text{m}^3$ [ELIAS *et al.*, 2012]. As stated before, the ratio of tidal flat over total surface area is about 0.7. The basin used to be considerably larger, because it included the Middelzee to the Southwest. However by the year 1500, most of the Middelzee was silted up and reclaimed [VOS AND KNOL, 2015]. Nevertheless, based on the erosion and sedimentation process over the last 70 years as described by [ELIAS *et al.*, 2012] and the fact that the reclamation was completed a long time ago, it seems unlikely that the inlet system is still impacted by this.

In recent years the Ameland Inlet basin is filling in, while the ebb-tidal delta has been eroding [ELIAS *et al.*, 2012]. Due to the effect of waves, the tide and the abundance of sediment, the ebb-tidal delta is highly dynamic [OERTEL, 1972]. The channels and bars on it show a cyclic behavior with a period of about 40 years [CHEUNG *et al.* [2007]. Due to the tidal flow and longshore wave driven sediment transport, they migrate eastwards. The main channel migrates towards the downdrift island, it loses importance, and on the western side a new channel emerges [WANG *et al.*, 2012; ELIAS *et al.*, 2012]. This channel grows and takes over the function of the role of the old channel [WANG *et al.*, 2012]. The old channel can cause severe erosion at the head of the downdrift island. However during different stages of the cycle, when a shoal reaches the coast of the barrier island, significant accretion can take place [HAYES, 1980; CHEUNG *et al.*, 2007]. Consequently, whether erosion or accretion takes place at the island tips depends on its stage in the cycle [ELIAS *et al.*, 2012]. Currently

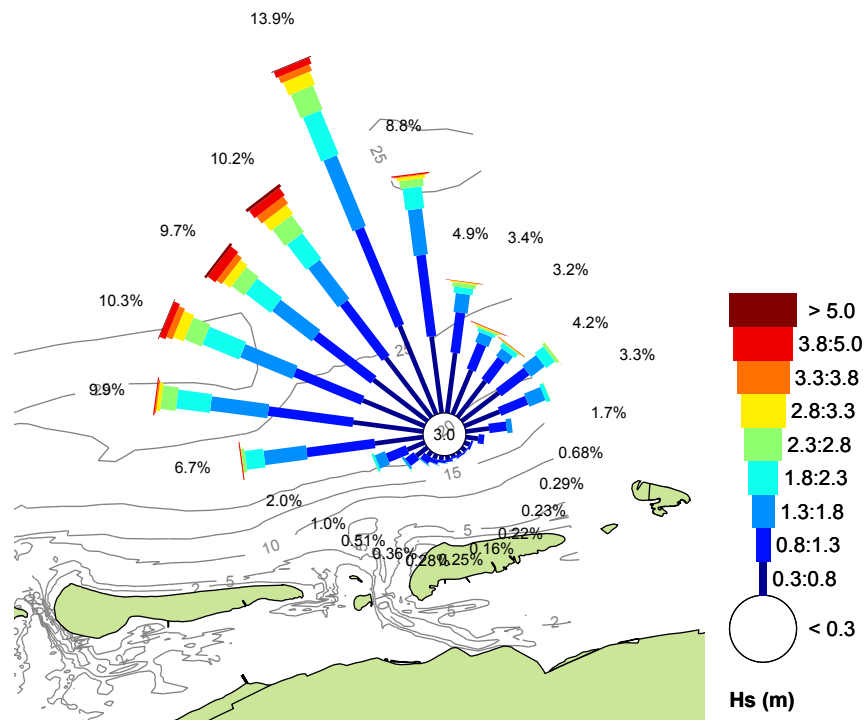


Figure 2.2: Wave rose for the SON measurement station, near Ameland, adapted from DE FOCKERT [2008]

the southwestern tip of Ameland is suffering from erosion [RIJKSWATERSTAAT, 2017]. The nature reserve Boschplaat, situated at the eastern tip of Terschelling is also eroding [ELIAS, 2017]. Figure 2.3 shows the development of the Ameland Inlet area over the last 100 years.

To protect the coastline near the inlet, both hard and soft measures have been taken. Channel wall protections, consisting of fascine mattresses, were constructed in 1947 and 1971 in order to fix the east side of the Borndiep channel [CLEVERINGA *et al.*, 2005; VAN HEUVEL, 1999]. However this was not sufficient, since the channel was still moving towards the east, causing erosion at the barrier island. In 1972 and 1989 rows of poles were installed at the Ameland coast, which were later reinforced with rip-rap. In 1979 an underwater dam was constructed at the Northwest coast of Ameland, in combination with a nourishment of $300.000m^3$ of sand. Moreover, groynes were constructed in the years between 1988 and 1995 [VAN HEUVEL, 1999; CLEVERINGA *et al.*, 2005]. In order to prevent further erosion of the beach, the rip-rap channel wall protection was increased up to $NAP - 0.50m$ in 1995 [VAN HEUVEL, 1999]. Soon after the completion, a phase of sedimentation started at the coast, and the protection lost its function. However during phases of erosion, it will gain back its function. The soft measures that have been taken include beach and shoreface nourishments, carried out at the Terschelling and Ameland coastlines [GRUNNET *et al.*, 2005; CLEVERINGA *et al.*, 2005].

Rijkswaterstaat is currently planning a $2.5 \cdot 10^6 m^3$ channel wall nourishment in Borndiep, to counteract the erosion at the southwestern tip of Ameland, which will be executed before the

end of this year [RIJKSWATERSTAAT, 2017]. No measures have been planned yet to protect the Boschplaat.

2.3 Sediment transport

Sediment is transported in and out of a tidal basin by the tidal currents. When an ebb current exports sediment out of the basin, it can continue its way downdrift. However, not all sediment is transported into the basin first. Part of it goes downdrift over the ebb-tidal delta. The sand accumulates west of the inlet and bypasses the ebb-tidal delta eastbound in the form of migrating bars, forced by the waves [FITZGERALD, 1984; SHA, 1989; CHEUNG *et al.*, 2007].

Bypassing

BRUUN AND GERRITSEN [1960] suggest a parameter r which indicates whether sediment transport is dominated by the tide, and consequently mainly via the inlet or by waves, bypassing the inlet. It reads [BOSBOOM AND STIVE, 2010]:

$$r = \frac{P}{M_{tot}} \quad (2.1)$$

In which:

$$\begin{array}{lll} P & \text{tidal prism} & [m^3] \\ M_{tot} & \text{total littoral drift} & [m^3/yr] \end{array}$$

For $r > 300$ the transport is mainly by the tidal currents, through the inlet. When r is small, the waves are responsible for most of the transport, which takes place over the ebb-tidal delta.

The mean tidal range at the inlet is $2.0m$ [SWINKELS AND BIJLSMA, 2012] and the average significant wave height is $1.1m$ [CHEUNG *et al.*, 2007]. The waves give rise to a littoral drift in the order of $1 \cdot 10^6 m^3/year$ [BRUUN, 1978]. Using equation 2.1, the result is an r value of 500, which indicates that the bypassing is predominantly tide induced, via the inlet.

Some researchers challenge the concept of sediment bypassing. SON *et al.* [2011] studied the sediment transportation patterns at the Otzumer Balje Inlet between Langeoog and Spiekeroog, in the East Frisian Wadden Sea, by analyzing sediment samples and swash bar patterns. They found that the sediment recirculates from the ebb channel towards the outer margin of the Otzum ebb tidal delta. From there the medium grained sediment is transported via the ebb tidal delta shoal in the form of swash bars, forced by waves and the tide, back towards the main channel. The fine sediment is also transported over the ebb tidal delta, but in the form of small dunes separate from the swash bars, forced by the flood current, towards the the marginal flood channel. According to the authors, sediment does not bypass the inlet through swash bars which migrate over the ebb tidal delta, as is believed to happen at many inlet systems [FITZGERALD *et al.*, 1984; CHEUNG *et al.*, 2007; DASTGHEIB, 2012]. They argue that due to the pile up of water in the funnel-shaped German Bight, no significant wave driven longshore current may develop. Their conclusions are among others based on the observation that the ebb tidal delta and the adjacent barrier island coasts are composed of fine sand, whereas the swash bars and the inlet channel bed

consist of medium grained sand. Moreover, their findings are supported by the sedimentary structures found in the samples and the orientation of the swash bars.

HERRLING AND WINTER [2014] also researched sediment transport patterns and processes for the same tidal inlet, although they performed a numerical study, using the process-based model Delft3D. Their results confirm the sediment recirculation as pointed out by SON *et al.* [2011]. Moreover, by alternating fair-weather and storm simulations, the model is able to reproduce the surface sediment grain size distribution as measured by SON *et al.* [2011]. However their model also shows a significant bypass of sediment towards the downdrift coast, which is in disagreement with the findings of SON *et al.* [2011].

ELIAS *et al.* [2006] find evidence for sediment recirculation at the Texel Inlet, based on field observations and numerical modeling. However the authors suggest that this is a response to the closure of the Zuiderzee. It is a self-organizing process that redistributes the sediment to reach a new equilibrium state. Their results show that the northward-directed littoral drift is important for sediment supply to the system. Moreover, they do provide evidence for a longshore current through which a part of the sediment bypasses the inlet, along the margins of the ebb tidal delta.

2.4 Sediment sorting

Due to the differences in hydrodynamic forcing at across the inlet and the ebb tidal delta, considerable sediment sorting occurs throughout the system. Coarse sediments will for instance be found mostly in areas with relatively high flow velocities, like the entrance channel. Following a channel into the basin, the grain size gradually decreases, due to the decreasing maximum current velocities [VAN STRAATEN AND KUENEN, 1958]. The most fine grained fraction settles in the back of the basin or at the tidal watersheds, in almost stagnant water.

As discussed previously for the case of the Otzumer Balje Inlet, sediments of different sizes can have different transport pathways. Some mechanisms driving the transport in and out of the basin for coarse and fine grained sediment are discussed here. Import and export of coarse versus fine sediment is driven by different processes. On the one hand, transport of coarse sediment is dominated by tidal asymmetry.

By definition the water level at high water is higher than at low tide and the shallow water wave speed increases for larger depths, high tide will generally propagate faster [DAVIS AND DALRYMPLE, 2010; BOSBOOM AND STIVE, 2010]. Moreover, the effect of friction is larger for shallower flows, causing relatively more damping of the amplitude and flow velocity during low water. These combined effects distort the symmetry of the tidal wave and may cause the rising period to be smaller than the falling period, which means that the maximum flood velocities are larger than the maximum ebb velocities [DAVIS AND DALRYMPLE, 2010; BOSBOOM AND STIVE, 2010].

Since sediment transport is usually expressed as a function of u to the power of 3-5, there will be a net transport of coarse sediment in the direction in which the maximum tidal velocity occurs.

Factors enhancing ebb dominance are: First, river discharge, which increases ebb velocities. Second, the fact that the average water level during flood is generally higher than during ebb, which gives rise to larger ebb velocities since the same volume has to be discharged through a smaller cross section [BOSBOOM AND STIVE, 2010]. Third, a large intertidal

storage, causing the high tide to propagate slower than the low tide. Finally wind-driven flow across the tidal watersheds and storm surge induced large water level gradients can cause the system to become temporarily ebb dominant.

On the other hand, the transport of fine sediment is dominated by settling lag and scour lag. Settling lag means that when the flow velocity drops below the critical level, the particles need some time and therefore travel some more distance before they reach the bottom [BOSBOOM AND STIVE, 2010]. If the high water slack duration is longer than the low water slack duration, particles will have less time to settle during low water and more particles will be in suspension during the next flood period. During high water slack relatively more particles will settle because of the longer high water slack duration [BOSBOOM AND STIVE, 2010]. This results in a net landward transport of fine sediment. This effect is only significant for fine sediment due to its lower settling velocity compared to coarse sediment.

Scour lag is related to the difference between the maximum flow velocity at which sedimentation occurs and the minimum flow velocity required for erosion of the same material. This difference is larger for smaller grain sizes [VAN STRAATEN AND KUENEN, 1958]. This process increases the tendency of fine sediments to accumulate in the back of a basin, compared to larger particles which respond instantaneously to forcing and do not experience scour lag.

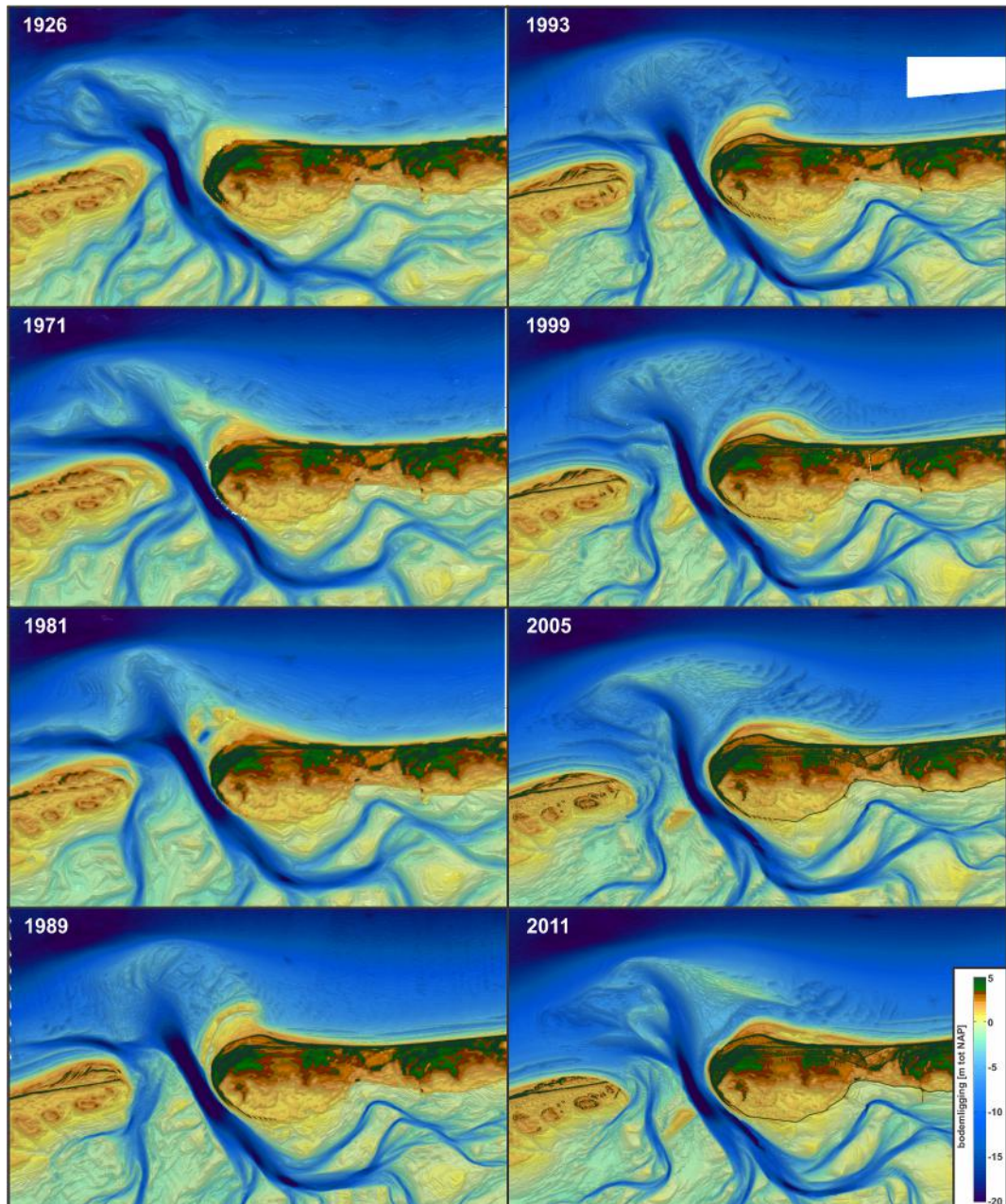


Figure 2.3: Evolution of the Ameland Inlet system, obtained from Deltares Beheerbibliotheek 2013

The process-based model Delft3D [LESSER *et al.*, 2004; DELTARES, 2014a] will be used as a means to analyze the Ameland Inlet and its response to a nourishment, in order to find answers to the research question and the various sub questions. In Sections 3.1, 3.2 and 3.3 the model set up is discussed. Section 3.4 deals with the bed composition generation, used to provide a suitable bottom as input for the nourishment models. In Sections 3.5 and 3.6, the sensitivity regarding relevant model parameters is treated.

A process-based model is chosen in order to resolve sediment transport pathways in detail. To answer the research questions, multiple sediment fractions must be traced as they move throughout the system with sufficient spatial resolution to identify their pathways and ultimate fate. This cannot be done using empirical or semi-empirical models such as ASMITA [WANG *et al.*, 2012], which are based on morphological equilibrium relationships for large idealized sections of the system.

In the present study, the Ameland Inlet will be modeled for a period of ten years. Due to this long modeling period and the limited time available for this research, a fast and exploratory model is used. The medium term morphological model used in this study is developed by DE FOCKERT [2008] and further improved by JIAO [2014] and WANG [2015]; WANG *et al.* [2016]. JIAO [2014] has performed sensitivity analyses regarding several numerical and input parameters, his recommendations are applied in this study. WANG [2015]; WANG *et al.* [2016] have studied the effect of bedform roughness in medium term modeling. These bedforms are included in the model at issue. In the next paragraphs a concise overview of the model will be provided. The reader is referred to the Delft3D manual [DELTARES, 2014a] and the paper by LESSER *et al.* [2004] for a more elaborated overview of the Delft3D modeling software. For an detailed overview of the Ameland model settings, see the reports by DE FOCKERT [2008]; JIAO [2014]; WANG [2015]; WANG *et al.* [2016].

3.1 Domain and parameter settings

The computational grids used in this study are based on STEIJN AND ROELVINK [1999]. The flow grid has 174 by 162 cells, varying from 60m by 80m in the inlet to 600m by 700m offshore. It extends from the mainland sea dikes in the south to outside the -20m depth contour in the north. In the east-west direction, the grid extends from the midpoint of Terschelling to the midpoint of Ameland and in the basin the grid continues until the tidal watersheds. The wave grid has the same resolution but extends slightly further in both directions, to prevent

artificial effects near the boundaries JIAO [2014]; DELTARES [2014b]. As a starting point, the 1999 bathymetry is applied in the model. Later in this research the 2016 bathymetry is constructed and used in the model.

3.2 Sediment transport

In the model sediment transport is calculated with the Van Rijn 2007 transport formula, for a detailed overview see the report by RIJN AND WALSTRA [2003]. The roughness is calculated by means of the Van-Rijn 2007 bedform-related roughness predictor [VAN RIJN *et al.*, 2007], including ripples, mega ripples and dunes. The active layer thickness in the model is 0.5m. This value is chosen, since it should be in the order of the bedform heights [DELTARES, 2014a] and the dunes typically have heights in the order of 10^{-1} - 10^0 m [WANG *et al.*, 2016].

The Delft3D model with the Van Rijn 2007 transport formula distinguishes between bed load and suspended sediment transport, for both a current and wave related part is calculated separately. First a reference height is determined based on the bed and wave related roughness heights. Sediment transported below this height is defined as bedload transport, above this suspended transport is supposed to take place DELTARES [2014a]. At this height the reference concentration is calculated for each sediment fraction, which depends on the availability of the sediment fraction, diameter, wave and current related shear stress and the Shields criterion [RIJN AND WALSTRA, 2003; VAN DER ZWAAG, 2014]. The Van Rijn 2007 transport formula are used to calculate the bedload and suspended transport below and above the reference height respectively.

3.3 Forcing

In each modeling stage, first only the tide is included, then complexity is added by including waves and wind. The effect of the waves is simulated by means of the Mormerge or Parallel Online Approach. In this approach the DELFT3D-FLOW simulations for all wave conditions are performed at the same time as separate calculations on different nodes [DELTARES, 2014a]. Each half time step the bed level is calculated for all conditions and subsequently the average bed level is calculated, weighted by the relative frequency of each condition [ROELVINK, 2006]. This level is then used by all conditions in the next calculation. Moreover, in the Mormerge approach a phase shift in the tidal signal is applied for the different wave conditions, see Figure 3.1. For each of the 12 consecutive wave conditions, the phase of the tide is shifted by $1/12^{th}$ of the tidal period. In this way the transports for some of the wave conditions will oppose each other during the same time step. As a consequence the amplitudes of the short term changes are reduced and a higher morphological acceleration factor (*MorFac*) can be applied [DE FOCKERT, 2008].

3.3.1 Tide

The tidal boundary conditions for the model are derived by JIAO [2014] after nesting the Ameland model in the Deltares Southern North Sea (ZUNO) model. The Northern boundary is divided in 8 different segments for which the water levels are determined. At the eastern and western boundaries Neumann conditions are prescribed.

In order to reduce the computational efforts for the simulations JIAO [2014] derived a morphological tide, based on LATTEUX [1995]. He constructed a morphological double tide

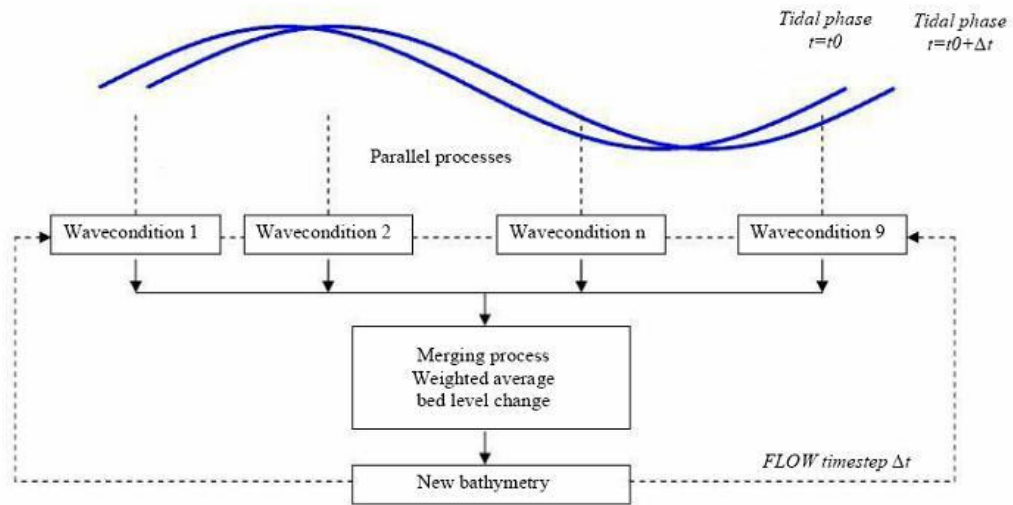


Figure 3.1: Phase shift in the tidal signal for the Parallel Online Approach, obtained from DE VRIES [2007]

based on the residual transport through the inlet and between different areas in the domain for a full spring-neap cycle. This tidal signal is applied in this study.

3.3.2 Waves and wind

The wave and wind climate in this study was developed by DE FOCKERT [2008]. He constructed a reduced wave and wind climate based on a measurements from the measurement station Schiermonnikoog North (SON). He schematized the full wave climate into 126 wave conditions. From these conditions he developed a morphological wave climate consisting of 12 wave conditions, each accompanied by the representative wind condition, see Table 3.1. A drawback of using this wave climate is that the SON measurement station is located quite far from the Ameland Inlet. A wind rose constructed from data from the SON measurement station is given in Figure 2.2.

3.4 Bed composition

The bed composition of the model is produced by means of bed composition generation (BCG) runs. In these BCG runs the bed level is static, but it does allow for the redistribution of sediment fractions [VAN DER WEGEN *et al.*, 2011]. In this way a more realistic bed composition can be generated based on an ill-defined initial bed composition.

3.4.1 Sediment fractions

BCG runs are performed with four different initial bottom compositions. Based on the results, the most suitable bed composition will be selected, which will be used as input for the nourishment simulations. Different sediment fractions are selected, based on the measured D_{50} values as shown in the sediment atlas, see Figure 3.2. In scenario 1 and 2 the bed consist of five fractions with a D_{50} of 50, 100, 200, 300 and 400 μm . In scenario 3 and 4

Table 3.1: Reduced wave and wind climate, obtained from DE FOCKERT [2008]

Wave condition	$H_{m0}[m]$	$T_p[s]$	$Dir[^\circ N]$	$U_{wind}[m/s]$	$Dir[^\circ N]$	Weight[%]
1	0.49	4.84	27.77	4.65	88.04	17.58
2	0.52	4.87	292.97	5.08	224.09	11.35
3	0.99	5.06	264.07	9.17	215.45	13.21
4	0.99	6.29	322.68	4.88	267.05	24.50
5	1.49	5.73	53.63	9.60	80.80	8.22
6	1.98	7.13	338.01	6.99	332.86	6.67
7	1.98	6.98	351.21	7.52	5.99	4.35
8	2.47	6.94	278.78	13.81	252.61	2.37
9	2.47	7.26	293.40	11.14	262.90	7.35
10	3.45	8.59	336.61	11.10	336.12	2.02
11	4.47	9.44	307.05	15.00	284.07	0.99
12	5.88	11.26	324.60	14.60	315.92	0.23

it consist of four fractions with a D_{50} of 100, 200, 300 and 400 μm . In order to successfully generate a bed that suits the hydrodynamic conditions, the initial distribution of the fractions over the domain should be close to the observed distribution [VAN DER WEGEN *et al.*, 2011]. Therefore a different initial bed composition is specified for the channels, tidal flats, basin and offshore area, based on the sediment atlas data. The different initial bed compositions are specified in Table 3.2, Figure 3.3 shows a map with the initial D_{50} distributions. In the model the transport layer has a thickness of 0.5m and four under layers of with a thickness of 5.0m are applied.

3.4.2 Tide only

First the bed composition is generated for the tide only scenario. An important stability criterion for the BCG run is that the sediment in the active layer should not be replaced in one time step [VAN DER WEGEN *et al.*, 2011]. Therefore the morphological acceleration factor (*MorFac*) is set to 50, half the value as suggested by JIAO [2014]. The model is run for a morphological period of 20 years.

The bottom changes were analyzed for four locations in the model domain, a point in the channel, on the ebb tidal delta, in the basin and on a tidal flat, numbers 1 till 4 respectively in Figure 3.4. Most of the change in bottom composition occurs in the first ten years (Appendix A). Since the relatively long modeling period and low *MorFac* of the BCG runs makes them time consuming, subsequent BCG runs will be stopped after this period. It is acceptable that the bottom composition still slightly changes after that period, because this also occurs in real life.

To further speed up the simulation process, it is assessed whether the *MorFac* can be increased to 100. Figures A.13 and A.14 show the results for composition 1 and 2. After ten years of simulation time the models with a *MorFac* of 100 show approximately the same results as

Table 3.2: Initial bed composition with 5 fractions

Morphological unit	50 μm	100 μm	200 μm	300 μm	400 μm
COMPOSITION 1					
Channels	-	-	-	50%	50%
Basin	15%	55%	15%	15%	-
Tidal flats	50%	40%	10%	-	-
Offshore	-	15%	55%	15%	15%
COMPOSITION 2					
Channels	-	-	33%	33%	34%
Basin	17%	33%	33%	17%	-
Tidal flats	33%	33%	34%	-	-
Offshore	-	17%	33%	33%	17%
COMPOSITION 3					
Channels	-	-	30%	40%	30%
Basin	-	40%	40%	20%	-
Tidal flats	-	80%	20%	-	-
Offshore	-	30%	30%	30%	10%
COMPOSITION 4					
Channels	-	-	-	50%	50%
Basin	-	20%	40%	40%	-
Tidal flats	-	80%	20%	-	-
Offshore	-	10%	50%	40%	-

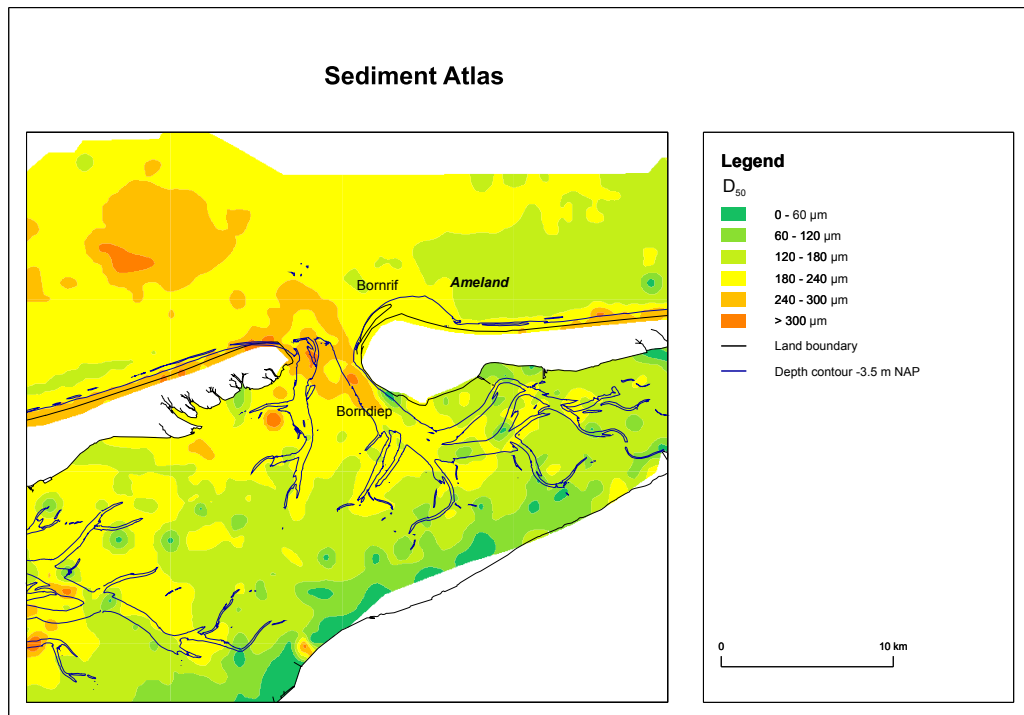


Figure 3.2: D_{50} distribution at the Ameland Inlet area, source: Wadden Sea Sediment Atlas

the models with a *MorFac* of 50; the difference in D_{50} values is less than 1%. Therefore the BCG runs for composition 3 and 4 were performed with a *MorFac* of 100.

The development of the D_{50} values for initial bottom composition 3 is shown in Figure 3.5, the results for the other compositions can be found in Appendix A. The fluctuations in the D_{50} values are a result of the morphological tide and the morphological acceleration factor. Figure 3.7 shows additional graphs for the bottom development on a tidal flat which is not connected to the shore, location 5 in Figure 3.4. For the resulting D_{50} maps after ten years, see Figure 3.6. These maps show that a significant amount of fines is transported out of the basin, which is even more clearly visible in animations. Moreover, the D_{50} graphs for location 4 and 5 show that for all initial bottom compositions, only slight changes in the composition of the tidal flats occur. And therefore it seems that the connectivity of the tidal flats with the rest of the system is low and occurs on very large time scales. The $50\mu\text{m}$ fraction mainly exists on the tidal flats, however when it remains static in the model, including it does not add much value. Therefore it was decided that the fraction with a D_{50} of $50\mu\text{m}$ will not be included in the nourishment model for the tide only scenario, with the additional advantage that about 20% calculation time is saved.

The resulting bottoms from the two four-fraction composition remain as options for the nourishment model. By comparing these (Appendix A) to the sediment atlas in Figure 3.2 the most suitable bottom was selected. According to the sediment atlas, the basin consists mainly of sand with a D_{50} of $120\mu\text{m} - 240\mu\text{m}$, in the main channel the D_{50} is $240\mu\text{m} - 300\mu\text{m}$ and even some larger material is found, in the offshore area the D_{50} is $180\mu\text{m} - 240\mu\text{m}$, but

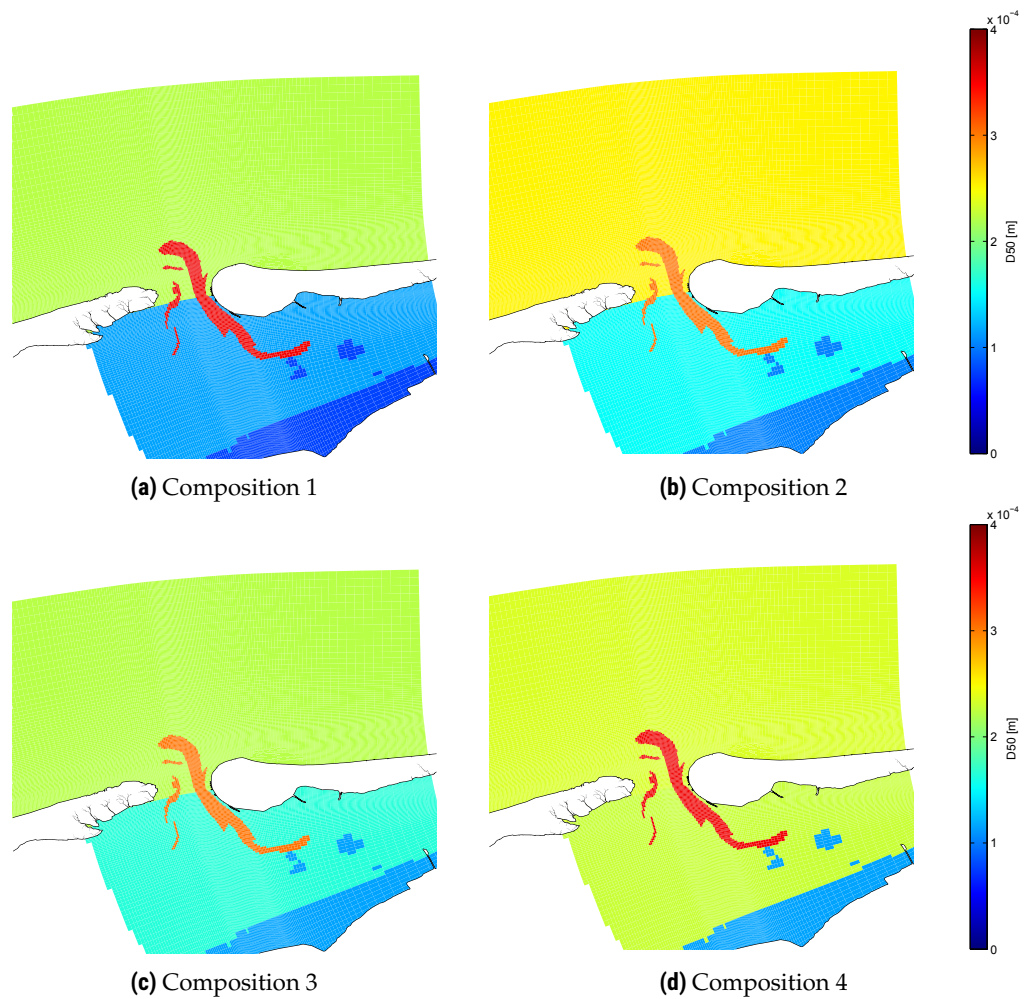


Figure 3.3: Initial D_{50} distribution for the different bottom compositions

some areas show larger or smaller fractions as well. Inside the basin the resulting bottom for both initial composition 3 and 4 corresponds well to the measurements, with D_{50} in the range of $150\mu\text{m} - 180\mu\text{m}$ and $180\mu\text{m} - 210\mu\text{m}$ respectively. In the channel the BCG models show D_{50} values of $350\mu\text{m}$ and $365\mu\text{m}$ respectively, which is somewhat larger than the atlas indicates. In the offshore area composition 3 corresponds best to the observed grain size distribution, with D_{50} in the range of $210\mu\text{m} - 235\mu\text{m}$. For composition 4 the model results slightly over-predict the measurements, with D_{50} values in the range of $235\mu\text{m} - 265\mu\text{m}$. In conclusion the resulting bottoms for both initial composition 3 and 4 correspond quite well to the observed values. However composition 3 seems to correspond slightly better and this generated bottom is therefore selected as input for the nourishment simulations.

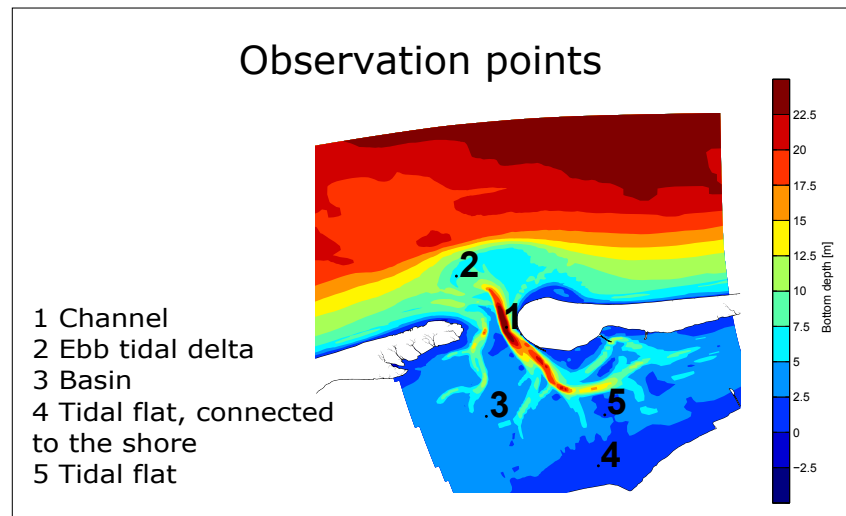


Figure 3.4: Locations of the observation points

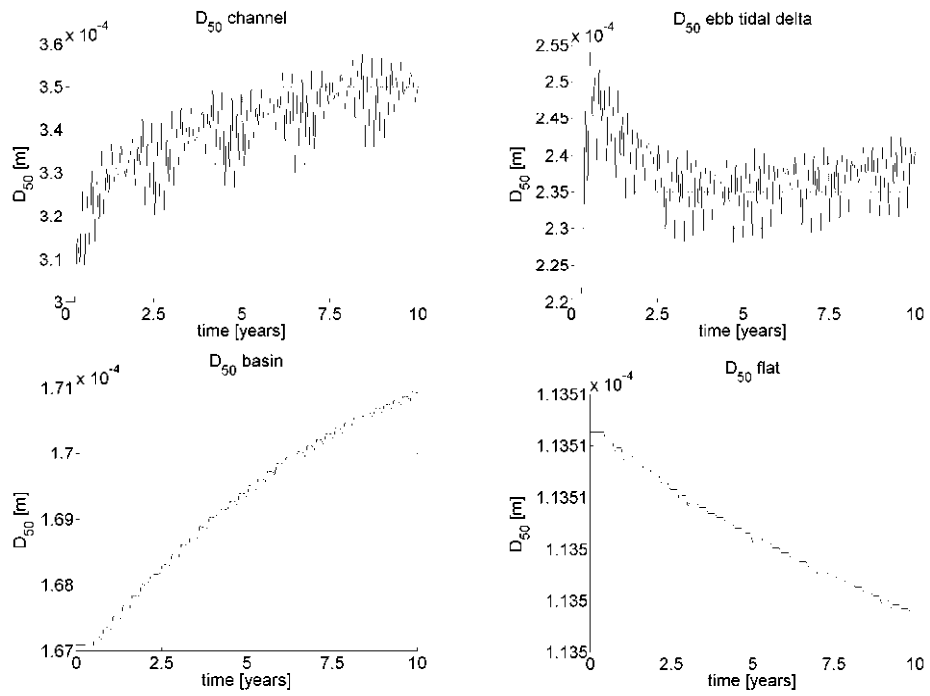


Figure 3.5: Composition 3 with a *MorFac* of 100, D_{50} evolution over time, tide only

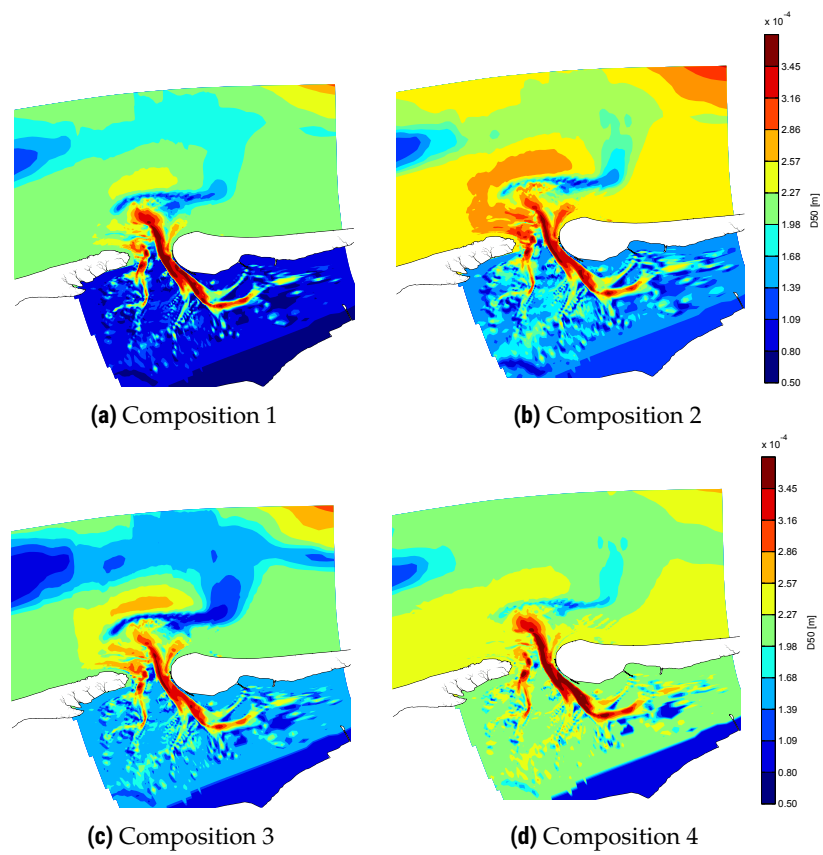


Figure 3.6: D_{50} distribution after 10 years, tide only

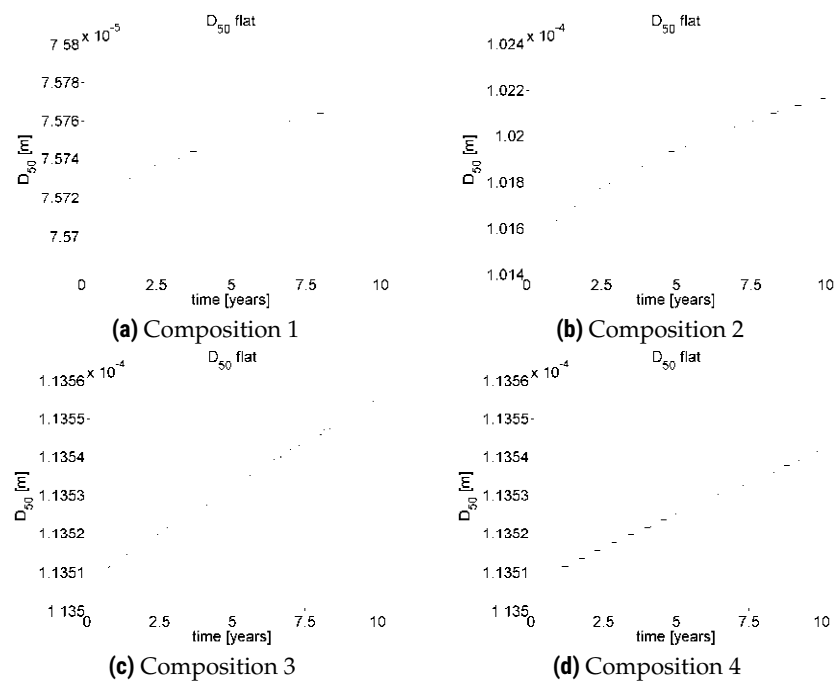


Figure 3.7: D_{50} evolution over time at a tidal flat, location 5, tide only

3.4.3 Tide, waves and wind

Now the procedure from the previous section is repeated for scenario 2, including tides, waves and wind. First the sensitivity regarding the *MorFac* setting is evaluated, by performing a BCG for composition 1 for *Morfac* values of 100 and 200, the value as suggested by JIAO [2014]. Both models show the comparable results, see appendix A. Therefore during subsequent runs the *MorFac* will be set to 200. Due to the long simulation time, the BCG run with a *MorFac* of 100 was stopped after about 17.5 years.

The results for the BCG runs with the different initial compositions can be found in Appendix A.2. Again it can be concluded that most change in bottom composition occurs in the first ten years. Therefore again the BCG runs will be limited to this period. The bottom composition maps resulting from ten year long BCG runs are displayed in Figure 3.9.

After comparing the D_{50} graphs and bottom maps of the tide only scenario to those of the tide, wind and waves scenario, the effect of the waves is clearly visible. The waves result in a substantial coarsening of ebb tidal delta. For initial composition 3, the BCG run results in a D_{50} of $238\mu m$ in the tide only scenario and $310\mu m$ for tide, waves and wind, about 30% larger. The D_{50} graphs for the tide, waves and wind scenario also show the fluctuations caused by the morphological tide in combination with the morphological acceleration factor.

Inside the basin the wave action also results in a significantly larger D_{50} than in the tide only scenario, for instance 17% larger for initial composition 3. The bottom composition of the channel is not much different for the two scenarios, which is expected because the bottom of the deep channel will not be reached by the action of most waves. For composition 1, both results are approximately equal, for compositions 2,3 and 4 the result for the scenario including wind and waves is about 3% larger. The near shore tidal flats (location 4) consist of slightly finer material when waves and wind are added, which might be the result of additional transport of fines from the basin to the flats by wave or wind driven processes.

From the D_{50} graphs it follows that under the influence of wind, waves and tide again the connectivity of the tidal flats (location 4 and 5) to the rest of the system is low. The $D_{50} = 50\mu m$ does not seem to play an important role in the model. To save computational time the BCG result of one of the two 4 fraction compositions will be used as input for the nourishment model. For composition 3, most of the bottom of the basin has a D_{50} of $140\mu m - 200\mu m$. For composition 4, this is coarser, with D_{50} values for most of the bottom ranging between $200\mu m$ and $260\mu m$. So in the basin composition 3 corresponds better to the values as observed in the sediment atlas. For the channel and ebb tidal delta, no major differences are observed between composition 3 and 4. Composition 3 shows a coarser bottom offshore than in the basin, similar as observed in the atlas. For composition 4, inside the basin the resulting bottom is quite similar as offshore. Based on these observations the result of the BCG run, for composition 3 is selected as input for the nourishment simulation, just as in the tide only scenario.

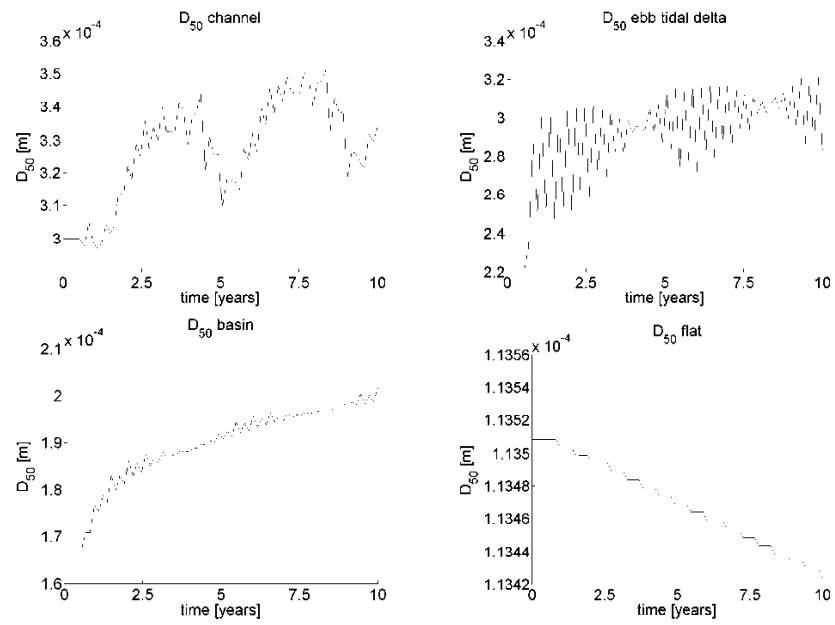


Figure 3.8: Composition 3 with a *MorFac* of 200, D_{50} evolution over time. Tide, wind and waves

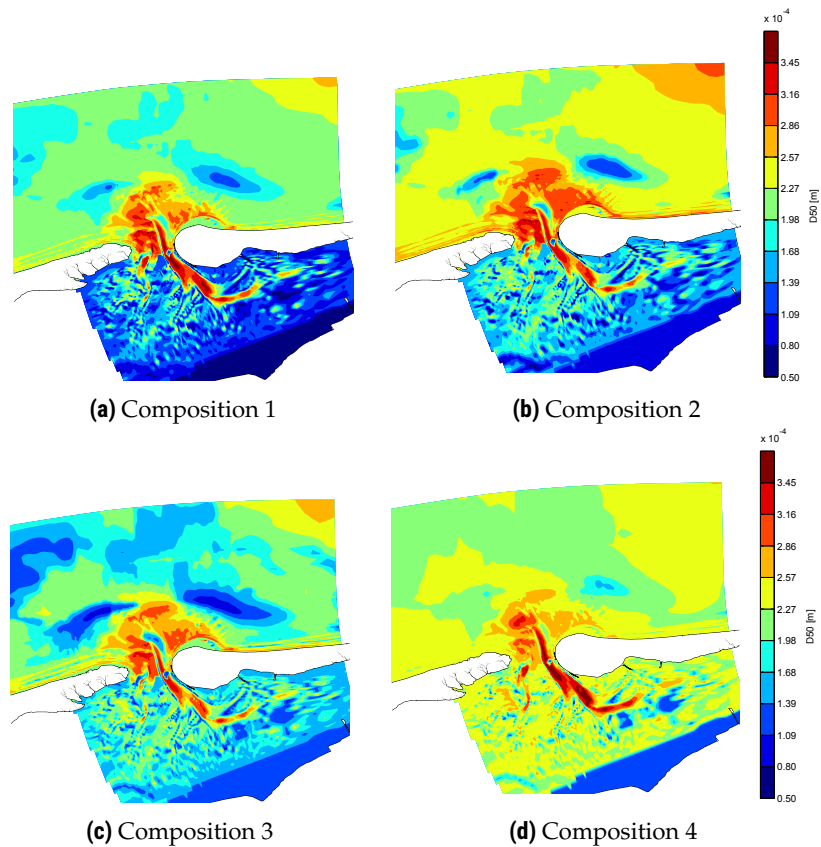


Figure 3.9: D_{50} distribution after 10 years. Tide, wind and waves

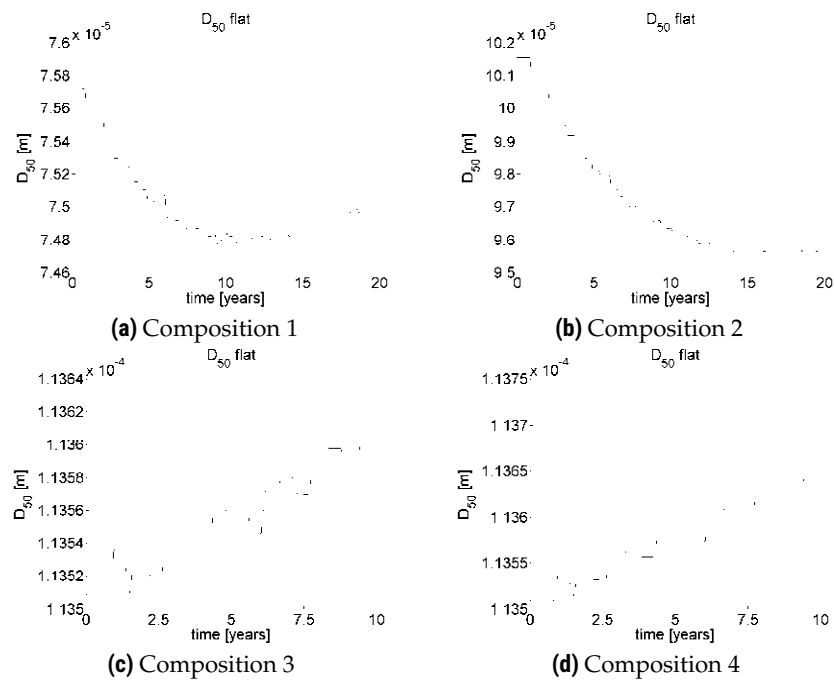


Figure 3.10: D_{50} evolution over time at a tidal flat, location 5. Tide, wind and waves

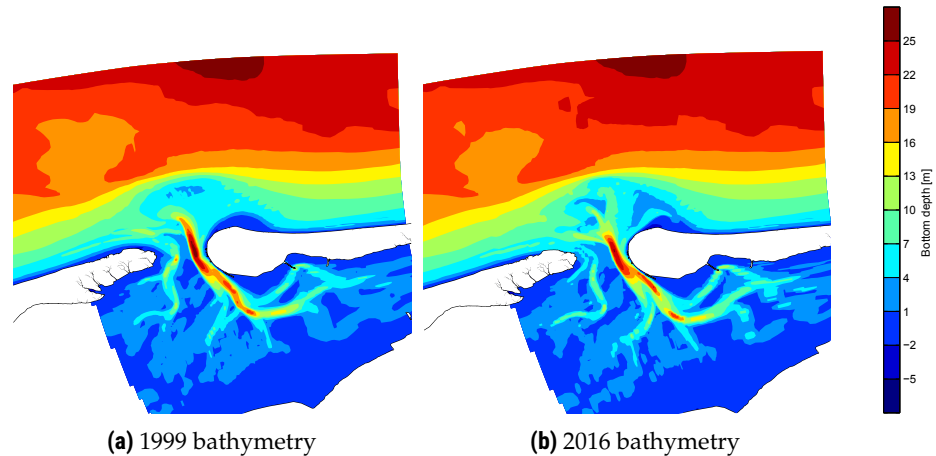


Figure 3.11

3.4.4 2016 bathymetry

The 2016 bathymetry is created based on the 2016 Vaklodingen for the area outside the inlet. Inside the inlet, the Vaklodingen 2011 data is used, which is the most recent bathymetry measurement covering the basin. However the older data for the basin is not expected to have a significant influence on the 2016 model results, since the bathymetry changes in that area appear to be small over time. The depth of the basin and the channel structure remained approximately the same for the period 1999 until 2011 (Figure 3.11).

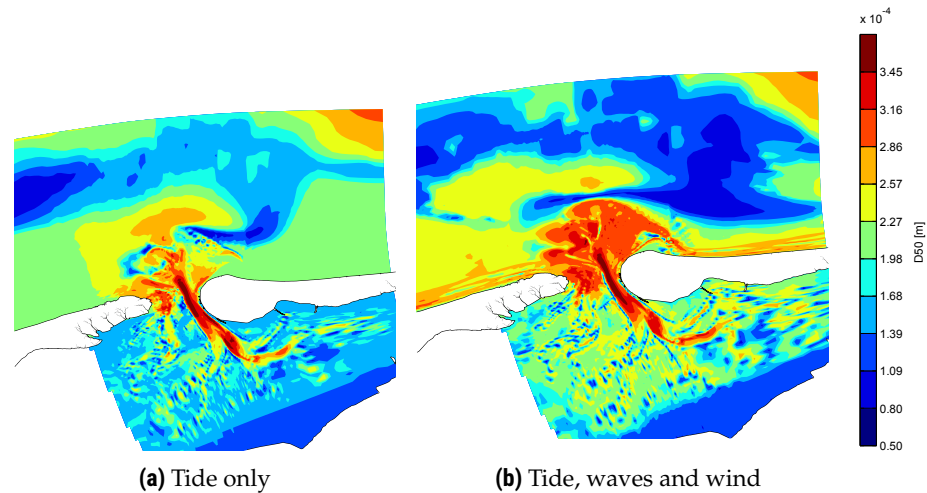


Figure 3.12: D_{50} distribution after 10 years

The bed composition for the 2016 bathymetry is generated by means of a BCG run with a duration of 10 years, starting with initial composition 3, see Table 3.2. An analysis of the results of different BCG runs with different initial compositions is not performed for the 2016 case, since no recent sediment atlas is available for the Ameland Inlet. The resulting D_{50} distributions for the tide only and tide, wind and wave scenarios are displayed in Figure 3.12

3.5 Morphological acceleration factor

The phase shift in the tidal signal for the different wave conditions in the Mormerge approach (see Section 3.3) appears to be very effective. In the simulation with equal phases for the different wave conditions, the results already show instabilities with a $MorFac$ of 200. With that $MorFac$ the nourishment sediment starts to shuffle back and forth with the tide significantly (Figure 3.13), which indicates the $MorFac$ is too high. With the phase shift, the $MorFac$ can be increased up to 600, while no instabilities are observed.

However when the $MorFac$ is increase further, instabilities can be observed for the phase shift approach as well. Starting from a $MorFac$ of 1000, the bed level change per time step starts to exceed 5% of the water depth and the model starts to become unstable. However the simulation is still completed. The morphological development modeled with these high $MorFac$ values is still comparable to the results with lower values and the nourishment sediment fractions move smoothly throughout the model domain, following the same pathways.

For $MorFac$ values of up to 800, the bathymetry predicted by the model after a period of 7 years is approximately the same (Figure 3.14). Some small differences can be observed, mainly at the western end of Westgat and the northern part of Boschgat.

Moreover the development of the bathymetry over time is analyzed. Figure 3.15 shows the development of a point at the bottom of Borndiep and a point at the Kofmansbult over time. For larger $MorFac$ values, the fluctuations of the bottom depth increase. At the point in Borndiep these fluctuations increase over time, at the Kofmansbult they decrease. For values

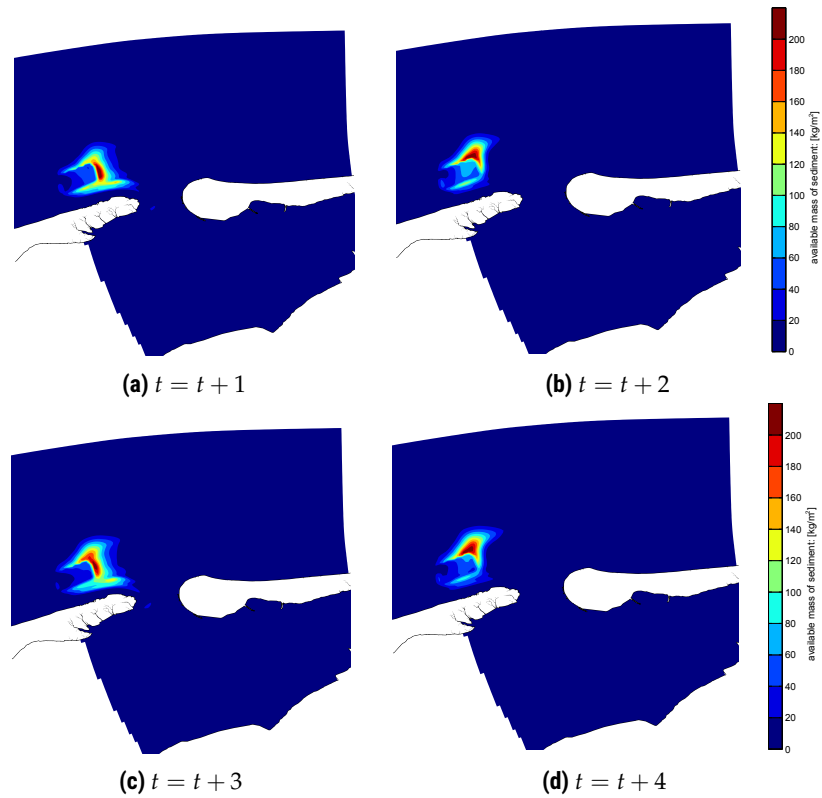


Figure 3.13: Unstable movement of a nourishment fraction, back and forth with the tide. No phase shift, $MorFac = 200$

of 800 and higher, the fluctuations become significantly larger. Therefore in this study a $MorFac$ of 600 is applied, since there are no significant differences in the results compared to simulations with lower values. Furthermore, it results in a computational time of 28 hours, which is acceptable.

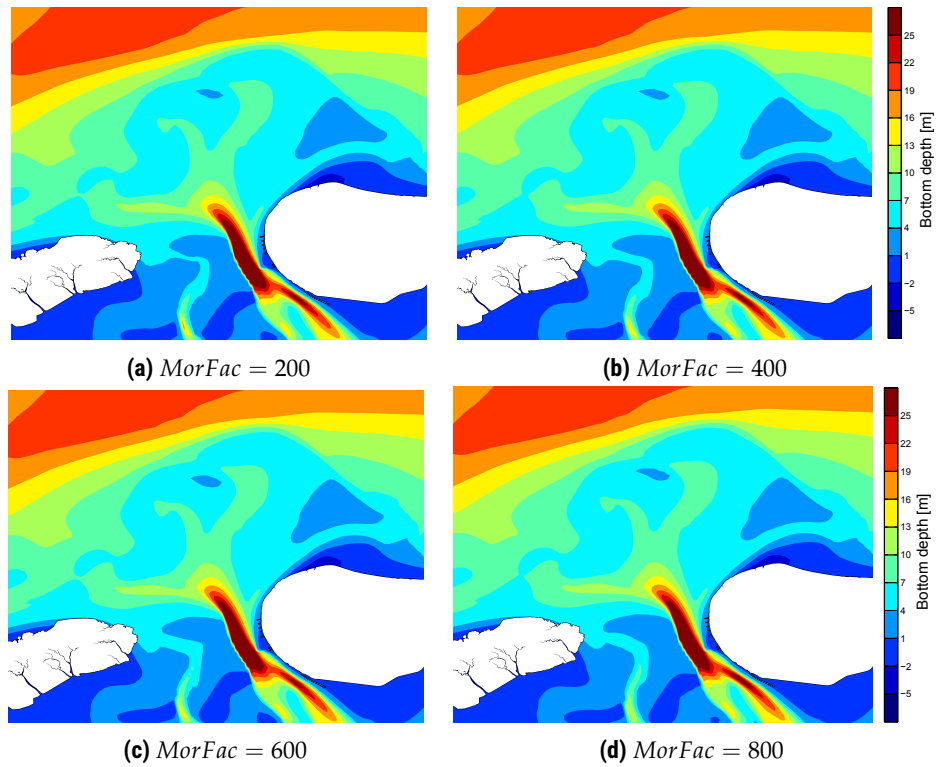


Figure 3.14: Resulting bathymetries after a modeling period of 7 years, for different $MorFac$ settings

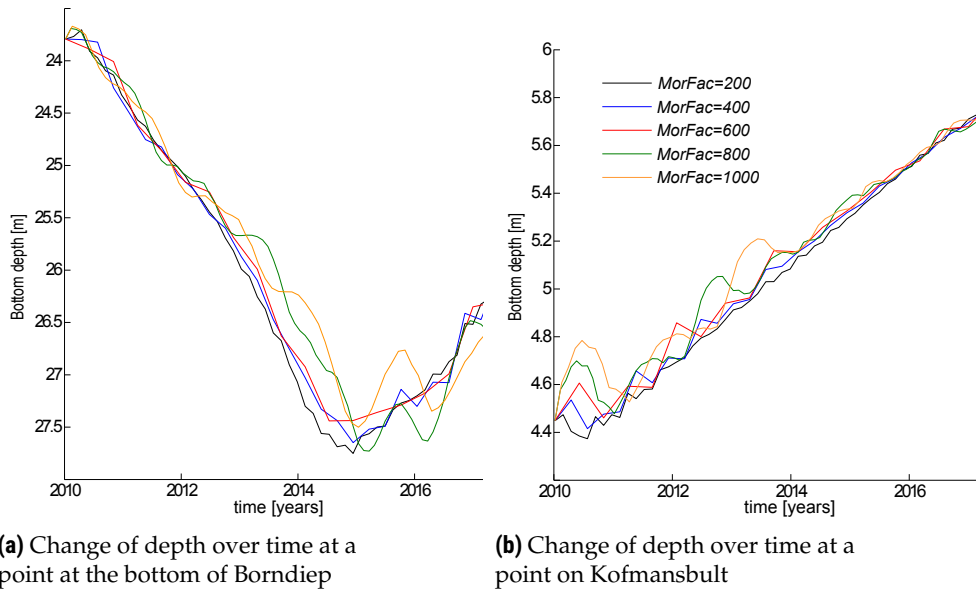


Figure 3.15: The development of a point at the bottom of Borndiep and a point on Kofmansbult over time for different $MorFac$ settings

3.6 Sensitivity to transport calibration factors

In Delft3D four parameters are included to calibrate the bedload and suspended sediment transport, *Sus*, *Bed*, *SusW* and *BedW* [DELTAIRES, 2014a; RIJN AND WALSTRA, 2003; VAN DER ZWAAG, 2014]. *Sus* and *Bed* are multiplication factors for the current-related suspended and bedload transport respectively. *SusW* and *BedW* are multiplication factors for the wave-related suspended and bedload transport. The default value of the four factors is 1, in case this value is used it is assumed that the formulations in Delft3D describe the sand transport process perfectly [BHATTACHARYA *et al.*, 2007]. By using different values, the sediment transport rates can be up- or downscaled, based on accurate transport or bathymetry data [BHATTACHARYA *et al.*, 2007].

The transport calibration factors are important for the purpose of this study, their effect on the model results are studied in greater detail. By influencing the transport vectors, they can have an effect on the way in which the nourishment fractions move throughout the model. Since no measurement data regarding the sediment transport is available to calibrate the parameters, previous studies are used to determine suitable settings (Table 3.3).

The sensitivity of the model to various settings is determined. Due to time and computer resources constraints, only a limited number of parameter combinations are simulated. See Table 3.4 for the parameter settings are tested.

First, the effect of the *Bed* and *Sus* parameters is analyzed. Figure 3.16 shows the availability of the coarsest sediment fraction in the upper 0.5m over the model domain at the start and after 10 years, for different *Bed* and *Sus* values. For the different settings, the location of the nourishment fraction after 10 years is approximately the same. They do not seem to influence the transport patterns of the nourishment fractions. However, for higher values of *Bed* and *Sus*, the bedload and suspended transport are increased. As a result a nourishment will erode faster in the model (Figure 3.17). The graphs show that for higher values of the *Bed* and *Sus* calibration factors, the height of the nourishment reduces more quickly.

Table 3.3: Transport calibration factors applied in different sediment transport studies

Topic	Author and year	<i>Sus</i>	<i>Bed</i>	<i>SusW</i>	<i>BedW</i>
Modeling of the Ameland	JIAO [2014]	1	1	0.2	0.2
Modeling of the Ameland Inlet	WANG [2015]	1	1	0.0	0.0
Sand Engine modeling	TONNON <i>et al.</i> [2009]	1	1	0.2	0.2
Sediment demand along the Dutch coast	VAN DER SPEK <i>et al.</i> [2015]	1	1	0.2	0.2
Modeling of a tidal inlet in Sri Lanka	DUONG [2015]	1	1	0.0	0.0
Sand Engine modeling	LUIJENDIJK <i>et al.</i> [2017]	0.5	0.5	0.2	0.2

The calibration factors *SusW* and *BedW* do influence the sediment transport patterns. Figure 3.18 shows the availability of the coarsest sediment fraction in the upper 0.5m over the model domain at the start and after 10 years, for different *SusW* and *BedW* values. The figures clearly show a decrease in onshore movement for smaller values of *SusW* and *BedW*, as explained in Section 3.2. This effect is most evident for the coarsest fraction, since this one is least affected by the alongshore transport processes, and therefore it remains quite stable in alongshore direction.

When both factors are set to 0.0, there is no onshore movement of the coarse fraction. If both

Table 3.4: Modeling scenarios with different transport calibration factors

Factor	Scenario 1	Scenario 2	Scenario 3	Scenario 4	Scenario 5
<i>Sus</i>	0.6	0.8	1	1	1
<i>Bed</i>	0.6	0.8	1	1	1
<i>SusW</i>	0.2	0.2	0.2	0	0.4
<i>BedW</i>	0.2	0.2	0.2	0	0.4

set to 0.2, the fraction moves about 500m in onshore direction after 10 years. When both are set to 0.4, the movement is about 1000m in 10 years. After analyzing the research of BRUINS [2016], who studied the behavior of 20 shoreface nourishments along the Dutch coast, it seems that a movement of 100m per year is too high. The maximum onshore movement observed by the author is 78.7m and the average is much lower, about 20m. Therefore a setting of 0.2 for both *BedW* and *SusW*, resulting in an onshore movement of 50m per year seems more reasonable. Moreover, these settings are applied in many other studies, see Table 3.3.

The value for *Sus* and *Bed* is of less importance for this study, since these do not significantly influence the sediment transport patterns. For both a value of 1 is chosen.

3.7 Morphological performance

In order to assess the performance of the model and to understand the limitations of the model, the simulated morphological development is compared to measurement data. The model with the 1999 bathymetry is run for a period of 9 years and the resulting bathymetry is compared to the Vaklodingen 2008 measurements. The model performance inside the basin is not evaluated, since no measurement data is available for the year 2008 (the basin is only surveyed every 6 years), moreover this area is much less morphologically active than the rest of the system. In Figure 3.19 the measurement and model results are displayed. Both show a two channel system and an extensive Bornrif tidal flat area. Moreover, both maps display that Akkepollegat bends towards the west at the northern end of the ebb tidal delta. However, some differences can also be observed. In the model results, both Borndiep and most of Bornrif are deeper. Furthermore, the model shows a deeper opening at the Northwestern side of Akkepollegat.

More insight in the model performance can be gained by comparing the simulated morphological development over the period 1999 - 2008 to the measured development. This is done by subtracting the measured 1999 bathymetry from the modeled and measured bathymetries, see Figure 3.20. The model does correctly predict a shift of Borndiep and Akkepollegat towards the east, however in the inlet it seems to over-predict this shift. Furthermore, the erosion and sedimentation patterns at the areas around the island tips seems to be predicted quite well, nonetheless the erosion just north of the tips is under-predicted. Moreover, just north of the tip of Ameland, the model predicts growth of Bornrif, which is in agreement with the measurements. However there are some discrepancies between the model results and the measurements. Again from these figures it can be observed that the channel incision in the model results is too large. Finally the model shows an outbuilding of the ebb tidal delta at its Northern end, while the measurements indicate erosion.

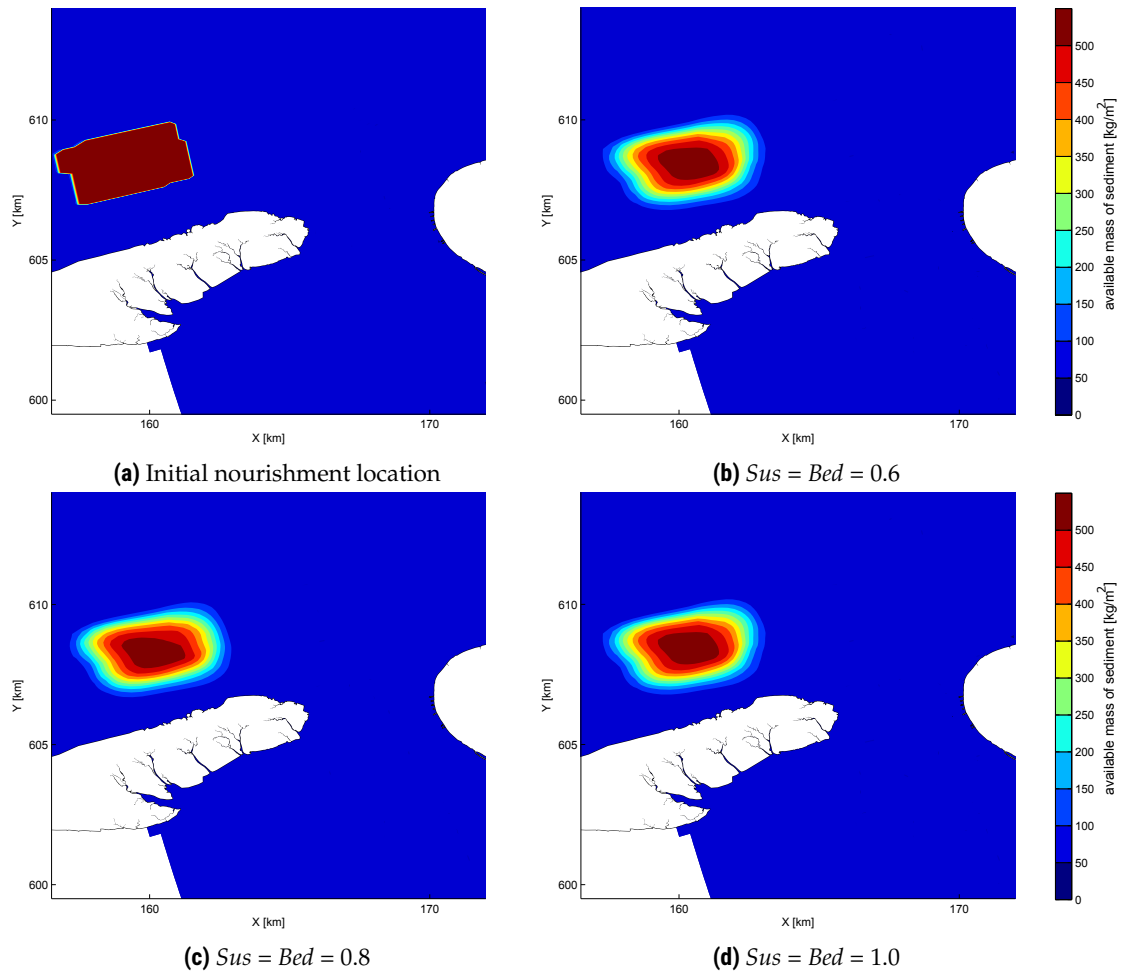


Figure 3.16: Available mass of the coarsest sediment fraction ($250 - 500\mu m$) after 10 years, for different settings of *Sus* and *Bed*

3.8 Particle tracking

In this study nourishments are implemented in the Delft3D model at different locations. The different nourishment sand fractions are labeled separately from the fractions in the rest of the domain. This allows us to evaluate for instance where in the model domain nourishment sand is available in the transport layer (upper $0.5m$) at different time steps in the simulation. In that way the transport pathways as well as the location where the sediment settles can be traced for each fraction. Furthermore, the total amount of nourishment sand ending up at different locations can be determined from the model results.

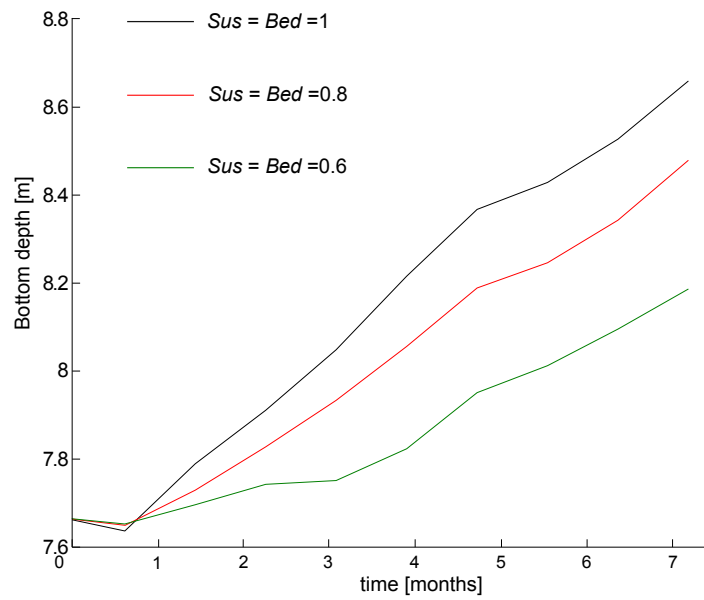


Figure 3.17: Change in bottom depth over time at a nourishment, for different settings of the *Bed* and *Sus* parameters

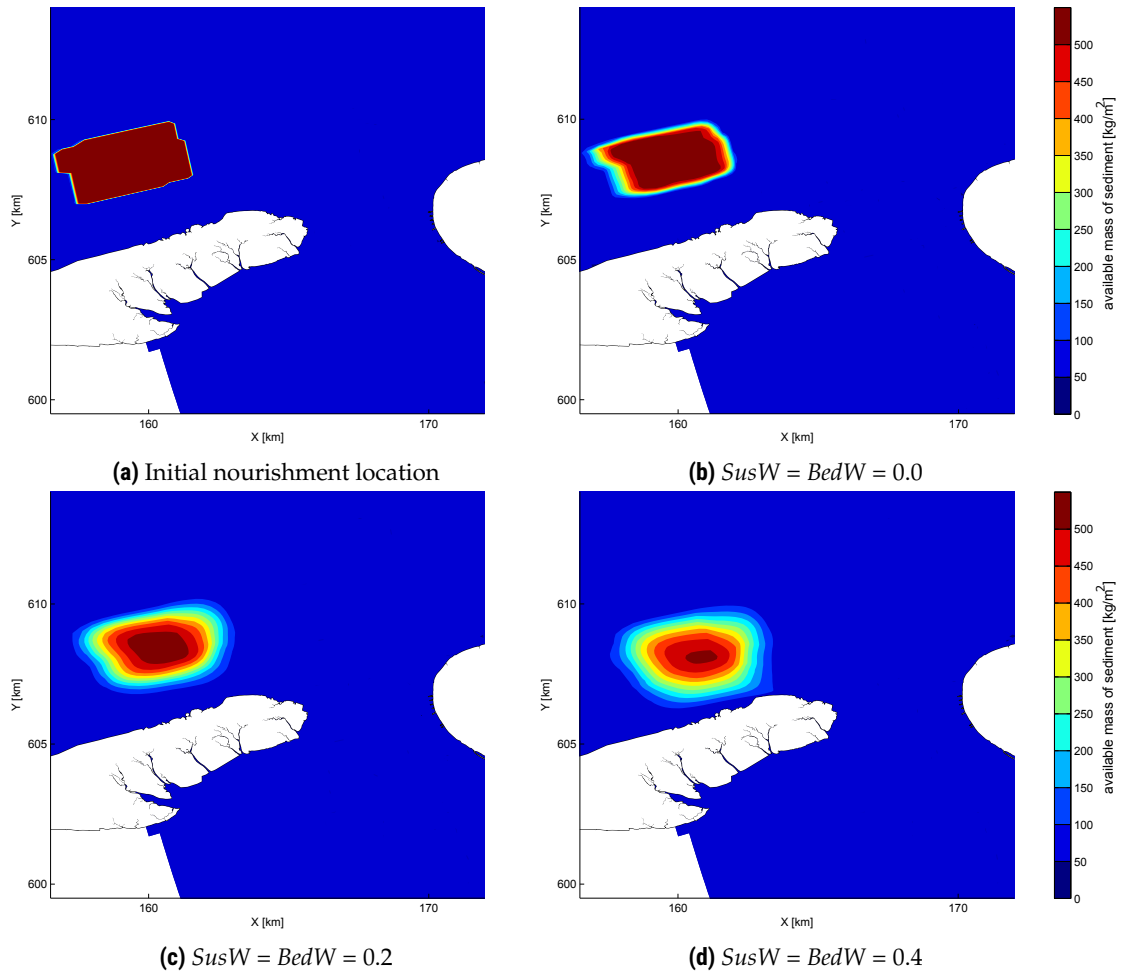


Figure 3.18: Available mass of the coarsest sediment fraction ($250 - 500\mu\text{m}$) after 10 years, for different settings of $SusW$ and $BedW$

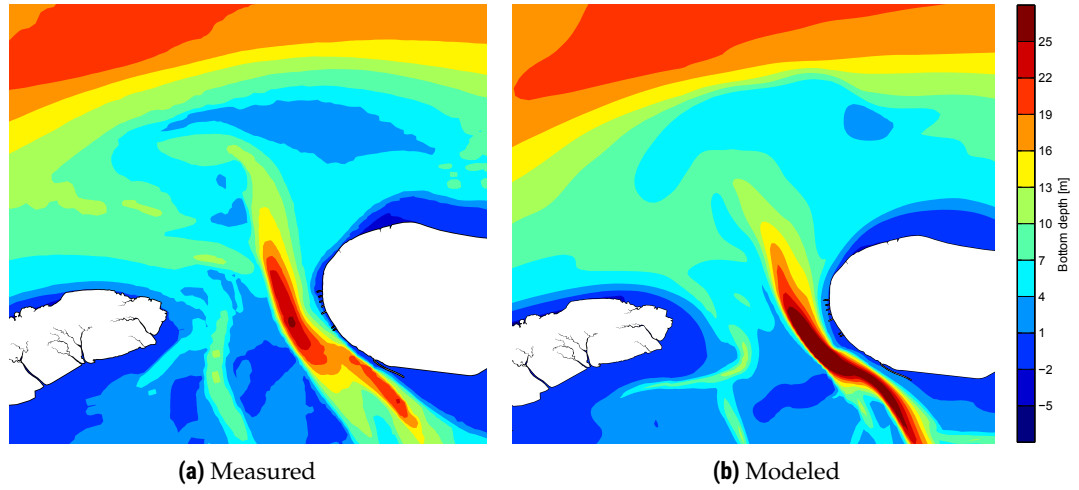


Figure 3.19: 2008 bathymetries

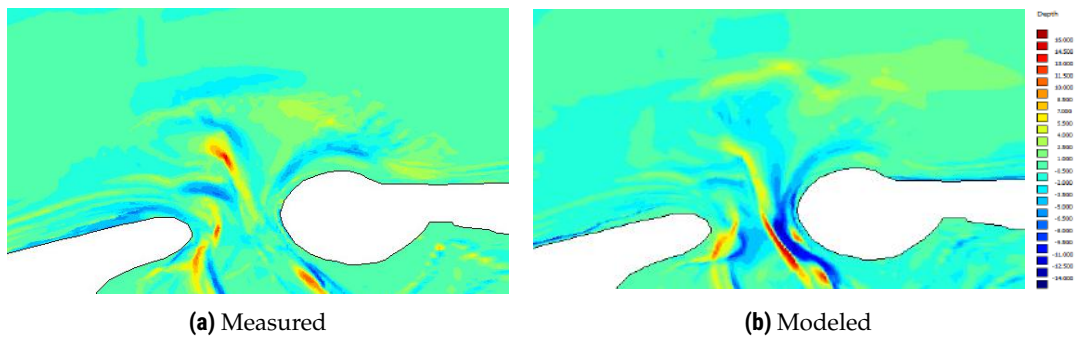


Figure 3.20: 1999 bathymetry subtracted from 2008 bathymetry, positive numbers indicate erosion

This chapter treats the design and model implementation of the nourishments. First in Section 4.1 the requirements that technology, ecology and society pose on a nourishment are discussed. Section 4.2 deals with the composition. In Section 4.3 an overview is provided of the residual sediment transport at the Ameland Inlet. The different nourishment locations and their score with respect to the nourishment requirements is discussed in Sections 4.4 and 4.5. The chapter concludes with the model implementation of the nourishments in Section 4.6 and the hypotheses regarding the transport of the fractions in Section 4.7.

4.1 Nourishment requirements

4.1.1 Technological requirements

To determine the different potential nourishment locations, the technical requirements need to be taken into account. This will be done by analyzing the properties of a trailing suction hopper dredger (TSHD). To minimize the sailing time, the borrow area for the nourishment material will be just outside the coastal foundation, close to the $-20mNAP$ depth contour. Figure shows a map of 3 potential borrow areas. The depth of the borrow area is about $-20mNAP$, the depth at the nourishment area is in the range of $-5to - 15mNAP$. For relatively shallow areas like these, a typical TSHD that would be used is of the type Shoalway (Figure 4.1). This vessel is highly maneuverable and is equipped with a powerful engine. Therefore it should be able to operate even in the inlet under high flow velocities.

The TSHD has a overall length of $90m$, the breadth is $19m$ and it has a hopper capacity of $4,500m^3$ [BOSKALIS, 1999]. When the hopper is fully loaded the draft is $6.82m$, the under keel clearance should be about $1m$, which is a conservative value and may be reduced when sailing carefully in calm conditions. With a reduced load of about $2000m^3$ the draft can be reduced to $5m$.

The TSHD can unload by dumping through the bottom doors, rainbowing, or pumping through floating pipelines. The bottom doors do not protrude under the TSHD when they open and therefore no additional clearance has to be taken into account while dumping. Therefore by dumping the full load, the nourishment can be placed up to a height of about $-7.5m$. When rainbowing half the load and dumping the rest, the sand can be dumped up to $-5.5m$. By making use of the tidal range, the sediment can be dumped up to $1m$ higher. By



Figure 4.1: The Shoalway, obtained from Boskalis Equipment Sheet

rainbowing the second half of the load on the shallow areas, the height of the nourishment can be further increased.

If the full load is rainbowed, the sand can be placed up to NAP or higher. When rainbowed with a large discharge distances of about $30m$ can be reached, with a reduced discharge this can be increased to about $80m$. If distances of over $80m$ over a shallow area need to be reached, for instance when nourishing on top of the ebb tidal delta, the dredged material can be pumped through floating pipelines. However when pumping the costs of the nourishment will be about twice as much compared to dumping. This is due to the extra equipment needed, such as pipelines, bulldozers to spread the sand and the extra time and man hours needed for the pumping operation.

When a nourishment is placed on a beach, first a bunt has to be constructed in between the mean low water line and mean sea level, in order to prevent the sediment from flowing away. Such a bunt is on average $1m$ to $2m$ high. Hereafter the sand is pumped on the beach and spread out by bulldozers.

The costs for the nourishment placement can be estimated by calculating the cycle time. For this calculation the following needs to be taken in consideration:

- The sailing speed of the Shoalway is on average $11kts(5.7m/s)$
- It takes about 1 hour to fill the hopper
- Dumping the full load through the bottom doors takes about 15 minutes
- Emptying by rainbowed takes about 1 hour
- Half rainbowed and half dumping the load takes about 30 minutes
- When pumping the load, the costs for a cycle are about twice the costs of dumping

In conclusion locations where the nourishment can be placed deeper than $-6.5mNAP$ at the offshore side of the Ameland inlet system are the most economically beneficial, since the sand can be placed by dumping and the sailing distance is the shortest. Constructing the nourishment at higher levels will require rainbowed, which takes more time and is therefore more expensive. Locations closer to the throat of the inlet will result in longer sailing times and consequently cost more. Most expensive are shallow areas which cannot

be reached by rainbowing. At these locations pumping is required, which takes more time and requires more equipment.

4.1.2 Ecology

When a nourishment is placed, the fauna living in and on top of the seabed are often destroyed. Furthermore, a nourishment may disturb the habitat of fish and birds. Moreover, the temporarily increased turbidity during the placement of the nourishment may harm the local organisms, however this will be the case for all nourishment locations and it will therefore not be included in this study. Recovery after the placement of a nourishment takes about 1 to 2 years, depending on the species concerned and local circumstances [CLEVERINGA *et al.*, 2004; SPEYBROECK *et al.*, 2006].

The offshore area

A lot of research has been performed regarding the ecology of the tidal basins of the Wadden Sea [E. VAN DER ZEE, A. RIPPEN, 2017; BAPTIST *et al.*, 2016], however not much is known about the area surrounding the ebb tidal delta [BAPTIST *et al.*, 2016; CLEVERINGA *et al.*, 2004].

Based on habitat models [BAPTIST *et al.*, 2016] argue that the circumstances at the ebb tidal delta are unfavorable for a rich bottom life, especially the shallow and morphologically dynamic areas. However life is present in the deeper and less dynamic areas. There are shellfish beds, inhabited by different kinds of shellfish such as the *Spisula subtruncata*, *Ensis directus*, *Tellina fabula* and *Macoma baltica* [VAN LEEUWEN *et al.*, 1994]. Most of these beds are situated on eastern offshore edge of the ebb tidal delta at depths of $-6mNAP$ to $-12mNAP$, since this area is sheltered from the dominant wave direction.

An abundance of fish is found in the region surrounding the ebb tidal delta. The sand eel (Dutch: Zandspiering) seems to be an important species in the area, as it prefers a bottom consisting of relatively coarse sand and high flow velocities. Furthermore, it is expected to be a keystone species [LEOPOLD AND BAPTIST, 2016], eaten by many other fish and possibly also by marine mammals such as seals. Areas with high flow velocities and coarse sand are for instance the inlet channels and the area where the main channel ends up on the ebb tidal delta. At these areas large amounts of sand eel are expected to be found.

Sea mammals use the higher elevated areas of the tidal inlet system, which fall dry during low tide, to rest. Grey seals prefer to lay down on the flats surrounding the ebb tidal delta, outside the basin. The ordinary seals prefer the tidal flats inside the Wadden Sea basins [LEOPOLD AND BAPTIST, 2016]. Therefore by nourishing areas near the flats inside or outside the basin, the habitat of seals may be disturbed. On the other side the nourishment may create new opportunities, when the nourishment is placed up to levels close to mean sea level, new resting areas for seal may be created.

Finally many sea birds regularly visit the ebb tidal delta to hunt. Gannets (Dutch: Jan van Gent) and terns (Dutch: stern) prefer to hunt near the ebb tidal delta, because due to the breaking waves there the fish become better visible. In the winter season large amounts of scoters (Dutch: zwarte zee-eend) are present at the Northern edge of the ebb tidal delta, hunting for the *Spisula* shellfish [JAK *et al.*, 2011; LEOPOLD AND BAPTIST, 2016].

The basin

The area inside the Wadden Sea basins consists of tidal flats and salt marches. This area is visited by millions of birds every year [H. MELTOFTE, J. BLEW, J. FRIKKE, H. U. ROSNER, 1994; KOFFIJBERG *et al.*, 2006], there is an abundance of shellfish banks [DANKER AND ZUIDEMA, 1995], the ebb and flood channels are important nurseries and feeding areas for fish [LOTZE, 2005], thousands of plant species are found on the salt marches [REISE *et al.*, 2010], finally seals use the tidal flats as resting areas. Therefore all areas inside the basin seem to be highly unfavorable as nourishment areas, when considering the ecological effects.

The nourishment may also have an indirect effect on the ecology. The location where the nourished sand ends up can also need to be taken into account. It is for instance undesired that the sand ends up on the tidal flats, since changes in the mud content will impact flora and fauna [WANG *et al.*, 2012].

Impact at different areas in the system

Based on this brief assessment of the ecological impact, the ecological vulnerability of different areas of the tidal inlet system is analyzed. Figure 4.2 provides an overview of 9 different locations of which the ecological sensitivity is discussed below. Inside the basin all areas are highly vulnerable, due to the abundance of bottom life, fish, birds and mammals.

1. The foreshore and backshore of Terschelling are relatively shallow and highly energetic, often exposed to breaking waves. Therefore it is a morphologically dynamic area. As a result not much life is expected to be found here. The impact of a nourishment will be relatively low.
2. The western end of the ebb tidal delta is situated in the dominant wave direction, therefore it is a morphologically active zone. However it is a relatively deep area and therefore some life is expected to be found here, so a nourishment will have a moderate impact.
3. This area, also at the western part of the ebb tidal delta, is more shallow compared to the previous one. Therefore it is expected to be more morphologically active and a rich bottom life is not likely to develop here. However as discussed previously birds use this area, which is exposed to breaking waves, to hunt. Therefore it is expected that a nourishment here will have a moderate impact.
4. The eastern part of the ebb tidal delta is relatively sheltered from wave impact. Shellfish banks are found in this area and therefore it seems likely that a nourishment will have a high impact.
5. Bornrif is at this location about 2m to 4m deep with respect to NAP. Therefore it is flooded most of the time, so birds and seals will not often use this area as a place to rest. Not much wave breaking takes place on the Bornrif flat, despite this it is an active area, with different migrating sand bars, quite large bathymetric changes can be observed over the years [ACHETE, 2011]. Therefore some bottom life may be present, however it is expected to be limited. Moreover, by placing a nourishment in this shallow area, a tidal flat can be created which can function as a resting place for birds and seals and a habitat for all kinds of bottom life. In this way initially the local ecology will be disturbed. However in a later stage it can benefit. All together the impact here is expected to be relatively low.

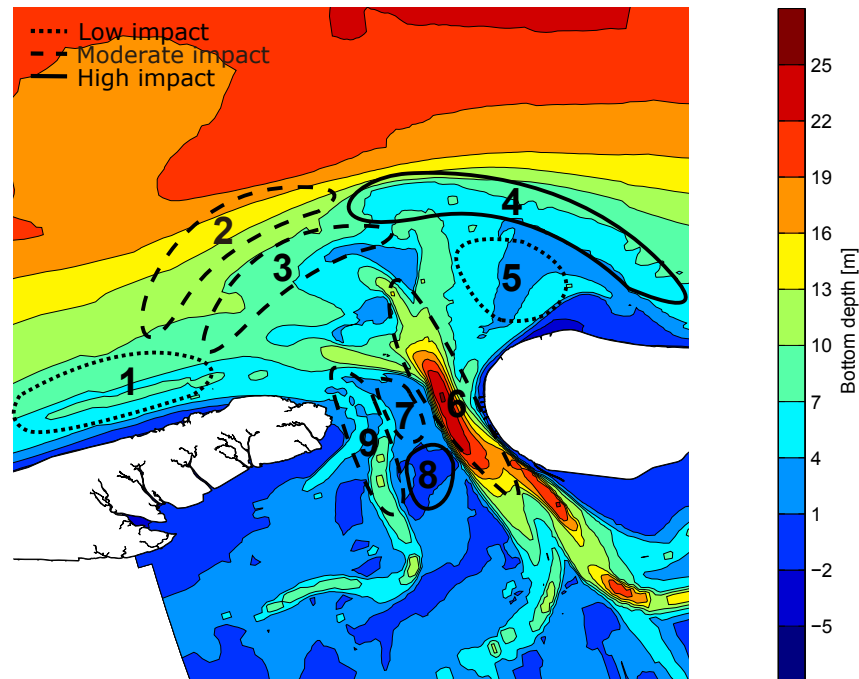


Figure 4.2: Regions with a different ecological impact

6. The deep Bornrif channel and active area due to the high flow velocities. Bedforms can be formed or moved over the channel bottom on short time scales. This bottom consists of coarse sediment, see Section 3.4. The combination of high flow velocities and coarse sand makes this area as an ideal habitat for the Sand Eel, which is expected to be a keystone species in this area. However not much other life expected to be found at this dynamic location. Therefore the impact is expected to be moderate.
7. This shallow area in between Boschgat and Borndiep is sheltered from wave impact by the ebb tidal delta, furthermore, local flow velocities are low. Therefore some bottom life may be present. The area is about $2mNAP$ deep and therefore too deep to be visited by seals or birds. However Robbeneiland (see next location) is just south of this area, and is often occupied by big groups of seals and birds. Therefore a nourishment in this area should be constructed far enough away from Robbeneiland to not disturb the seals and birds. If enough care is taken a nourishment here may create an extra tidal flat area for these animals. Keeping these things in mind, the impact will be moderate.
8. The tidal flat in this area is known as Robbeneiland (Seal Island) [AMELANDGANGER, 2017], many seals and birds use it as a place to rest. Therefore in this area a nourishment is expected to have a high impact.
9. In Boschgat a nourishment is expected to have the same influence as in Borndiep, Location 6. Therefore the local ecological impact will also be moderate.

4.1.3 Social requirements

A nourishment may also have an impact on society. In the area considered in this study tourism and recreation will be affected most. Nuisance to the fishery will be limited, since not much fishing is expected to take place near the ebb tidal delta, due to the energetic environment with breaking waves and locally high flow velocities. There is no commercial shipping in the area.

Different boat tour providers offer seal watching trips to tidal flats where the seals lay down. They depart from the harbor in Nes, on the south side of Ameland and sail towards Robbeneiland through Borndiep [AMELANDGANGER, 2017]. Therefore, dredging works near this tidal flat disturbing the animals will negatively affect the tour providers and the tourists.

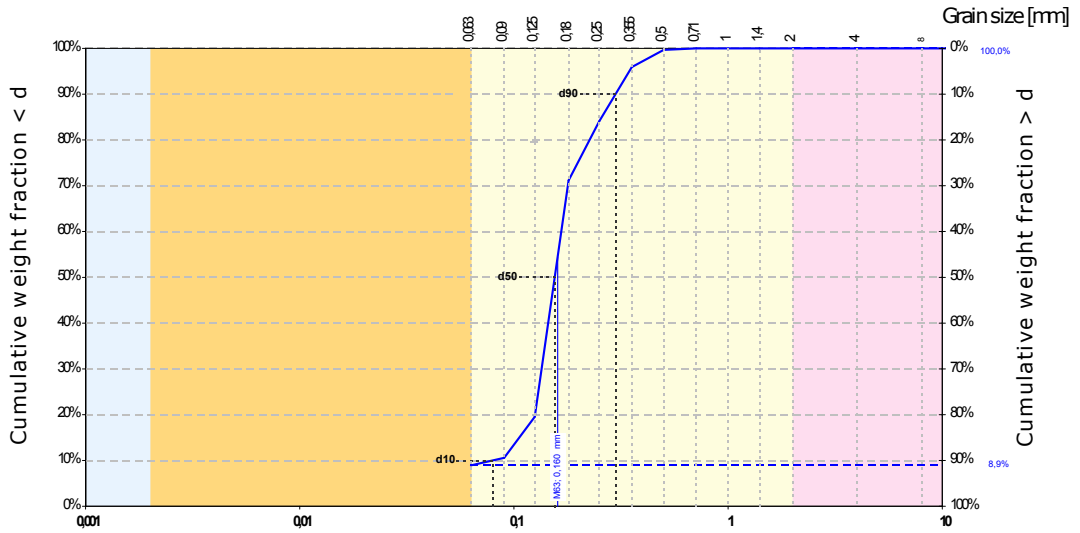
Furthermore, there is pleasure navigation in the area. Boschgat is a sailing channel for pleasure navigation, demarcated with navigation buoys. Filling this channel with the nourishment will negatively impact pleasure navigation. However, as long as the sediment is not placed too high, it is not a problem as the draft of yachts is generally not more than 2m. During the works, navigation may experience hindrance, since they need to keep a safe distance from the TSHD.

Finally, the local community and tourists will experience nuisance from the placement of a nourishment, when it is located near the coast. A clear example is the construction of a beach nourishment. During the construction a part of the beach will be closed and heavy equipment will be working on it, causing noise, smell and visual pollution.

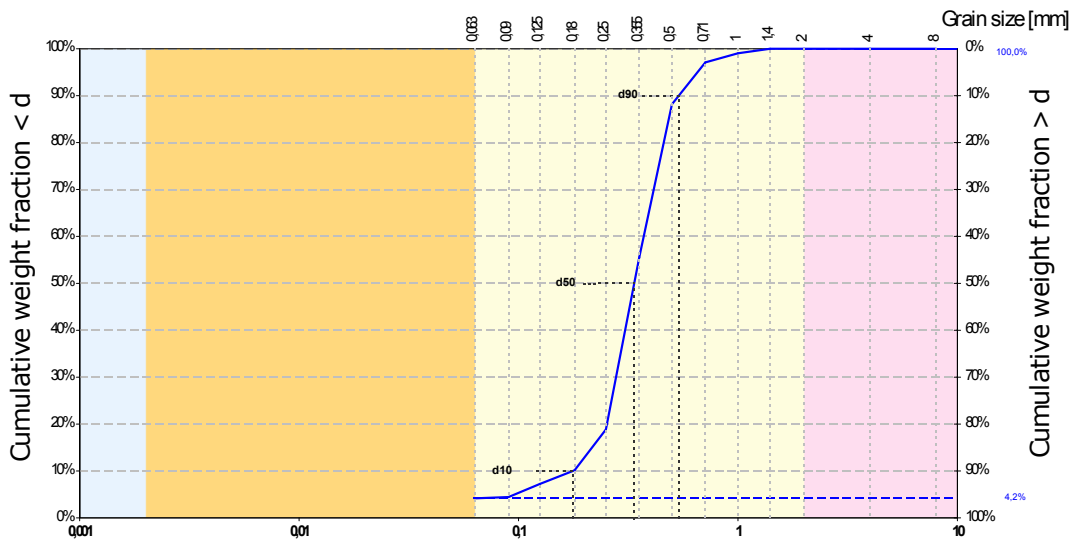
Looking at the locations in Figure 4.2, it seems likely that a nourishment at Location 2 will have the biggest negative influence on residents and tourists. A nourishment on or close to the beach will result in noise, smell and visual pollution. Therefore, the social impact there will be high. At Location 9, pleasure navigation will experience hindrance of the TSHD during construction. Moreover, if the nourishment is placed too high, the Boschgat may become too shallow for navigation. The impact here is expected to be moderate. At Location 6, a nourishment should not result in major problems for navigation. Borndiep is a large channel and boats should be able to sail around the TSHD. However, if a channel wall nourishment is constructed, the local community and tourists at Ameland will experience noise, smell and visual pollution. The impact is therefore assessed to be moderate. At Location 8, disturbing the seals and birds will have a negative effect on the tourists and the tour providers. Therefore, the impact at this location will be high. At the other locations, the effect on society is expected to be minimal.

4.2 Nourishment composition

In order to design a nourishment with a realistic composition, the bottom investigation report of one of the borrow areas near Ameland is analyzed [LABAN, 2014]. Most of the borrow area consists of sand with a D_{50} of 140 – 180 μm . However, there is also a large area consisting of coarse sand with a D_{50} of 300 – 420 μm . The effect of different nourishment compositions will be evaluated in this thesis. Therefore, two representative sediment samples are selected from the report: a relatively fine and a coarse one, see Figure 4.3. The grain size distribution of the modeled nourishments will be based on this data. For one of the nourishment locations, both a fine and coarse distribution will be modeled, in order to assess the effect of the composition. At the other locations, only the fine composition is applied.



(a) Fine area



(b) Coarse area

Figure 4.3: Grain size distribution at the borrow area, adapted from LABAN [2014]

4.3 Sediment transport at the Ameland tidal inlet system

In order to gain system understanding and to predict how nourishments at the Ameland Inlet system will behave, the residual sediment transport patterns are analyzed for the different sediment fractions included in the BCG analysis. This is done by running the model without a nourishment with the bottom that resulted from the BCG analysis, for a period of 12 tidal cycles, for the tide only scenario and for the scenario including wind and waves. Hereafter the mean total transport over this period is evaluated. Figures 4.4 through 4.11 show the tide driven suspended and bedload transport for the 100, 200, 300 and 400 μm fractions respectively, for the 2016 bathymetry. Figures 4.12 through 4.19 show these transports forced by a combination of tide, wind and the 12 wave conditions. The total transports can be found in Figures C.01 through C.08. For each fraction the scale of the total, suspended and bedload transport is the same, to show the relative importance of the different transport modes. It should be noted that a nourishment will change the bathymetry and will effect the sediment transport in that way. Therefore the transport patterns may differ in the nourishment models.

4.3.1 Tide-driven transport

From Figures 4.4 through 4.11, it becomes clear that the tide driven transport is for the most part confined to the two inlet channels Borndiep and Boschgat. Outside these channels not much transport takes place, due to the low flow velocities. Fractions with larger grain sizes are increasingly confined to the channels, since larger flow velocities are required to move the grains. Significant transport of the 400 μm fraction only occurs in Borndiep. The tidal currents in Boschgat are hardly able to transport this sediment (Figures 4.10 and 4.11).

For each of the four fractions, sediment is primarily transported in suspension. For the 100 μm and 200 μm fractions the relative contribution of the bedload transport is negligible (Figures 4.5 and 4.7). For the coarser fractions, this contribution increases. This is expected, since it requires more energy to bring heavier particles into suspension, and therefore they are relatively more likely to be transported as bedload.

In Borndiep a recirculation is visible inside the inlet, with flood dominant transport governing the western part of the channel, and ebb transport dominating the eastern part. Sediment leaving Borndiep is transported onto the Kofmansbult or it flows in offshore direction through the Akkepollegat. Boschgat shows a flood dominated transport, resulting in a residual transport into the basin for all fractions. In the Westgat there is a residual transport of sediment into Borndiep.

The bedload and the suspended load show comparable transport patterns for the 400 μm fraction see Figures 4.10 and 4.11. A similar recirculation is visible in Borndiep, and at the northern end of the channel export of the 400 μm fraction is visible.

4.3.2 Tide, wind and wave-driven transport

By comparing the transport fields for the tide-only to the tide, wind and waves scenario, the effect of the waves becomes clearly visible. The area surrounding the ebb tidal delta and at the north-eastern tip of Terschelling is exposed to the dominant wave conditions (see Figure 2.2). In this area, strong wave breaking results in wave driven currents which transport the sediment. The transports are thus not confined to the channels as they were in the tide only scenarios.

Just like in the tide-only scenario, each of the four fractions is predominantly transported in suspension. Only for the larger fractions does bedload transport show a significant contribution to the total transport. The effect of the waves on the transport patterns becomes less pronounced when the grain size increases. By comparing Figures 4.10 and 4.18, it is evident that the patterns of 400 μm fraction remain relatively unchanged when waves are added. This holds true for both the suspended and the bedload transport. Therefore, it seems that the coarser fractions are less influenced by wave driven transport. This may be due to the fact that the transport of the coarse fractions is restricted to the relatively deep channels, where the flow velocities are large. In these areas where the water depth is large, sand on the bottom does not experience much wave action. This also seems to be the case for the other fractions in the channels: adding wind and waves does not significantly affect their transport.

Along the island tips, wind and wave action drive a residual transport into the basin for all fractions. At the northern end of the ebb tidal delta, a strong bypassing mechanism is present especially for the 100 μm and 200 μm fractions (Figures 4.13 and 4.11). The 300 μm and 400 μm fractions also show a bypassing behavior at the northern and eastern side of the ebb tidal delta. However at the western end, the transport is very weak for these coarse fractions. The currents there appear to be too weak to result in a significant transport. At the northeastern side of the Kofmansbult, the breaking waves give rise to a residual transport in southeast direction, for all fractions.

The bedload transport of the coarse fractions shows similar patterns as the suspended transports (Figures 4.17, 4.16, 4.19 and 4.18).

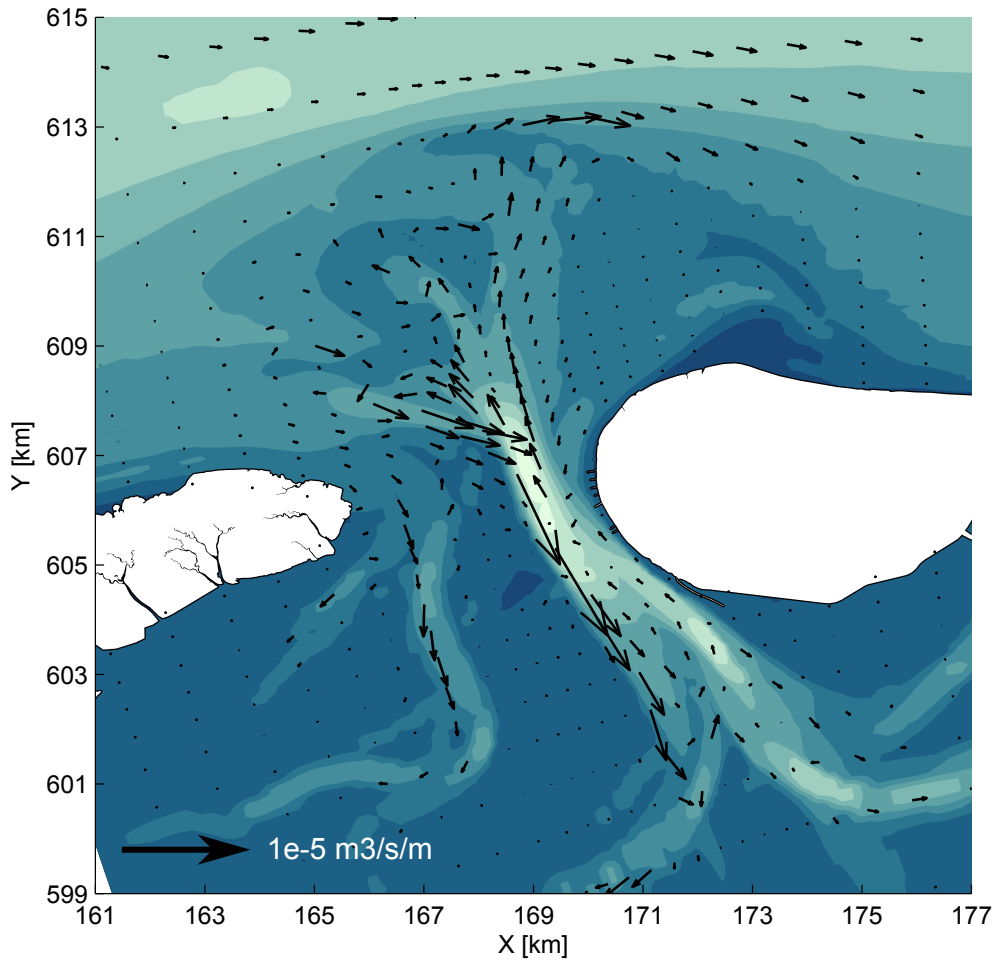


Figure 4.4: Tide driven suspended transport of the $D_{50} = 100\mu\text{m}$ fraction, tide-averaged

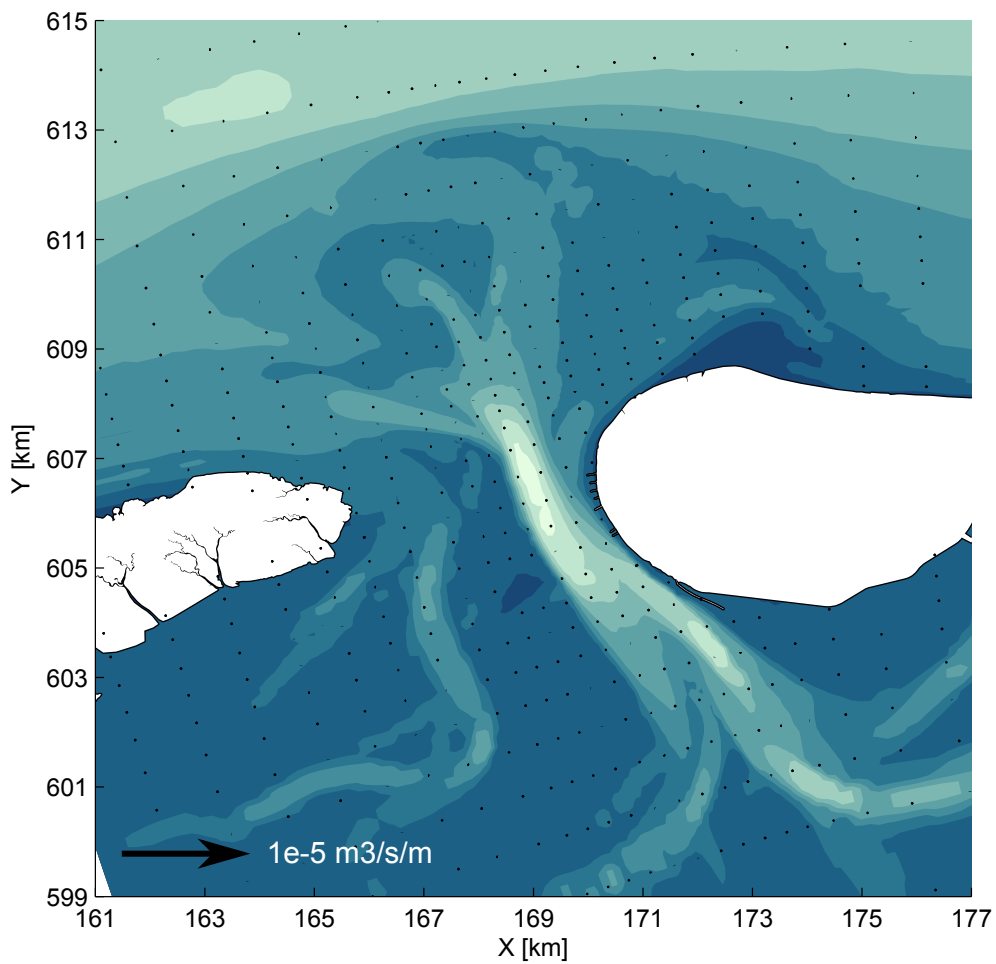


Figure 4.5: Tide driven bedload transport of the $D_{50} = 100\mu\text{m}$ fraction, tide-averaged

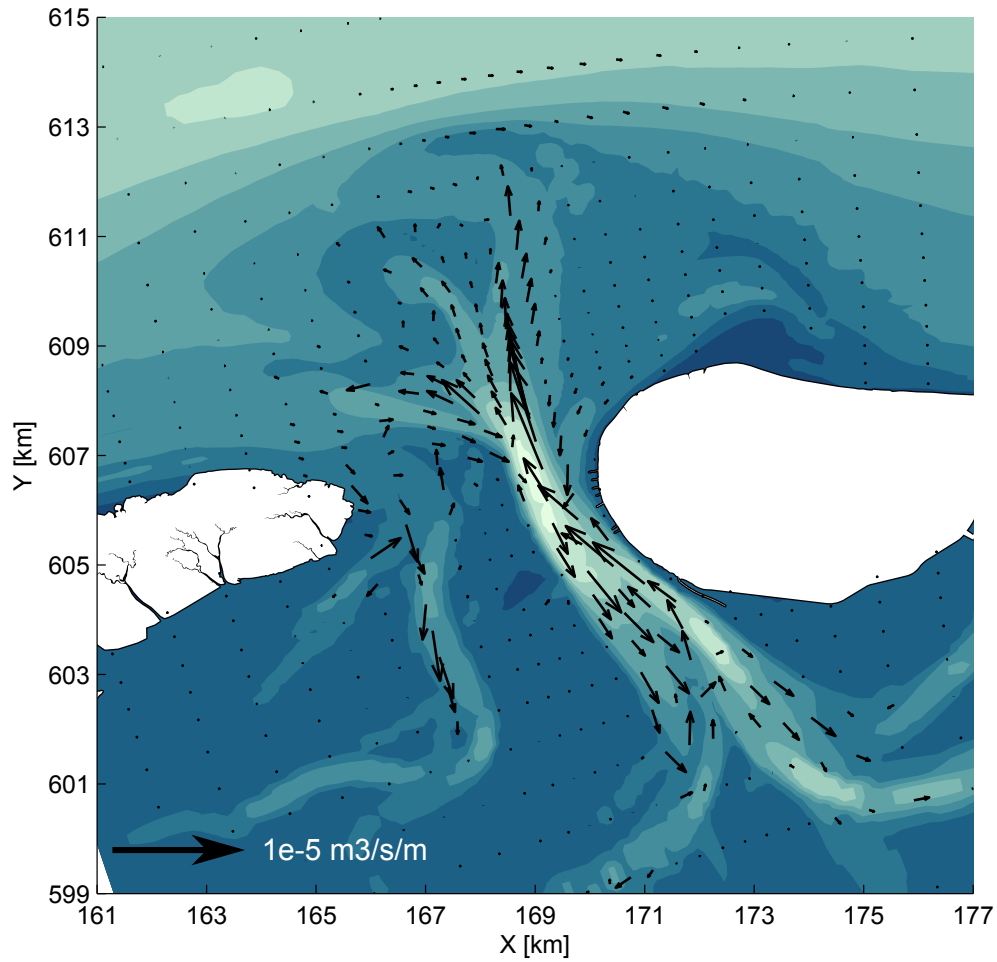


Figure 4.6: Tide driven suspended transport of the $D_{50} = 200\mu m$ fraction, tide-averaged

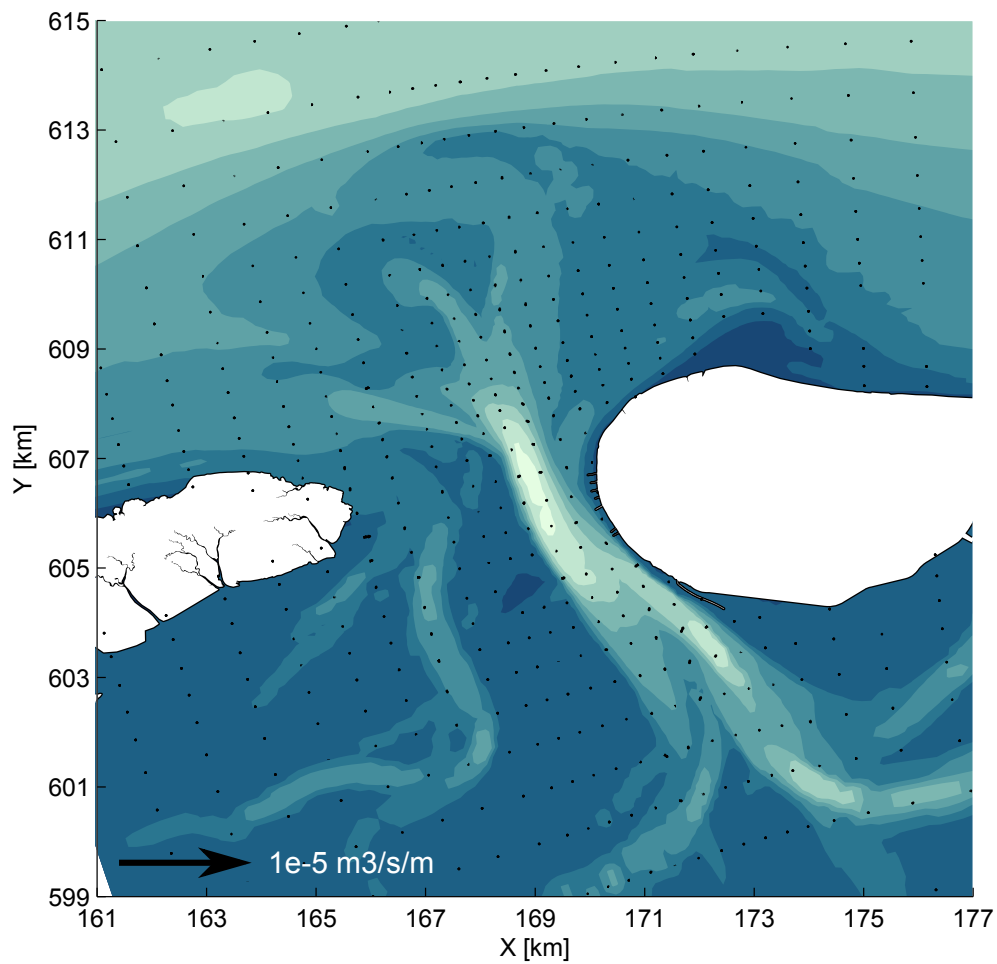


Figure 4.7: Tide driven bedload transport of the $D_{50} = 200\mu m$ fraction, tide-averaged

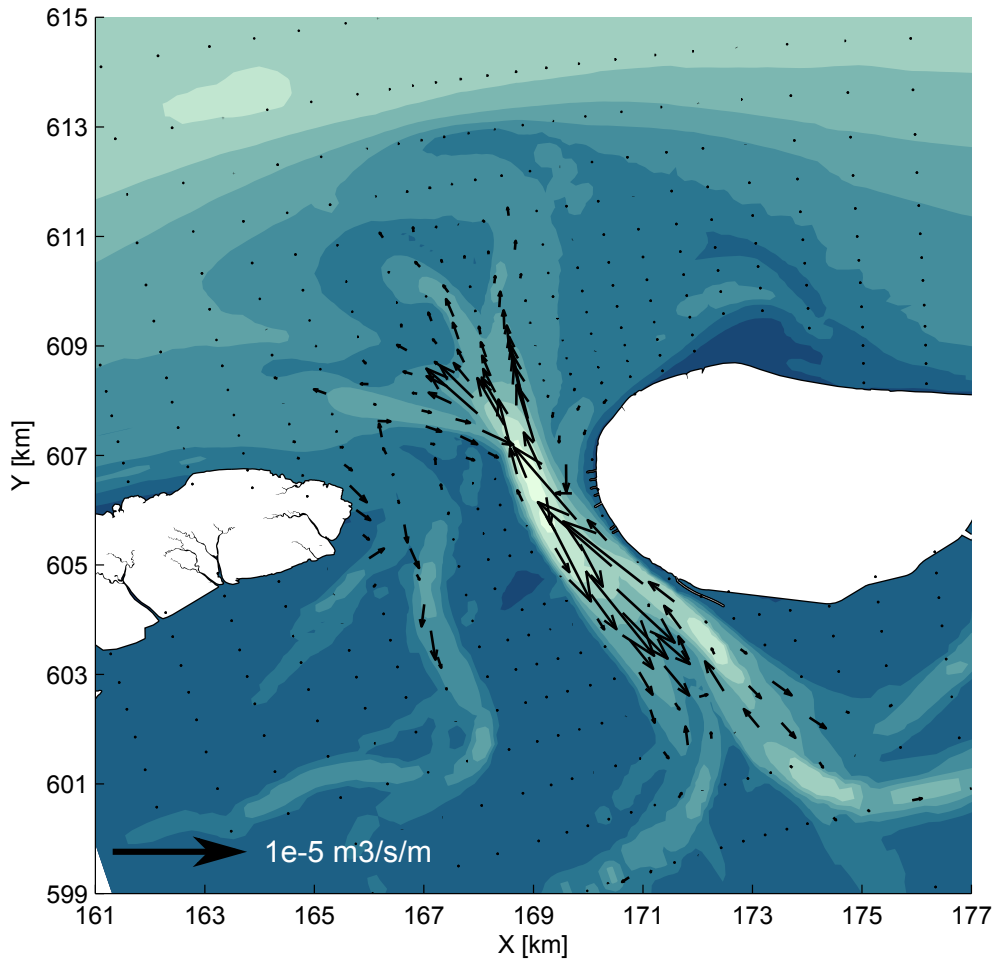


Figure 4.8: Tide driven suspended transport of the $D_{50} = 300\mu\text{m}$ fraction, tide-averaged

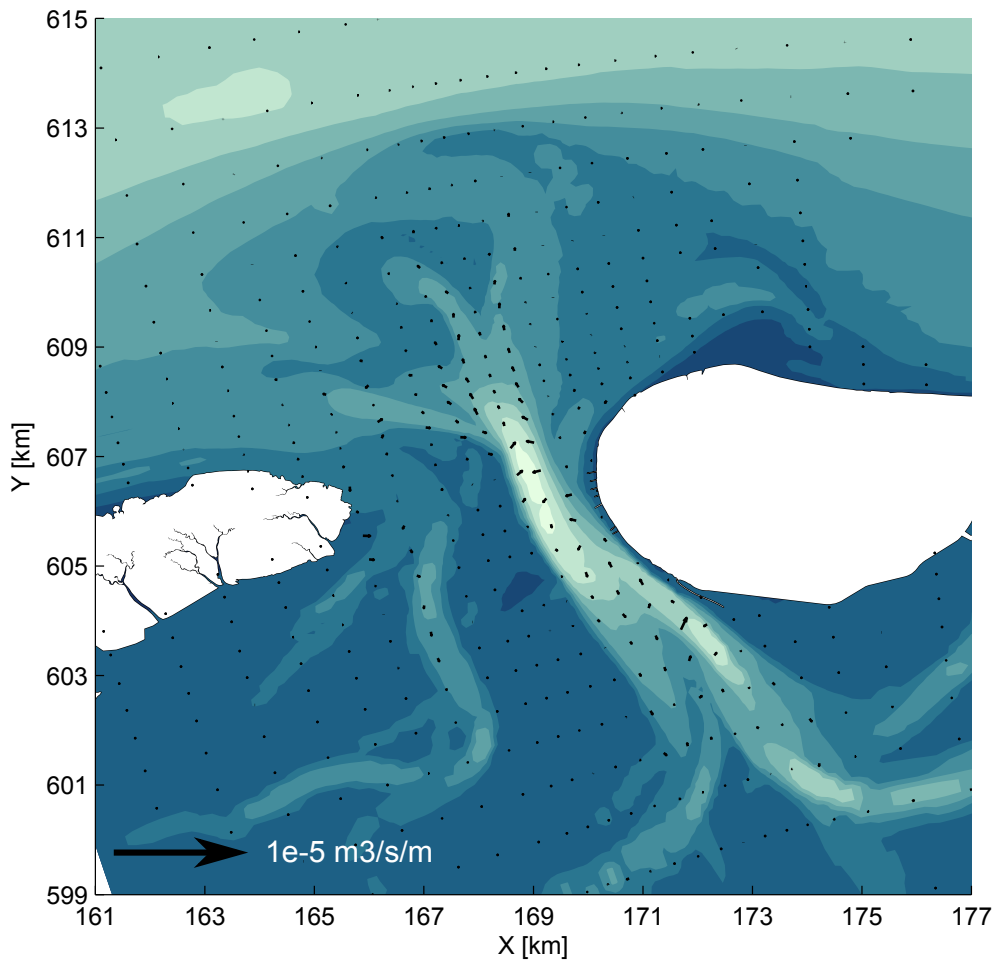


Figure 4.9: Tide driven bedload transport of the $D_{50} = 300\mu\text{m}$ fraction, tide-averaged

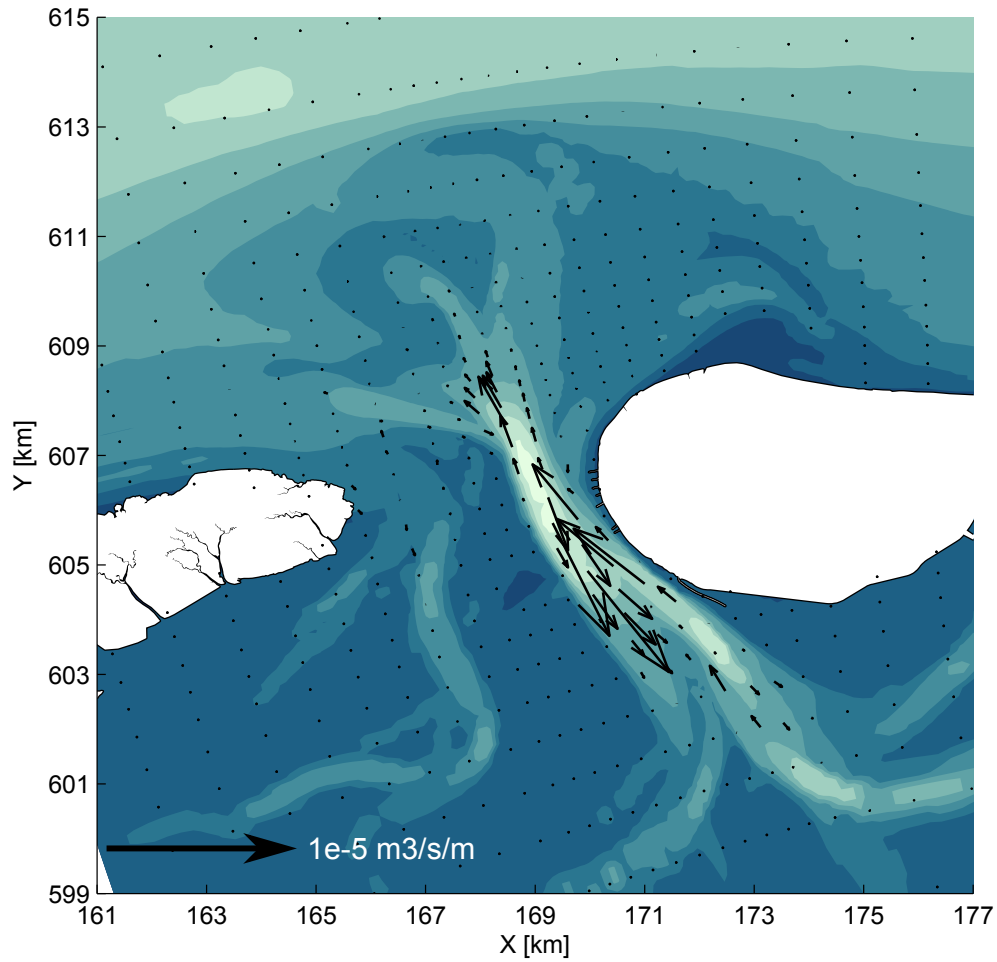


Figure 4.10: Tide driven suspended transport of the $D_{50} = 400\mu\text{m}$ fraction, tide-averaged

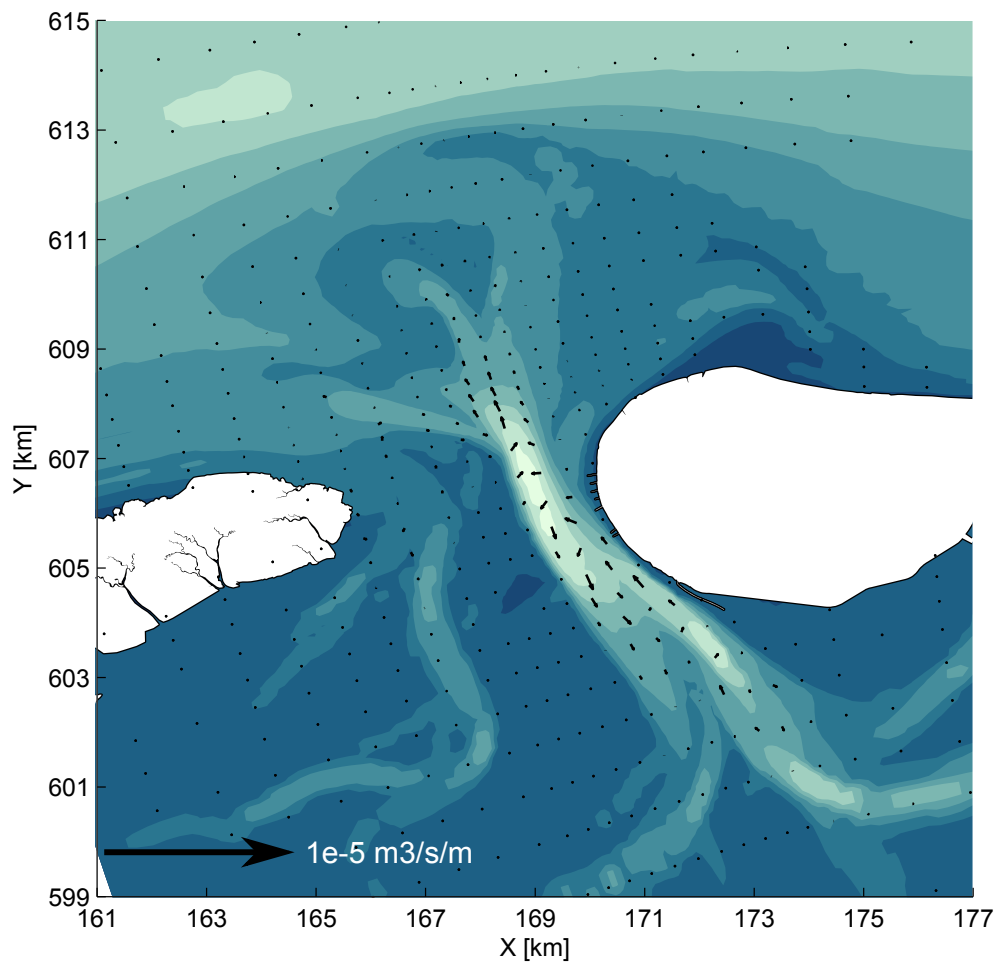


Figure 4.11: Tide driven bedload transport of the $D_{50} = 400\mu\text{m}$ fraction, tide-averaged

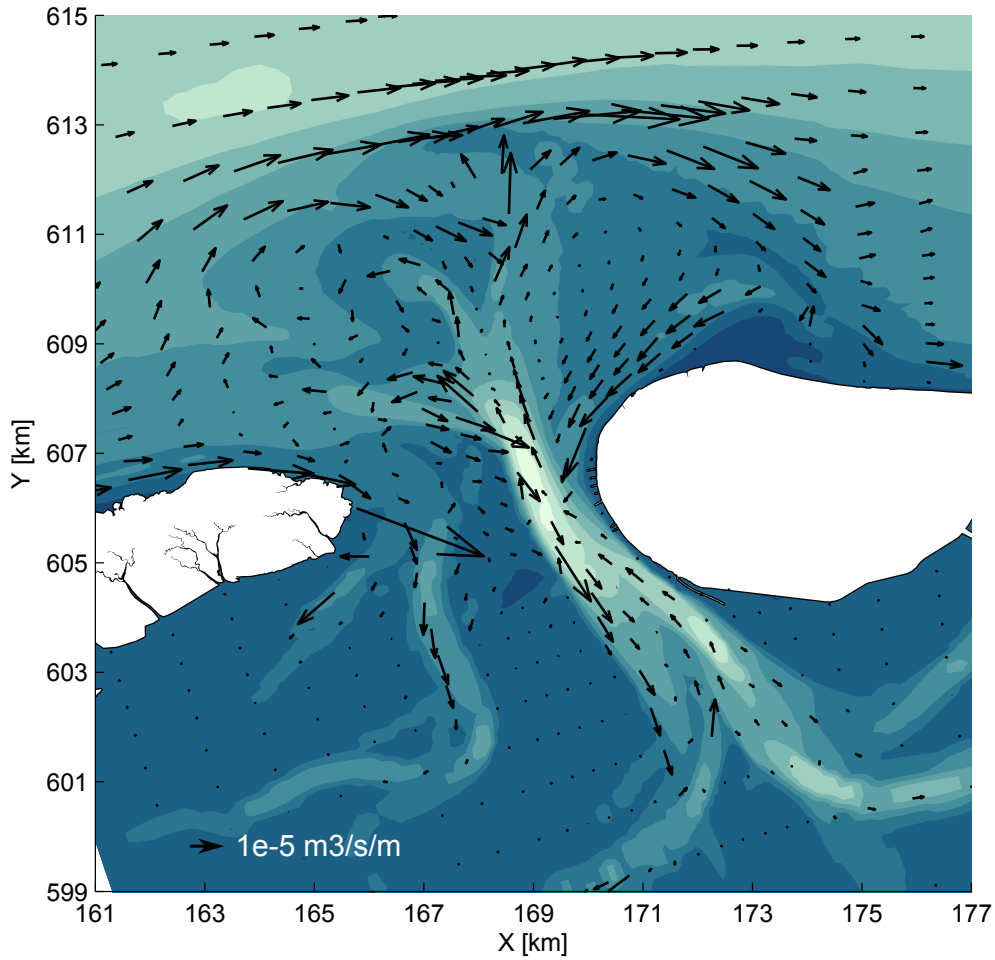


Figure 4.12: Tide, wave and wind driven suspended transport of the $D_{50} = 100\mu\text{m}$ fraction, tide-averaged

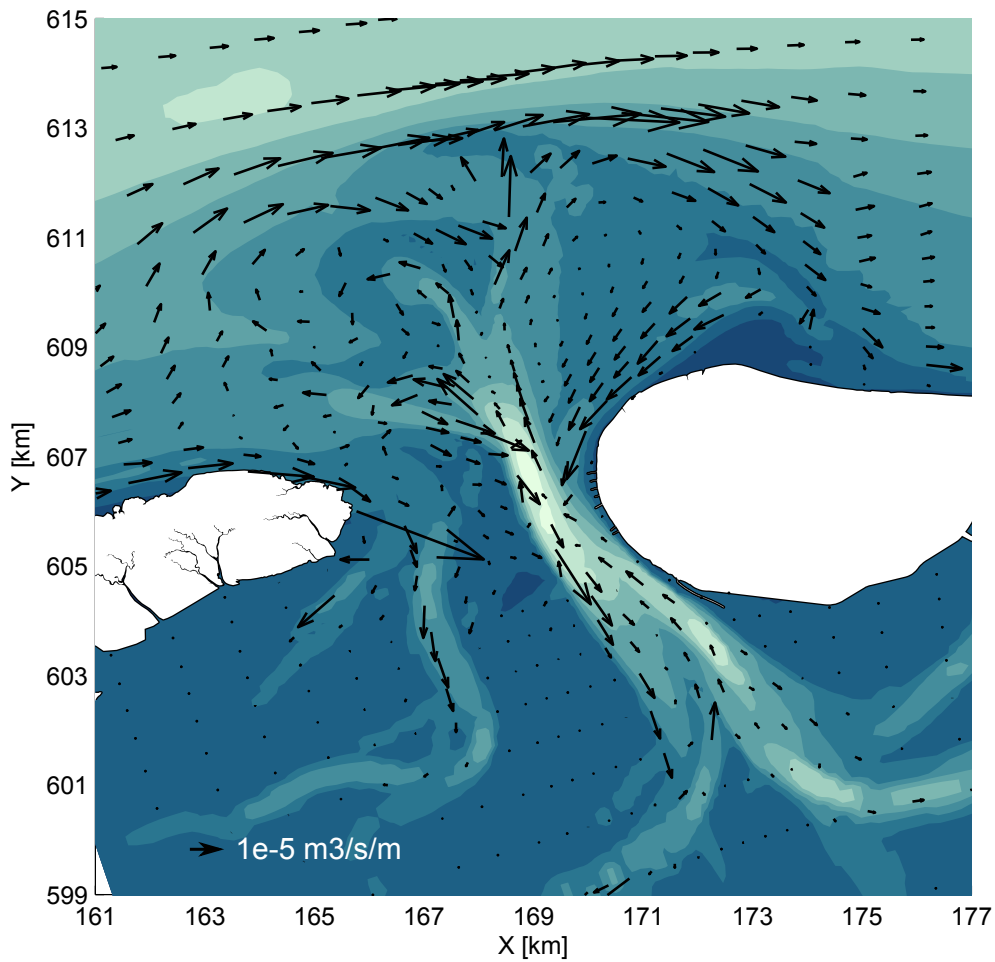


Figure 4.13: Tide, wave and wind driven bedload transport of the $D_{50} = 100\mu\text{m}$ fraction, tide-averaged

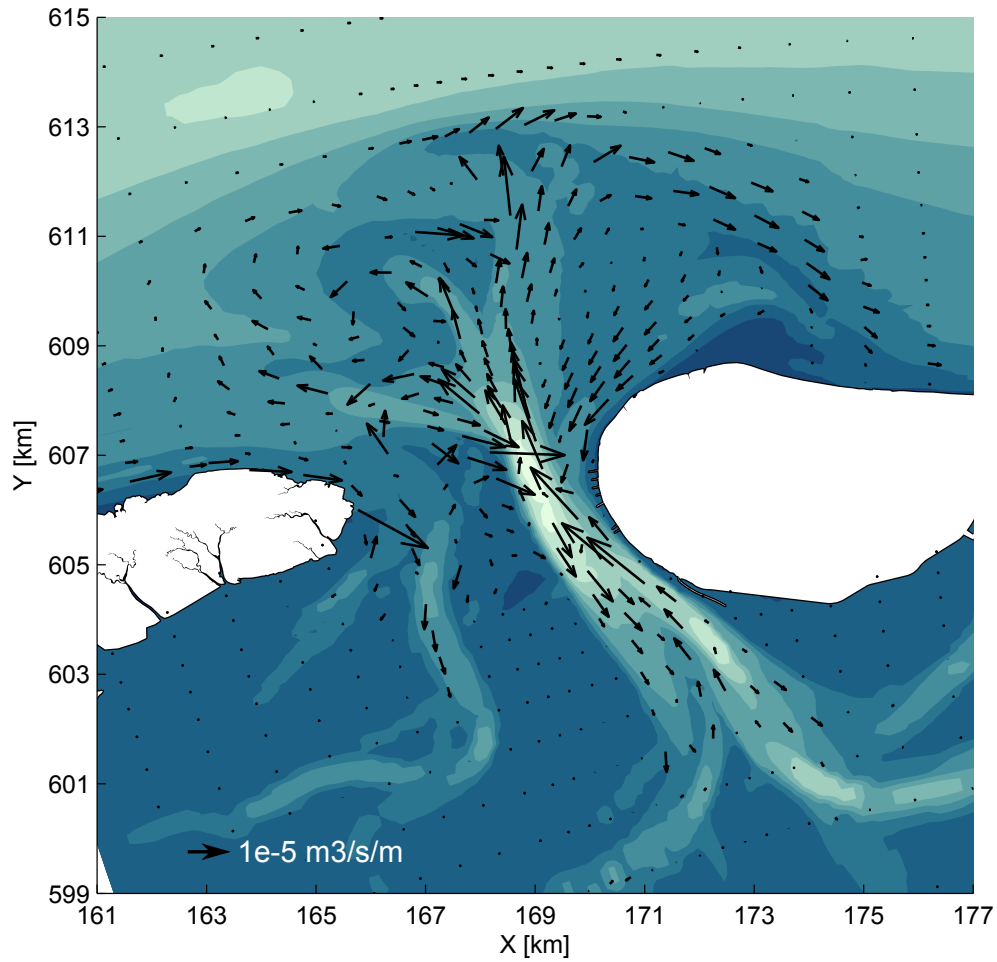


Figure 4.14: Tide, wave and wind driven suspended transport of the $D_{50} = 200\mu\text{m}$ fraction, tide-averaged

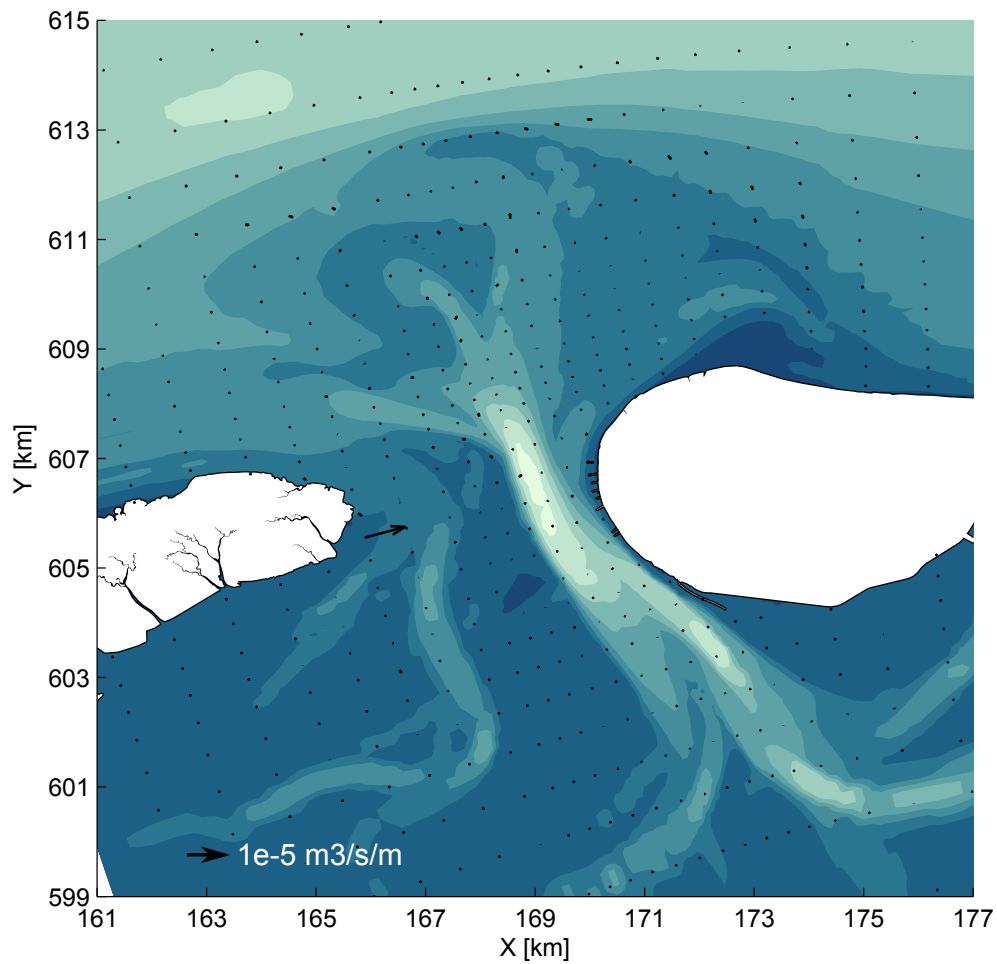


Figure 4.15: Tide, wave and wind driven bedload transport of the $D_{50} = 200\mu\text{m}$ fraction, tide-averaged

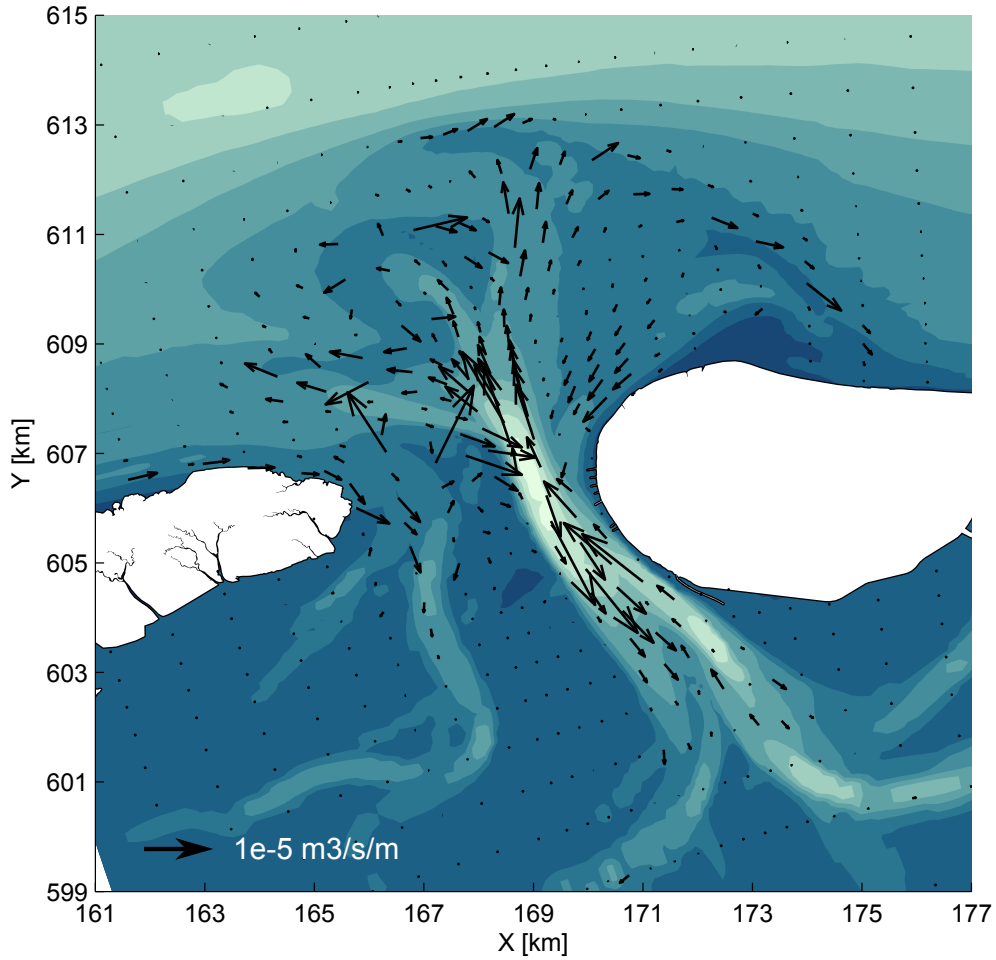


Figure 4.16: Tide, wave and wind driven suspended transport of the $D_{50} = 300\mu\text{m}$ fraction, tide-averaged

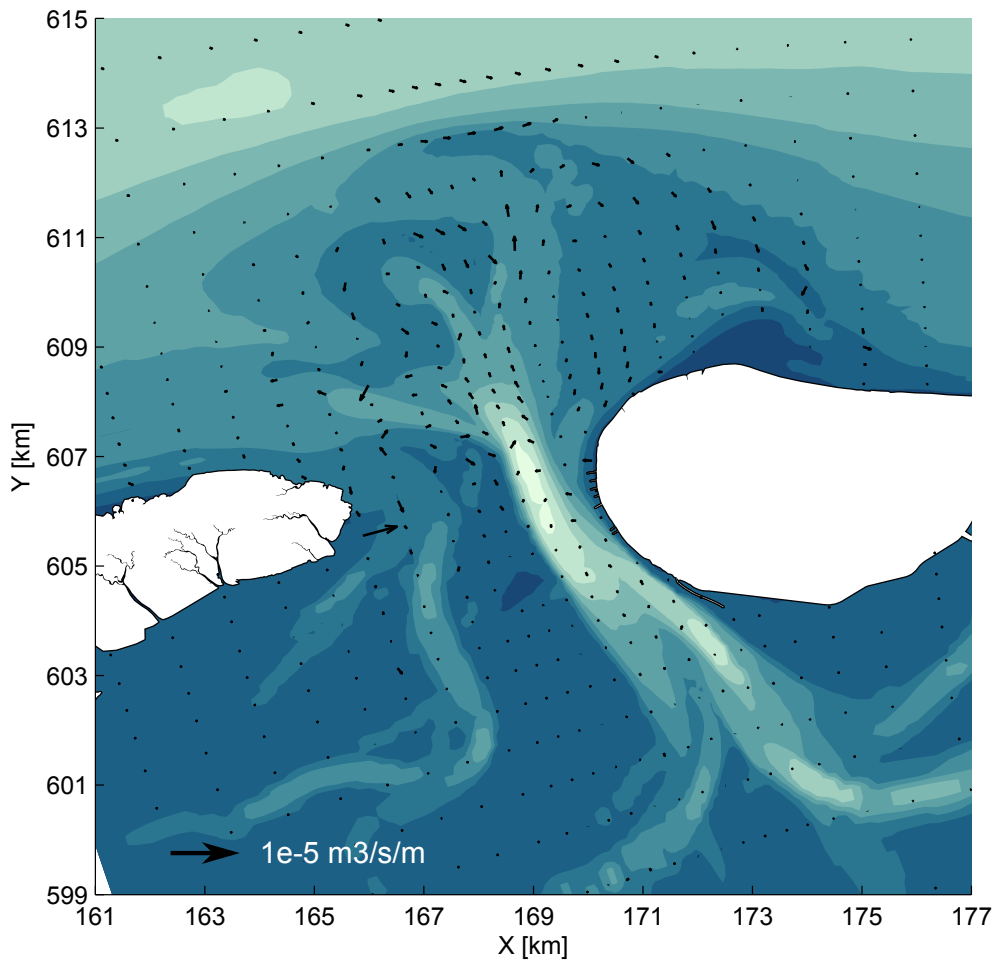


Figure 4.17: Tide, wave and wind driven bedload transport of the $D_{50} = 300\mu\text{m}$ fraction, tide-averaged

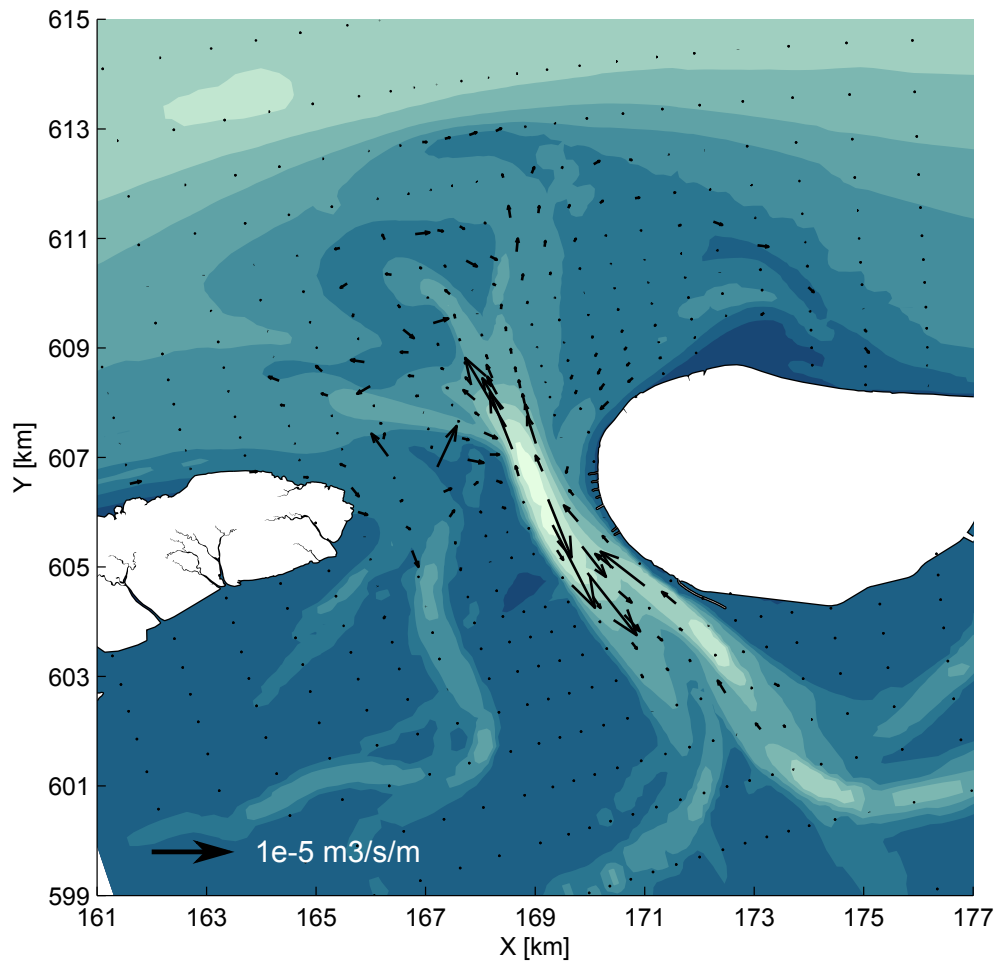


Figure 4.18: Tide, wave and wind driven suspended transport of the $D_{50} = 400\mu\text{m}$ fraction, tide-averaged

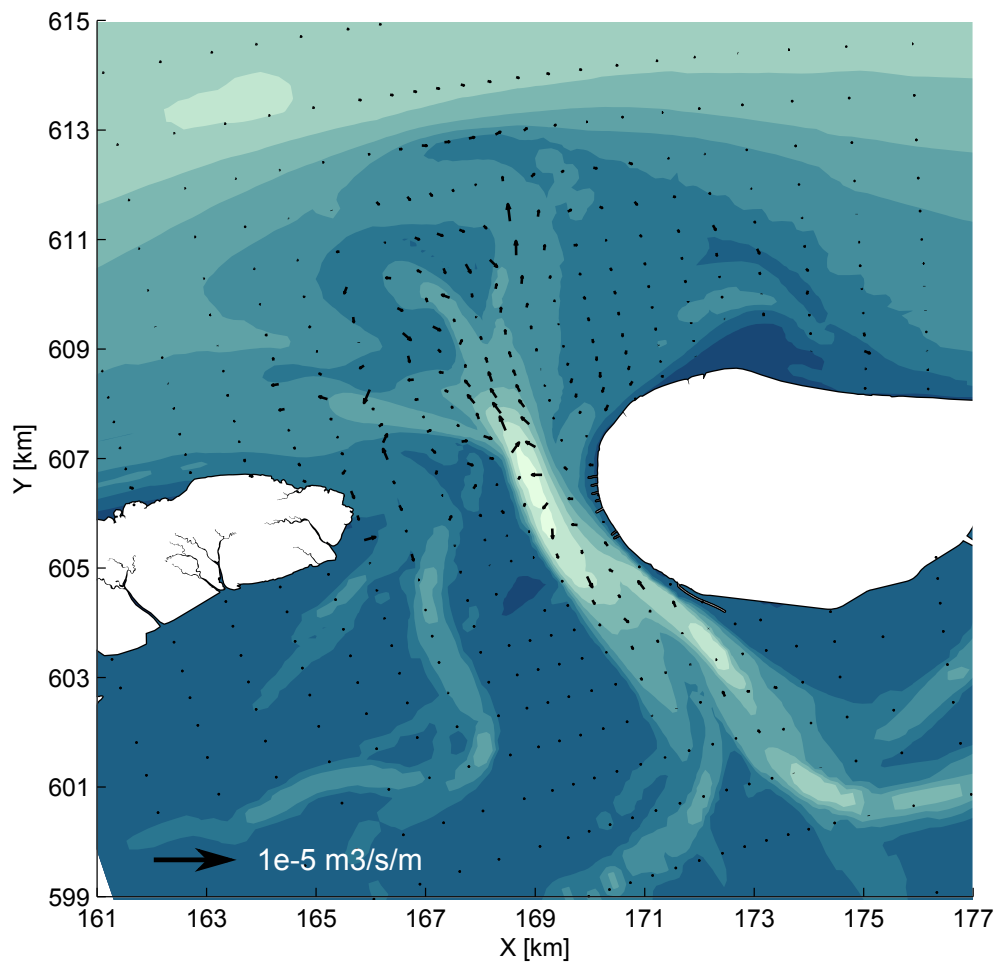


Figure 4.19: Tide, wave and wind driven bedload transport of the $D_{50} = 400\mu\text{m}$ fraction, tide-averaged

4.4 Proposed locations

Eight different nourishment locations are evaluated in this study, see Figure 4.20. At some of the locations mega nourishments are possible, with a size of $20 \cdot 10^6 m^3$, comparable to the sand engine. At other locations regular nourishments will be evaluated, since larger sizes don not fit. The nourishments are designed with the help of the Boskalis Production Department.

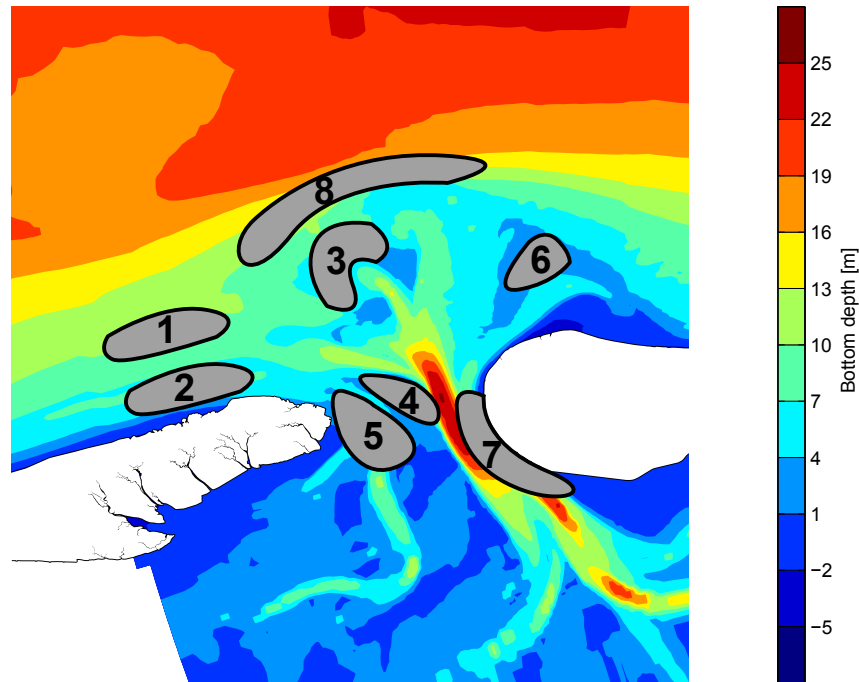


Figure 4.20: 8 nourishment locations

The main characteristics of the nourishments are:

1. Mega foreshore nourishment Terschelling

A mega nourishment of $20 \cdot 10^6 m^3$ is designed here at a distance of about $2 km$ off the shore of Terschelling. In between the $5 m$ and $12 m$ depth contours a layer of $3 m$ of sand is placed. Therefore most of the sediment can be placed by dumping.

2. Beach nourishment Terschelling

A beach nourishment of $5 \cdot 10^6 m^3$ is modeled. This is a large volume for a beach nourishment, which are on average $0.5 \cdot 10^6 m^3$ in The Netherlands HANSON *et al.* [2002]. The sediment is placed around mean sea level, a layer of $1.5 m$ is applied. For the construction of this nourishment the sediment has to be pumped on the beach through pipelines, on the beach bulldozers will work to spread out the sediment.

3. Pilot nourishment location, Kofmansbult

This location is included because Rijkswaterstaat is planning a pilot nourishment there, which will be executed in 2018. This location is selected, not necessarily because it

is the best location for a nourishment, but because it is expected that we can learn valuable lessons from it. Nourishments at a location like this on an ebb tidal delta have not been performed before. It will be interesting to see what the effect of this nourishment on the wave breaking will be and how the channel cutting through the Kofmansbult will respond. Just as in the pilot, $5 \cdot 10^6 m^3$ sand is placed in the model at this location. The maximum height of the nourishment here is $-4.5mNAP$. Therefore the sand will be placed by a combination of dumping and rainbowing.

4. Nourishment in between Boschgat and Borndiep

For this location a $5 \cdot 10^6 m^3$ nourishment is designed. The nourishment is placed up to $0mNAP$. Due to the limited depth in this area it has to be placed by pumping through pipelines.

5. Nourishment in Boschgat

The channel will be filled up to a depth of $-3.5mNAP$. $5 \cdot 10^6 m^3$ is placed here. This will be done through a combination of dumping and rainbowing.

6. Mega nourishment at Bronrif

This is a mega nourishment of $20 \cdot 10^6 m^3$. A large sand flat is created up to $0mNAP$. Due to the limited depth over large distances, the sand has to be placed by pumping through pipelines. This nourishment provides a large intertidal area, which can be used by birds and seals.

7. Channel-wall nourishment

A volume of $2.5 \cdot 10^6 m^3$ of sand is placed at the eastern channel wall of Borndiep, at the southwest corner of Ameland. It is placed below $6.5mNAP$ and can therefore be placed by dumping the hopper. Rijkswaterstaat planned this nourishment to be executed this year. In the past multiple channel-wall nourishments have been carried out at this location.

8. Mega ebb tidal delta nourishment

At this location, on the northern end of the ebb tidal delta a mega nourishment of $20 \cdot 10^6 m^3$ is designed. The highest point of the nourishment is about $5mNAP$ deep, therefore most of the nourishment can be placed through dumping. At the shallower areas the sand will be placed by dumping half of the load and rainbowing the rest.

4.5 Nourishment location evaluation

Based on the technological requirements and the ecological and social impact assessments above, the 8 nourishment locations, see Figure 4.20 are rated, see Table 4.1.

The construction costs rating is based on the cycle time of one cycle and the dredging method that is used, see Sections 4.4 and 4.1.1. One cycle includes the time required to fill up the hopper, sail to the nourishment location, unload the sand and sail back to the borrow area. The sailing distance is determined from the borrow area, assuming this is area M9J, see Section B. The sailing route is via Westgat, since a loaded TSHD of the type Shoalway can only enter the tidal inlet system via this channel.

Table 4.1: Evaluation matrix for the nourishment locations. ++ In the table stands for the shortest distance, the most positive impact or the lowest cost and – for the longest distance, highest costs or most negative impact. -/+ Indicates that there is a negative impact, however extra ecological value can be created by placing the nourishment as explained in Section 4.1.2.

Location	Distance	Construction Costs	Ecological Impact	Social Impact
1	-	0	0	-
2	-	--	0	--
3	++	+	-	0
4	-	--	-/+	0
5	-	0	-	-
6	++	--	0/+	0
7	--	0	-	-
8	++	++	--	0

4.6 Model implementation

In the model the nourishment is placed on top of the existing bathymetry. This is done by specifying the nourishment layers in thickness files, in these files the layer thickness is $0m$ everywhere, except at the nourishment, where the thickness is prescribed based on the nourishment characteristics. The maximum under layer thickness is $1m$. Applying multiple under layers (in which the sediment is well-mixed), allows for armoring to take place. In this way the fine fractions, which are buried deeply enough under coarser fractions, are not just simply washed out of the bottom, but will remain there until further erosion occurs.

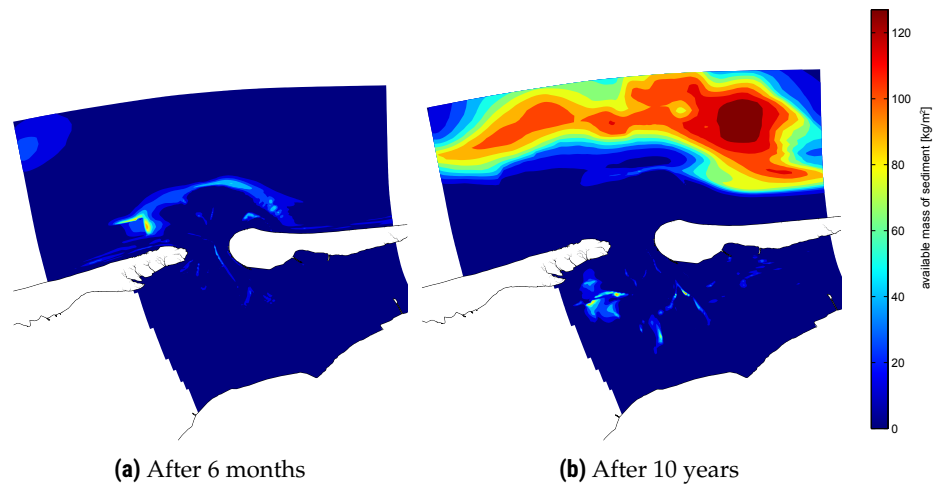
The fractions in the nourishment layers are labeled separately from the fractions in the rest of the domain. In order to create a realistic nourishment, the two previously mentioned grain size distributions of the borrow area are approximately reproduced in the model. These distributions are schematized into four sediment fractions, which are specified in the model by a minimum and maximum sediment diameter and loguniformly distributed, see Table 4.2. Based on these distributions Delft3D determines the D_{50} , D_{10} and D_{90} for each fraction, which it uses in the calculations, the values are given in Table 4.2. The corresponding grain size distributions graphs are shown in Figure 4.22. The fine composition is the most representative for the borrow area. This one will be implemented in the model for all eight locations. The coarse one will only be applied for Location 1, in order to evaluate the effect of a different composition.

However when model runs are performed with the nourishment fractions on top of the existing bathymetry, a problem arises at one of the boundaries. In the model results, the finest nourishment fraction arises at the western boundary, see Figure 4.21. At the end of the simulation period, such a large amount of the nourishment fraction has entered the model domain at the boundary, that it cannot be distinguished anymore from the real nourishment fraction. This issue appears to be the result of the fact that Delft3D tries to keep the bottom level and the bottom composition constant at the boundaries. The program uses the first specified layer to do this, which is a nourishment layer in this case. It does not understand that this first layer is empty at the boundaries. Therefore the nourishment fractions can arise at the boundaries and are subsequently transported throughout the model by the currents.

Table 4.2: Nourishment compositions

Sediment fraction [μm]	Proportion [%]	D_{50} [μm]	D_{10} [μm]	D_{90} [μm]
FINE COMPOSITION				
63 - 125	19.5	89	67	117
125 - 180	51.6	150	130	174
180 - 250	13.0	212	186	242
250 - 500	15.9	354	268	467
COARSE COMPOSITION				
63 - 180	10.1	107	70	162
180 - 250	8.7	212	186	242
250 - 355	36.8	298	259	343
355 - 500	44.4	421	367	483

This issue is solved by specifying a top layer, consisting of only the regular fractions, with a thickness of $1m$ everywhere except at the nourishment location, there it is $0m$.

**Figure 4.21:** Boundary issue

4.7 Hypotheses

Following the approach of ELIAS [2017], the residual transport patterns discussed in Section 4.3 are analyzed in order to formulate hypotheses for the different nourishment designs. At Location 1 the fine and coarse composition are implemented and therefore both will be evaluated. At the other locations we only look at the fine composition. The sand fractions in the model domain ($D_{50} = 100, 200, 300$ and 400) are different from those in the nourishment, since they were imposed previously in the Bed Composition Generation, see Section 3.4. Therefore the hypotheses regarding the movement of the different nourishment fractions

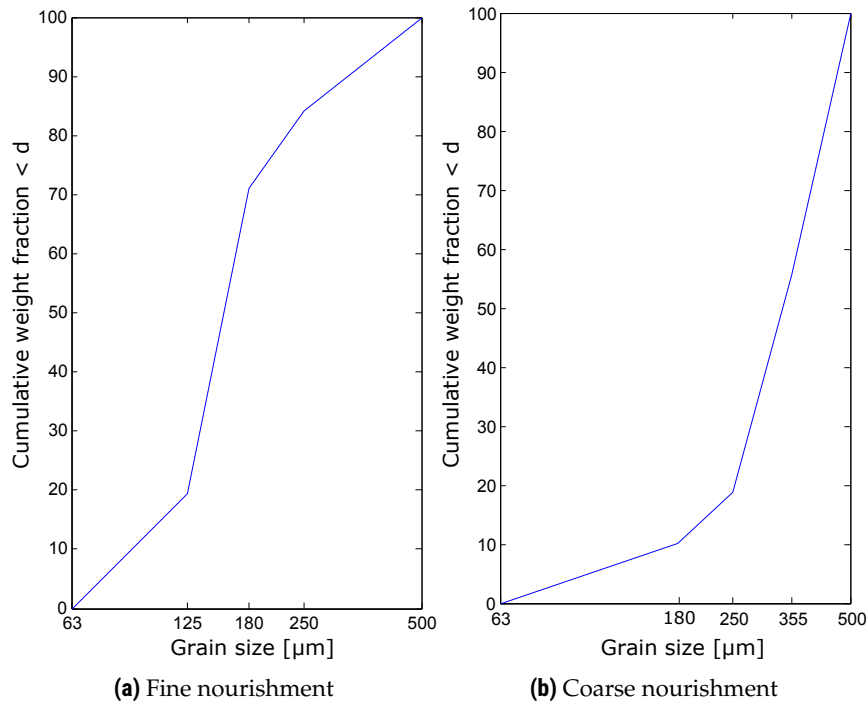


Figure 4.22: Modeled grain size distribution

are based on the residual transport patterns of the fractions in the domain with the most similar D_{50} values.

As noticed previously, suspended transport is the dominant transport mode for each of the sediment fractions. For the coarsest fractions some bedload transport can be distinguished, however its contribution is minimal and the patterns are comparable to the suspended transport. Therefore the hypotheses below are based on the suspended transport.

1. Foreshore nourishment Terschelling

At this location a coarse and a fine nourishment are simulated.

Fine composition For all sediment fractions, there is hardly any influence of the tide. The change in bathymetry may give rise to some increased sediment transport, due to the larger flow velocities on top of the nourishment. However it is expected to be quite stable in the tide only scenario.

When the effect of wind and waves is added, this changes. The longshore drift will transport the sediment towards the inlet, for the coarser fractions this will happen more slowly. Closer to the inlet, it is likely that most of the $63 - 125\mu\text{m}$ and the $125 - 180\mu\text{m}$ fractions bypass the inlet via the northern end of the ebb tidal delta. However some of these sediment fractions will be imported into Borndiep, via the tide driven flow in Westgat. Especially the smallest fraction is then likely to be transported into the basin. The coarser fraction will mainly be exported through Akkepollegat or over the Kofmansbult, towards the northern and northwestern end of the ebb tidal delta. From there the sediment will then be transported towards the Ameland coast,

via the northern end of Bornrif.

For the 180 – 250 μm and 250 – 500 μm fractions a bypassing mechanism seems less evident. When these fractions come closer to the inlet, they are likely to be transported in northwestern direction, therefore they are less likely to arrive in Westgat than the other fractions. From the West of the ebb tidal delta they will bypass the inlet, but much slower than the finer fractions. At Kofmansbult the patterns show some transport in southeast direction, into Akkepollegat. From there the coarse sediment is expected to be exported relatively fast again and then it will follow its way towards the Ameland coast.

Coarse composition With this composition the finest fractions is coarser than in the previous one, moreover the proportion of relatively coarse sediment is much larger. Therefore this nourishment will be less mobile and for instance the bypassing will occur on larger time scales. Furthermore, the fine sediment buried below other layers is less likely to be moved, due to an increased armoring by the coarser fractions.

2. Beach nourishment Terschelling

A nourishment close to the shore of Terschelling is expected to follow a significantly different transport pathway compared to further offshore. Again for this nourishment the tide is initially of minor importance. The waves however result in a transport towards Boschgat, along the tip of Terschelling. From there most of the sediment will be imported into the basin via Boschgat by the tide driven flood currents. Therefore it seems likely that a nourishment at this location will feed the basin. Some of the sediment may end up in Borndiep, either via Westgat or transported over the shallow area in between Boschgat and Borndiep, see also the tracer study by ELIAS [2017].

The coarse fractions are less likely to be transported over this shallow area, due to the low flow velocities locally. Besides this the different fractions show similar pathways here, however for the coarse fractions the time scales will be larger. Especially the 250 – 500 μm will move slowly, since the transport of this fraction is mostly confined to the Borndiep channel, see Section 4.3.

3. Pilot nourishment location, Kofmansbult

The tidal currents at this location will transport the sediment fractions in offshore direction. The 63 – 125 μm placed on the east side of Kofmansbult shows a transport with the tide towards Akkepollegat in the east, the other fractions don not show this movement.

When the influence of waves is included, the offshore tidal transport is counteracted. At the eastern part of the Kofmansbult, waves drive a residual transport towards the Akkepollegat, from where the sediment is exported over the ebb tidal delta and subsequently transported in southeast direction towards Ameland. In the southwestern part, a net transport towards the south is observed and from there towards the west, from where it will follow the same pathway as described for Nourishment 1. This seems to hold for all fractions.

Differences in the transport patterns between the fractions can be observed in the middle of the Kofmansbult. There the 63 – 125 μm fraction is expected to move towards the south, from where part of it will be circulated back up north. The coarser fractions will move more towards the west or southwest from this location and from there

follow the same pathway as described for Nourishment 1.

Again for this nourishment the 250 – 500 μm fraction is expected to remain much more stable than the other fractions.

4. Nourishment in between Boschgat and Borndiep

A nourishment at this location may reduce the transport from Boschgat over the shallow area, towards Borndiep. As a result the erosion of the Boschplaat may be counteracted. From this location transport of the 63 – 125, 125 – 180 and 180 – 250 μm fractions will take place towards Borndiep, through Westgat and over the top of the nourishment, by the tide driven currents. The 250 – 500 μm fraction will hardly be affected by the tide at this location.

Wind and waves do not seem to have a significant effect on the residual transport patterns of the 63 – 125 μm fraction. For the three coarser fractions it is expected to result in a transport from on top of the nourishment in northeastern direction towards Westgat. Furthermore, wind and waves may increase the transport from the nourishment directly into Borndiep, for all fractions.

Due to the low transport capacity at this shallow area, the 250 – 500 μm fraction is again expected to remain relatively stable here.

5. Nourishment in Boschgat

By partly filling up Boschgat up to -3.5mNAP it is expected that less sediment will be transported towards the basin by the tide driven currents. In this way less sand will be removed from the Boschplaat. Therefore this alternative may also counteract the erosion at Boschplaat.

A part of the 63 – 125, 125 – 180 and the 180 – 250 μm fraction will be transported by the tidal currents from this location into the basin, through Boschgat. Another part may end up in Borndiep through Westgat, or over the top of the shallow area between Boschgat and Borndiep in the same way as explained for Nourishment 4.

Again, not much movement of the 250 – 500 μm fraction is expected here.

6. Nourishment at Bronrif

Due to the low transport capacity locally, all fractions are expected to be relatively stable at this area.

At Bornrif the effect of the tide is negligible for the four fractions. The residual transport locally is driven by wind and waves. These result in a circulating pattern in clockwise direction around the edges of Bornrif. This circulation will be much weaker for the coarser nourishment fractions and the 250 – 500 μm fraction will probably hardly move. The other fractions are expected to move to the north, following the residual transport through Bornrif and Akkepollegat, when situated in the west. In the north the movement is in southeast direction, towards Ameland. Nourishment fractions in the southeast will be transported towards Borndiep. Therefore some of the sediment is expected to end up in Bornrif, while the rest is transported towards Ameland, via the edges of Bornrif. The sediment in the middle of Bornrif will remain stable.

7. Channel-wall nourishment

In this nourishment the $250 - 500\mu m$ fraction will be much more mobile than at the other locations. The effect of waves and wind is expected to be small compared to the tidal forcing in this deep channel. Since a recirculation in the channel is observed for all fractions, with the flood dominated transport in the west and the ebb dominated transport in the east of the channel, the nourishment fractions may move back and forth through the channel for a while. The $D_{50} = 100\mu m$ fraction shows a residual transport into the basin. Therefore import of the $63 - 125\mu m$ and to a lesser extent of the $125 - 180\mu m$ nourishment fractions is expected.

Most of the coarsest two nourishment fractions will be exported out of Borndiep, by the ebb dominant transport via Akkepollegat, over the Kofmansbult and to some extent through Westgat. Subsequently the fractions are expected to be transported towards Ameland.

8. Mega ebb tidal delta nourishment

With this mega nourishment the wave sheltering function of the ebb tidal delta may be reinforced. The nourishment fractions are expected to behave quite the same as for the pilot, at Location 3. This nourishment is located a bit more offshore and it will therefore experience loss of the tidal flow over the Kofmansbult. However further offshore a strong residual transport is present, which will especially affect the fine nourishment fractions.

However, this mega nourishment may have important consequences for wave breaking around the ebb tidal delta. Therefore the model results featuring this nourishment may differ from these expectations, which are based on the undisturbed bathymetry.

The nourishment designs discussed in Chapter 4 are implemented in the model discussed in Chapter 3, the results are presented here. Furthermore, they will be compared to the hypotheses presented in Section 4.7. First the results for the different nourishment locations are treated. Hereafter the model outcomes for the two nourishment compositions at Location 1 are compared.

5.1 Effect of the nourishment location

Figures 5.1, 5.2 and 5.3 show the total percentage of the nourishment sand in the transport layer, the upper $0.5m$, after a morphological period of 10 years. On the left the results are shown for the tide only scenario. In the figures on the right the sediment transport is driven by tide, wind and waves. Figures 5.4 and 5.6 to 5.12 show the same results, but then for the different sediment fractions separately. This gives a clear picture of the destination of the different nourishment fractions after 10 years.

However, below the transport layer nourishment sand is present as well. To quantify where the fractions end up after a period of 10 years, the Ameland Inlet is divided in separate morphological units, see Figure 5.13. For these different units the fractions in all layers are added up and divided by the total volume of the nourishment fraction, see Table 5.1 and Figure 5.19. In Figures 5.14, 5.15, 5.16 and 5.17 this is displayed in pie charts for all eight nourishment locations, for each fraction separately. The percentage of the total nourishment volume ending up in the morphological units is also determined and displayed in the table and in the pie charts in Figure 5.18.

5.1.1 Location 1, mega foreshore nourishment Terschelling

For the smallest fraction, $63 - 125\mu m$, the tidal influence is already limited. It is moved a bit into the direction of the inlet by the tidal flow. The transport of the nourishment fractions is mainly driven by wave forcing. Wave-driven flow results in a bypassing mechanism, through which about a third of this fraction has bypassed the inlet after 10 years, ending up about $25km$ downdrift of the initial nourishment location. By that time also about a third is still in the area of the ebb tidal delta. As soon as the sediment approaches the inlet, a small proportion is imported into the basin, via Boschgat and through Westgat and Borndiep. After 10 years 8% of this fraction is in the basin. According to the model 32% remains

at the Terschelling coast, at the initial nourishment location, armored under the coarser nourishment fractions.

The tidal currents are not strong enough to move the $125 - 180\mu\text{m}$. When waves are taken into account it moves in a similar way as the $63 - 125\mu\text{m}$ fraction, however much slower. According to the model results after 10 years most of the sand is located at the ebb tidal delta, about 1km downdrift of the initial nourishment location. For this fraction there is also some import into the basin via Boschgat and Westgat, however only about 1% ends up there.

After 10 years the $180 - 250\mu\text{m}$ fraction is still bypassing the inlet via the ebb tidal delta by wave driven flow. 57% is located at the ebb tidal delta by that time, the rest is then still at the Terschelling coast. A small amount is transported in the direction of Boschgat, however there is no import yet into the basin.

The coarsest fraction, $250 - 500\mu\text{m}$ remains relatively stable even in the scenario with wave forcing. There is some spreading in the down drift direction and towards the Terschelling coastline.

For most part the model results are in line with the hypotheses, see Section 4.7. However, the $180 - 250\mu\text{m}$ fraction also clearly shows bypassing, which was not predicted. The $250 - 500\mu\text{m}$ fraction does not follow the hypothesized pathway but remains stable.

5.1.2 Location 2, beach nourishment Terschelling

Figure 5.6 shows the model results for the beach nourishment at Terschelling. As hypothesized, the tide only has no influence on the nourishment fractions.

When taking waves into account, the $63 - 125\mu\text{m}$ fraction is mainly imported into the western part of the basin via Boschgat, a small percentage is bypassed to the Ameland coast.

The $125 - 180\mu\text{m}$ fraction behaves in a similar way, however relatively more remains at the Terschelling coastline and less is transported into the basin.

For the $180 - 250\mu\text{m}$ fraction, again less import into the basin takes place. It moves slower and therefore a larger percentage is still feeding the Boschplaat after 10 years.

The $250 - 500\mu\text{m}$ fraction is transported into the direction of Boschgat as well, it folds around the tip of Terschelling, feeding the Boschplaat. According to the model about 95% is still at the Terschelling coastline after 10 years.

The observed model results are in line with the hypotheses, except for the movement of the $250 - 500\mu\text{m}$ fraction, which was expected to be more stable.

5.1.3 Location 3, pilot nourishment Kofmansbult

The tide only already results in bypassing of the $63 - 125\mu\text{m}$ fraction at this location. In the east of the nourishment offshore and eastbound transport is observed. Furthermore, the tide drives an import of some of the sediment into the basin, first via Westgat and later also via Akkepollegat and Borndiep. When waves are included both the bypassing and import of sediment are strongly reinforced. After 10 years the model predicts that 35% is transported to the Terschelling coastline, 53% is in the ebb tidal delta region and 11% is imported. No transport to Ameland is observed.

The tidal influence on the 125 – 180 μm fraction is more limited. Movement towards Akke-pollegat occurs much slower and there is no import. Again under the effect of waves and tide the transport is significantly increased. Sediment bypasses the inlet and is imported into the basin in the same manner as for the previous fraction. However, the coarser fractions stay closer to the Ameland coastline, since they are less influenced by tidal currents out of the inlet. After 10 years, significantly more sediment remains in the ebb tidal delta region and less is bypassed or imported.

The 180 – 250 μm fraction is hardly effected by the tide at this location. The influence of waves is also limited. After 10 years some of the sand has just reached Borndiep via Westgat. By this time the complete fraction is still in the ebb tidal delta unit.

The coarsest fraction of 250 – 500 μm remains quite stationary. After 10 years it has spread out towards the east in the northern part of the nourishment. In the south it moves towards the Terschelling coast.

The hypothesized strong eastbound transport of the 63 – 125 μm fraction in the eastern part of the nourishment is confirmed. Furthermore, in the middle of Kofmansbult the sediment moves indeed to the south, this effect is again stronger for the smaller fractions.

5.1.4 Location 4, nourishment between Boschgat and Borndiep

When a nourishment is placed between Boschgat and Borndiep, the tidal flow picks up the 63 – 125 μm fraction from the edges of the nourishment. A part is transported via Westgat towards the western part of the ebb tidal delta. Another part is imported into the basin either via Boschgat or via the flood dominated western part of Borndiep. Wave action stirs up the sand at the shallow nourishment area and thereby significantly increases the transport. Moreover, wave forcing drives an offshore transport of the sediment leaving via Westgat. Subsequently this sediment is bypassing the inlet. Furthermore, the wave forcing drives a flow from Westgat to Borndiep, transporting sediment over the shallow area. At the end of the modeling period 56% is in the basin, 22% is on the ebb tidal delta and 21% has bypassed the inlet towards Ameland.

The 125 – 180 μm fraction behaves in a similar way as the 63 – 125 μm fraction, resulting in about the same distribution over the morphological units after 10 years.

The tidal currents are not strong enough to transport the 180 – 250 μm through Boschgat. Movement into Borndiep and Westgat is still observed, but to a much lesser extent. With waves included, sand starts to enter Boschgat again, however it is first transported over the shoal area in southern direction. However, transport into the basin via Borndiep is dominant. The distribution over the morphological units after 10 years is again approximately the same.

The 250 – 500 μm fraction moves in a similar way as the 180 – 250 μm fraction, however it moves slower and therefore more of the sediment remains in the northern part of the basin and bypassing is weaker.

All fractions show some movement over the shoal area in southern direction, reinforcing Robbeneiland. The transport from the nourishment into Boschgat was not foreseen in the hypotheses.

5.1.5 Location 5, nourishment in Boschgat

The 63 – 125 μm fraction of the nourishment in Boschgat is for most part imported into the basin in the tide only scenario. Another part is first transported into Westgat, from where it is partly exported to the western part of the ebb tidal delta and partly into the basin via Borndiep. In the scenario with waves, the sediment leaving Westgat is bypassing the inlet. Furthermore, the wave action drives the sediment further into the basin. After 10 years 56% ends up in the basin, 16% is located at the Terschelling coast, the rest is divided over the Ameland coast and the ebb tidal delta.

The transport of the 125 – 180 μm fraction occurs in a similar fashion as the smaller fraction, however more slowly. Therefore after 10 years more sediment is located at the Terschelling coast, 23% compared to 16% for the 63 – 125 μm fraction. And more sediment is located at the ebb tidal delta by that time, 19% compared to 16% for the 63 – 125 μm fraction. The import into the basin is reduced for the 125 – 180 μm fraction, compared to the smaller fraction (48% instead of 56%).

The tidal flow is strong enough to transport the 180 – 250 μm fraction in the south in the direction of the basin and in the north towards Westgat. However, after 10 years the fraction still has not entered Westgat and therefore no movement into Borndiep or export towards the ebb tidal delta is observed. Under the effect of tide, waves and wind Westgat is reached and the sediment is partly bypassing the inlet and partly imported via Borndiep, however for this fraction import is mainly via Boschgat.

For the 180 – 250 μm fraction the influence of the tide is limited. Wave forcing again splits up the nourishment, a part is transported towards Westgat and the rest is transported into the basin, however the movement remains limited. Therefore significantly more remains near the Terschelling coastline, 38% compared to the 26% of the 180 – 250 μm fraction, thereby this fraction still feeds Boschplaat after 10 years.

The results are mostly in agreement with the hypotheses. However, the transport via Westgat and subsequently via the ebb tidal delta towards Ameland was not considered.

5.1.6 Location 6, mega nourishment at Bornrif

The influence of the tide on the 63 – 125 μm fraction is already minor. There is only a small import into Borndiep, from where the sediment is recirculating in the channel with the tide. Under wave action the fraction behaves as a sand bar and moves towards the western tip of Terschelling where it folds around and reinforces Bornrif Strandhaak. From there the sediment is transported downdrift along the Ameland coast. Furthermore, waves strongly reinforce the import into the eastern part of the basin, along the Northwestern tip and the western edge of Ameland. Some of the sand entering Borndiep in this way is exported again via Akkepollegat and transported towards Ameland over the eastern part of the ebb tidal delta.

The 125 – 180 μm fraction behaves in a similar way as the smallest fraction, only slower.

For the 180 – 250 μm fraction no influence of the tide is visible. When waves are considered, the behavior again is quite similar to the previously discussed fractions. The movement is slower and the import is less far into the basin. Strong sand bar behavior can be observed. After about a third of the simulation time the fraction is folded around Bornrif Strandhaak, traveling over a distance of about 2 km. The 2014 and 2016 Vaklodngen measurements

in Figure D.01 show that the $-5m$ depth contour has been shifted over about $2.5km$ after 2 years. According to the sediment atlas in Figure 3.2 the sediment in this area has a D_{50} of $180 - 250\mu m$. Therefore the distances over which sediment transport is predicted in the model seem to be reasonable.

The $250 - 500\mu m$ fraction spreads out to a lesser extent than the previous fractions. After 10 years the sand bar has folded around Bronrif Strandhaak however there is not much transport further downstream. Some sediment also reaches Borndiep, where it is transported back and forth. However, the model results do not show import into the basin.

For all fractions after 10 years most sediment remains at the ebb tidal delta region, or is transported downdrift along the Ameland coastline. There is a small import into the basin. The effect of the tide at this location is according to the hypotheses. However, the effect of waves was expected to be more limited for the fine fractions, especially in the middle of the nourishment

5.1.7 Location 7, channel wall nourishment Borndiep

At this location the tide is strong enough to transport the different nourishment fractions over considerable distances. The $63 - 125\mu m$ fraction is transported back and forth through Borndiep. After 10 years part of the sediment is transported out of the inlet through Akkepollegat. Waves drive this sediment downdrift along the Ameland coast. The rest is imported into the east side of the basin. Inside the basin waves further disperse the fraction.

The $125 - 180\mu m$ fraction shows a similar pathway, however transport downdrift the Ameland coastline occurs considerably slower. Additionally the downdrift transport is closer to the Ameland coastline. The tidal flow pushes the coarser fractions less far out of the system, as a consequence these fractions are transported downdrift closer to the shore, compared to finer fractions.

After 10 years most of the $180 - 250\mu m$ fraction has just left the inlet and is in the ebb tidal delta area, 55% is located there. This leads to the strongest reinforcement of this area, compared to the other fractions. Furthermore, the sediment is transported less far into the basin.

The tidal flow moves the $250 - 500\mu m$ fraction less far into the basin in the south and less far onto the ebb tidal delta in the north. Moreover, the wave forcing at the ebb tidal delta is not strong enough to result in a significant downdrift transport.

There is a relatively large import into the basin for all fractions at this location, however it must be noted that southern part of Borndiep is considered as part of the basin. For the present schematization the initial nourishment location is partly in the basin. Nourishment sediment, which is armored under other layers and still at the initial location after 10 years therefore belongs to the basin. The hypothesized recirculation in the channel, import of sediment into the basin and export via Akkepollegat are confirmed by the model results. Transport into Westgat is not observed.

5.1.8 Location 8, mega ebb tidal delta nourishment

This nourishment is located in the same area as the pilot nourishment discussed in Section 5.1.3, but it extends over a much larger area. The tidal and wave influence is the same for both nourishments. After 10 years the larger nourishment results in relatively less transport

towards Ameland, 12%, compared to the 17% for the pilot nourishment. There is also less import in the basin, 1% instead of 5%. Relatively more sediment remains in the ebb tidal delta region.

5.2 Effect of the nourishment compositions

Figures 5.4 and 5.5 show the availability of the sediment fractions in the transport layer after 10 years for the fine and coarse nourishment compositions respectively. In the first two sections of Table 5.1 the distribution of the fractions over the morphological units after 10 years is shown for these two scenarios. The bar graphs are shown in Figures 5.19 and 5.20.

Some important differences in the results for the two compositions are observed. First of all, the fractions in the coarse composition show a slower movement. Moreover, more armoring occurs of the finer fractions under coarser fractions. As a result a smaller amount of the fractions of the coarse nourishment is transported in the direction of the ebb tidal delta and to the coast of Ameland. Consequently after 10 years, 92% of the nourishment is still at the Terschelling coastline, instead of 45% for the fine nourishment.

For nourishment Locations 2, 4 and 5 some of the sediment ends up in Boschgat. However, for all these scenarios the minimum depth of the channel is larger than $4mNAP$. Therefore not much hindrance is expected for pleasure navigation.

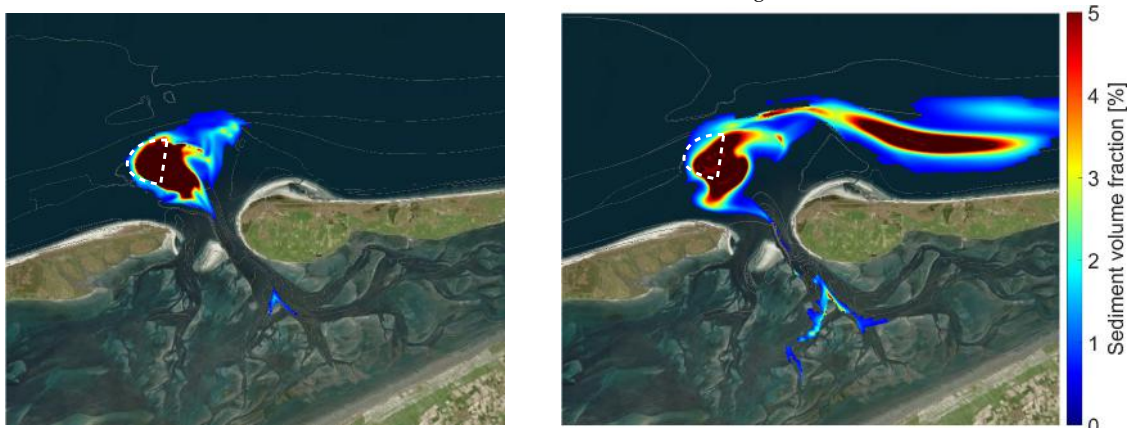
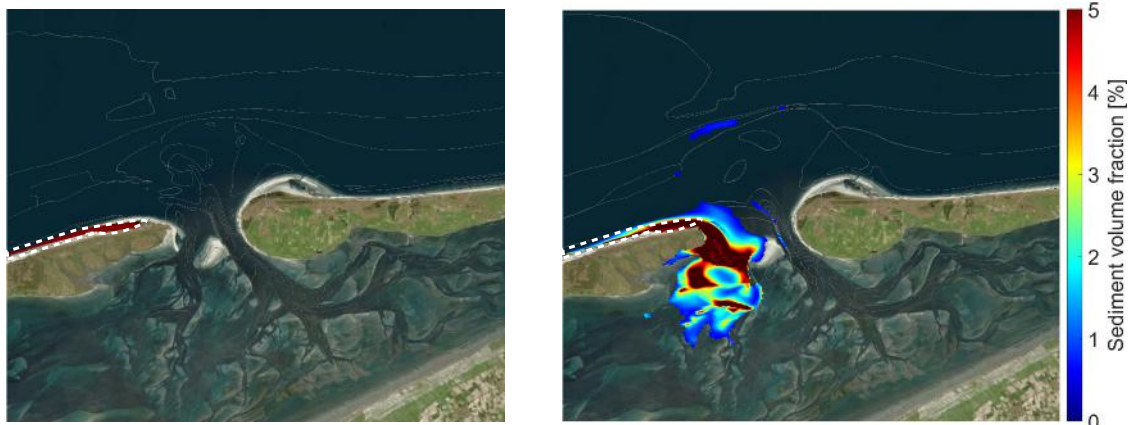
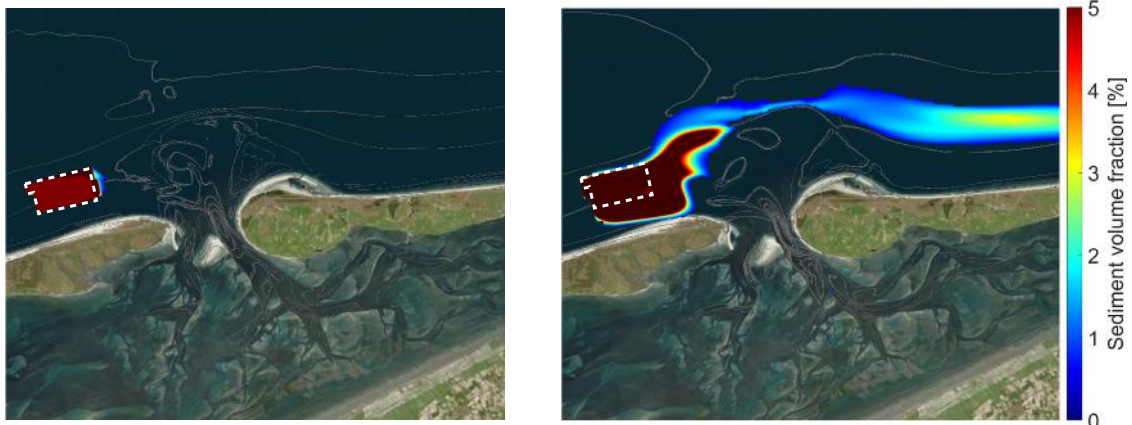
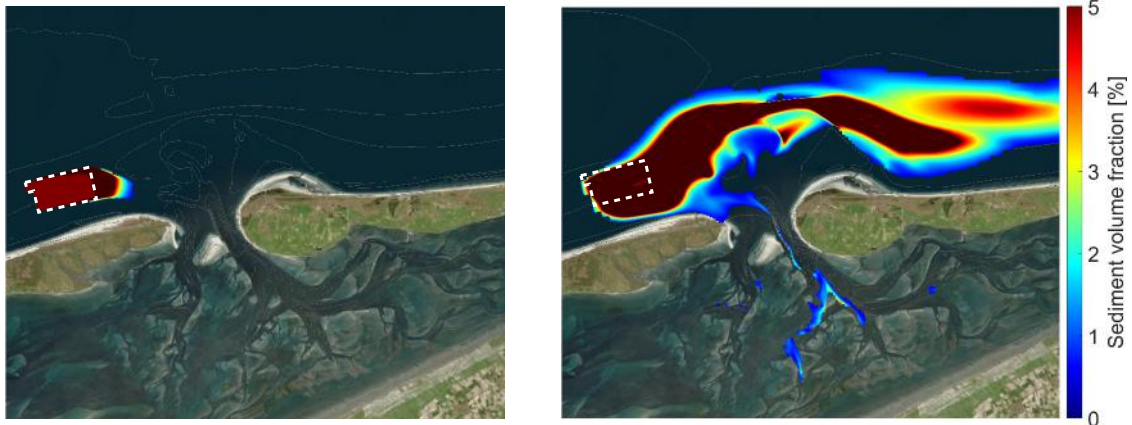
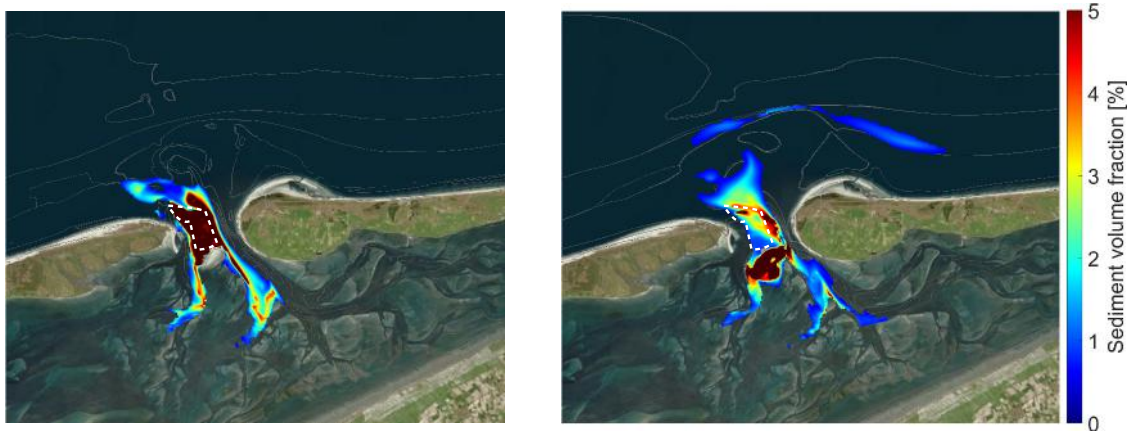
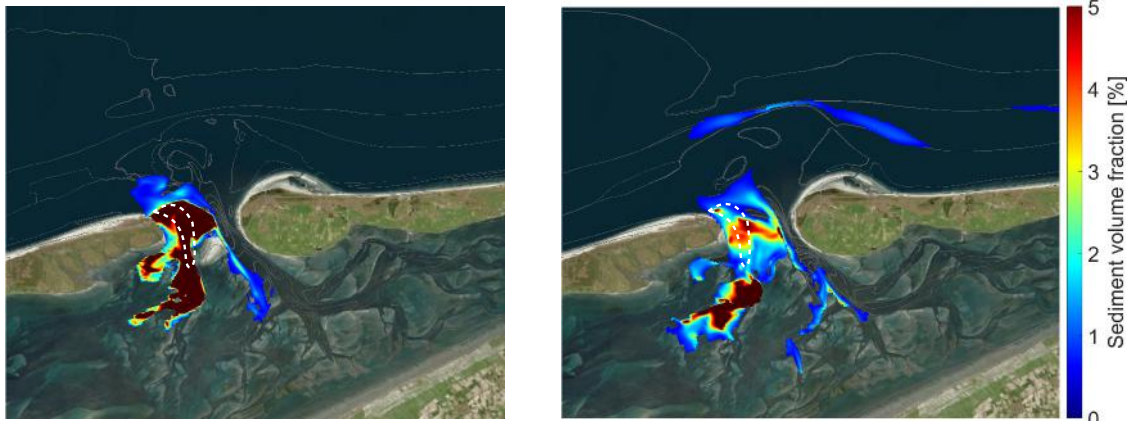


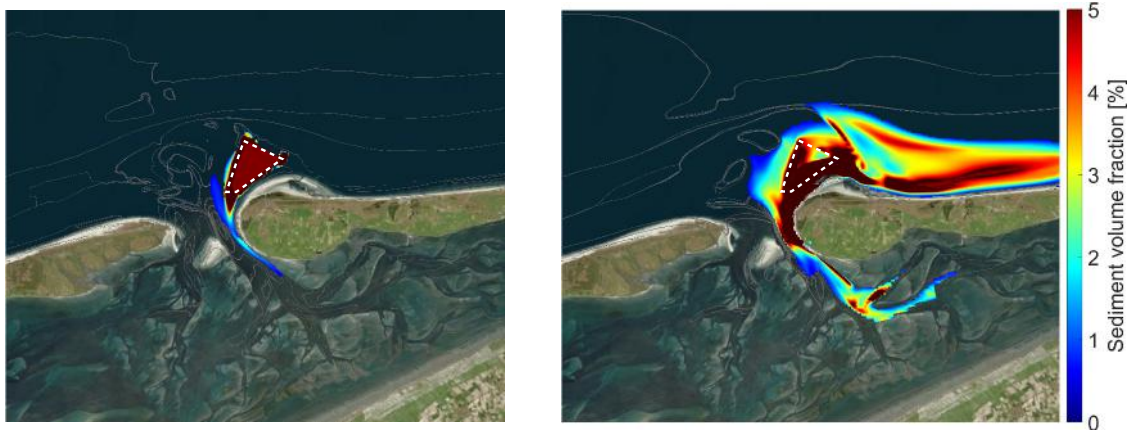
Figure 5.1: Total percentage of nourishment sediment in the transport layer (upper $0.5m$). The figures on the left show the effect of the tide. The figures on the right show the effect of tide, wind and waves. The dashed boxes indicate the outline of the initial nourishment locations



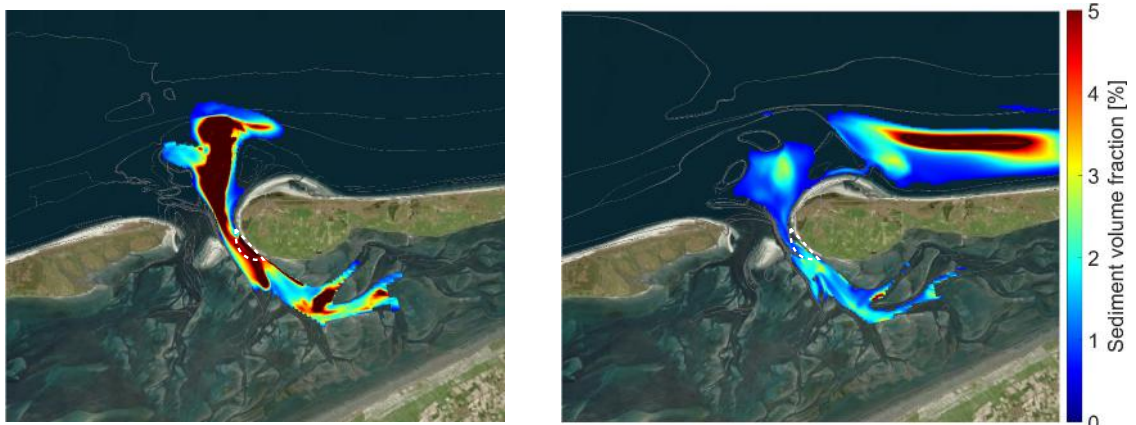
Location 4, nourishment between Boschgat and Borndiep



Location 5, nourishment in Boschgat

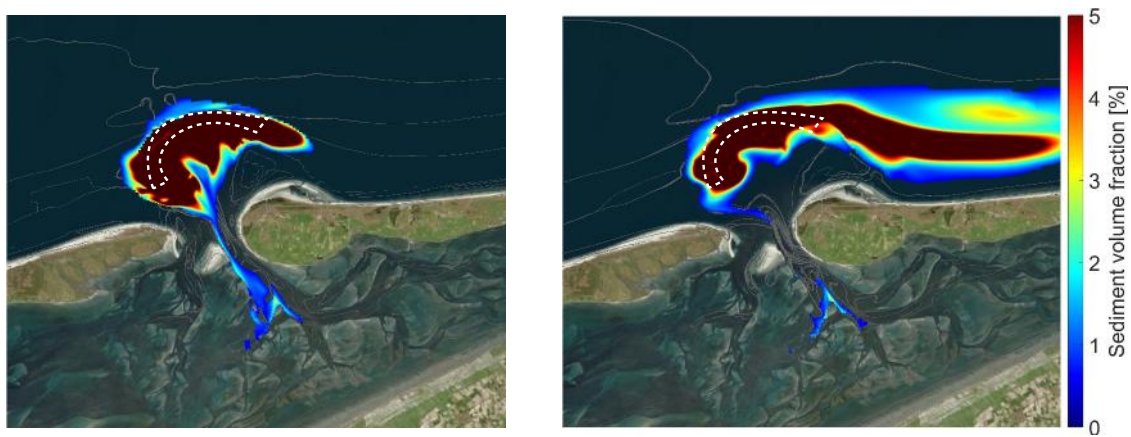


Location 6, mega nourishment at Bornrif



Location 7, channel wall nourishment Borndiep

Figure 5.2: Total percentage of nourishment sediment in the transport layer (upper $0.5m$). The figures on the left show the effect of the tide. The figures on the right show the effect of tide, wind and waves. The dashed boxes indicate the outline of the initial nourishment locations



Location 8, mega ebb tidal delta nourishment

Figure 5.3: Total percentage of nourishment sediment in the transport layer (upper $0.5m$). The figures on the left show the effect of the tide. The figures on the right show the effect of tide, wind and waves. The dashed boxes indicate the outline of the initial nourishment locations

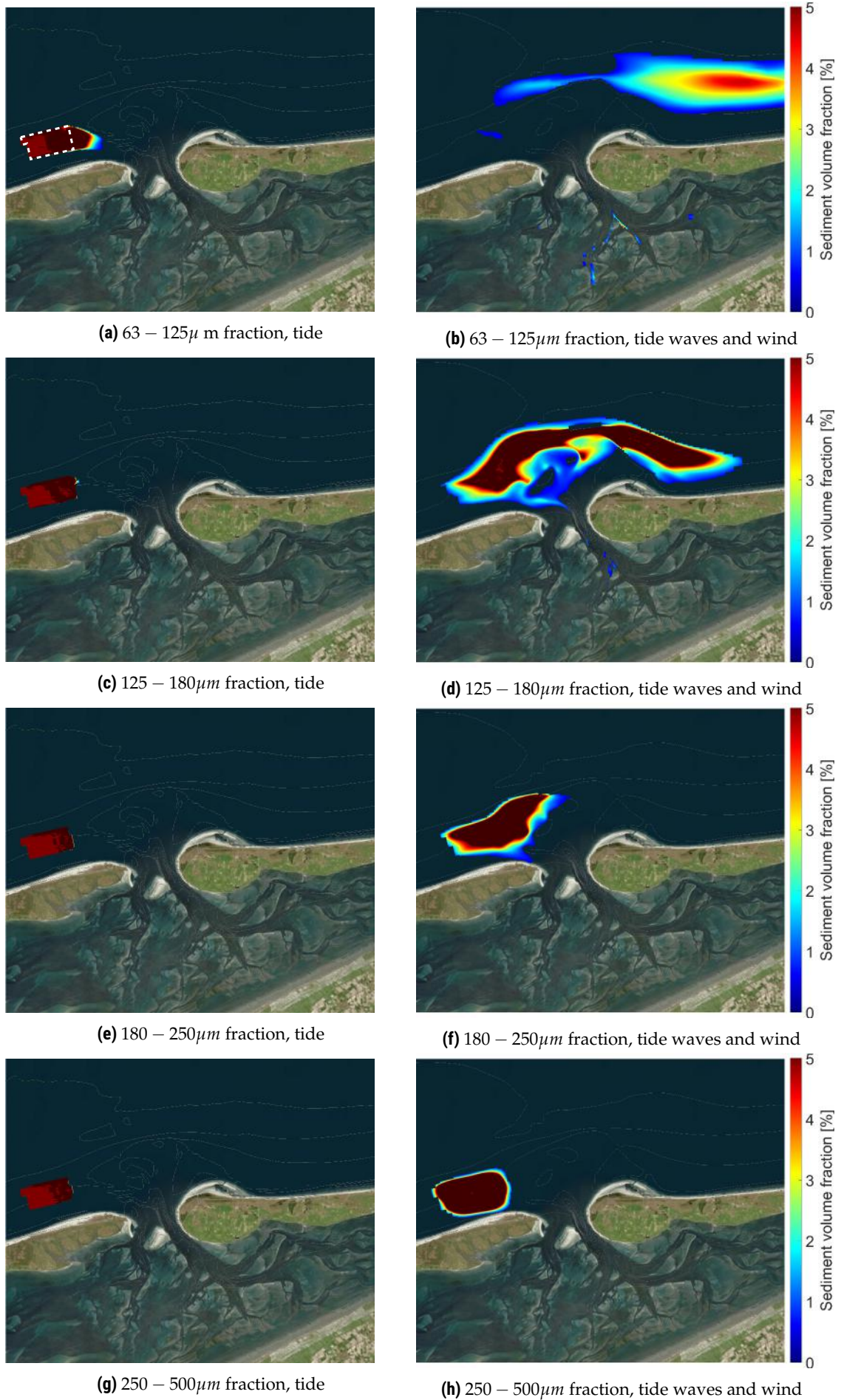


Figure 5.4: Nourishment location 1, mega foreshore nourishment Terschelling, fine composition: Percentage of nourishment sediment in the transport layer (upper 0.5m), per fraction. The dashed box in figure (a) indicates the outline of the initial nourishment location

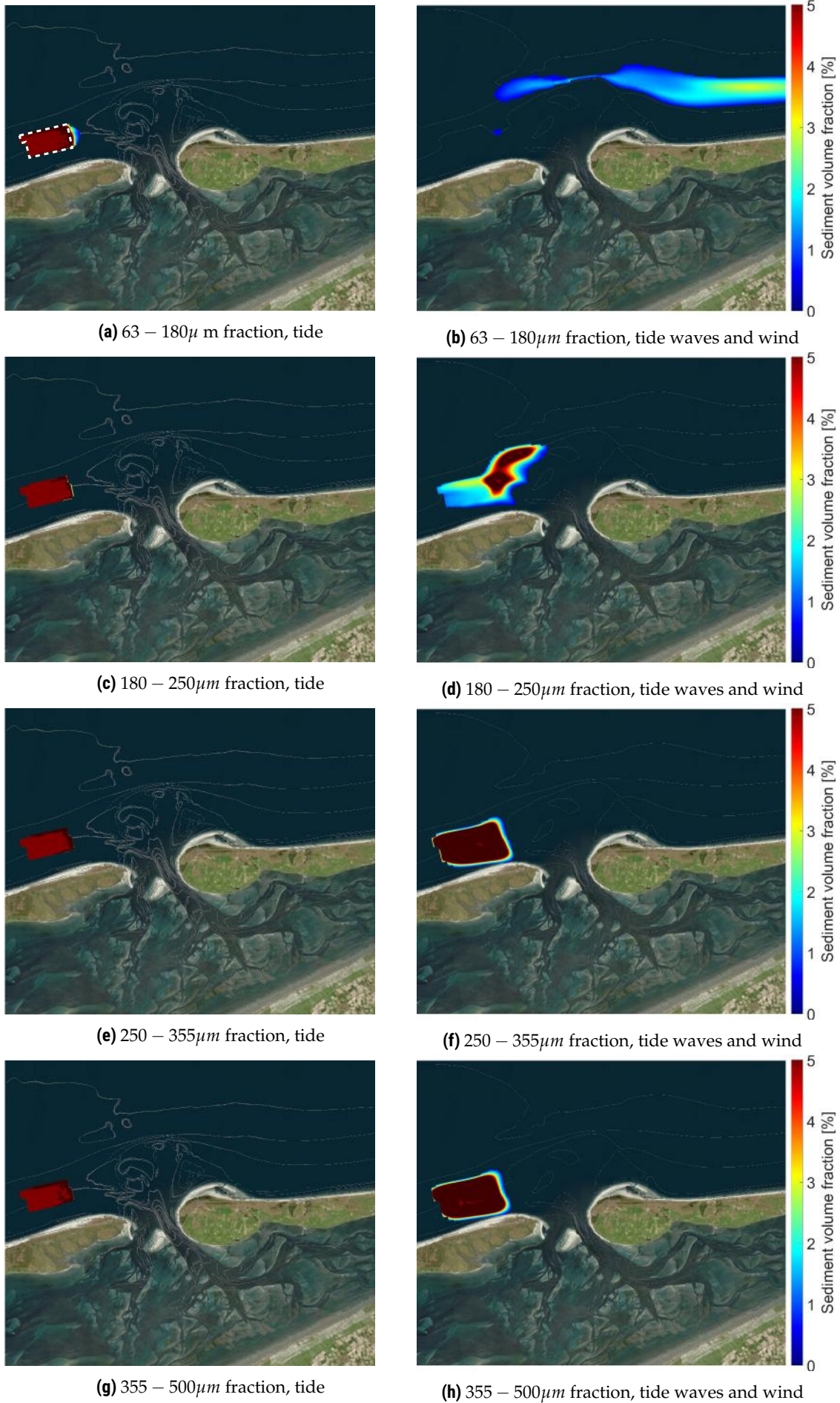


Figure 5.5: Nourishment location 1, mega foreshore nourishment Terschelling, coarse composition: Percentage of nourishment sediment in the transport layer (upper 0.5m), per fraction. The dashed box in figure (a) indicates the outline of the initial nourishment location

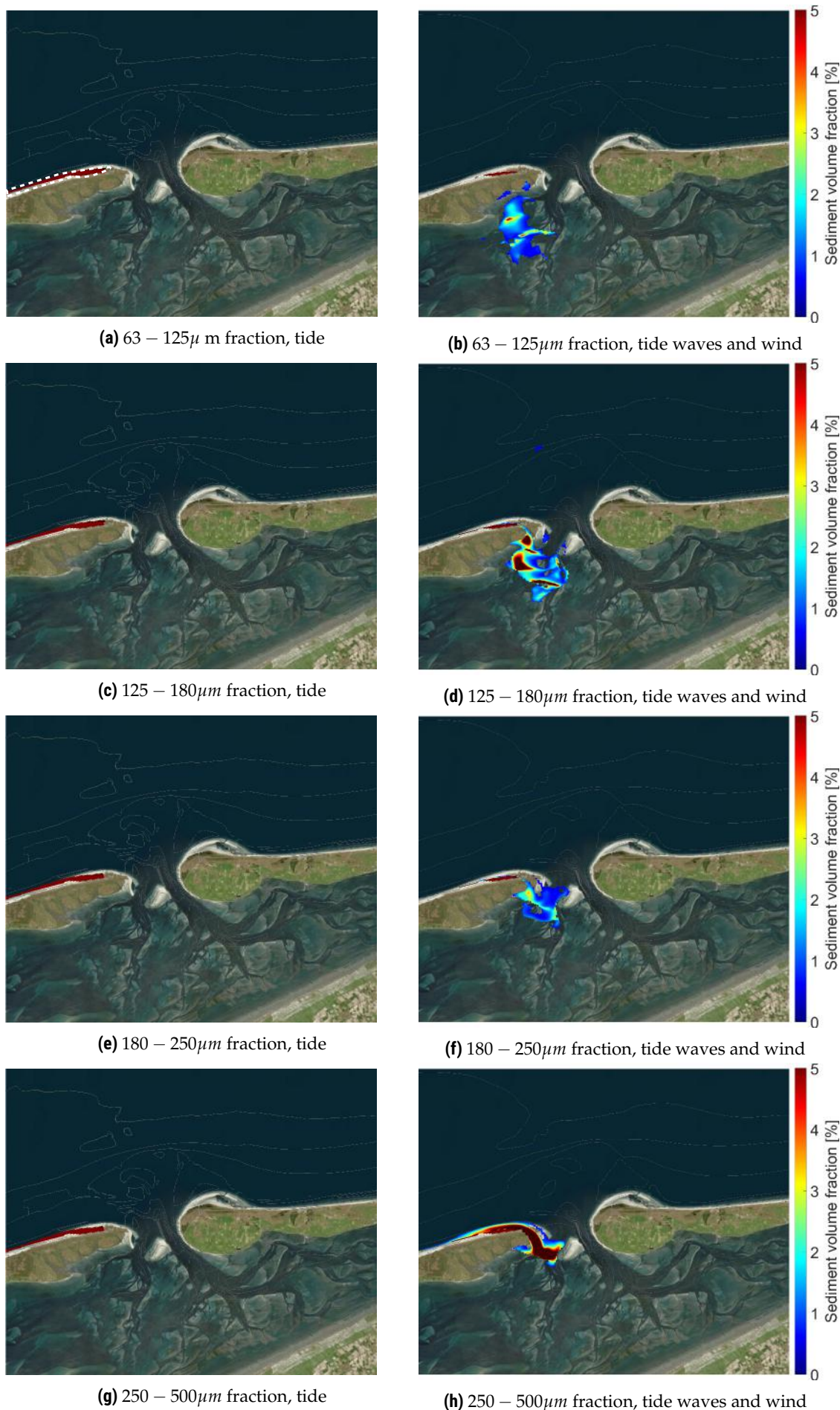


Figure 5.6: Nourishment location 2, beach nourishment Terschelling: Percentage of nourishment sediment in the transport layer (upper 0.5m), per fraction. The dashed box in figure (a) indicates the outline of the initial nourishment location

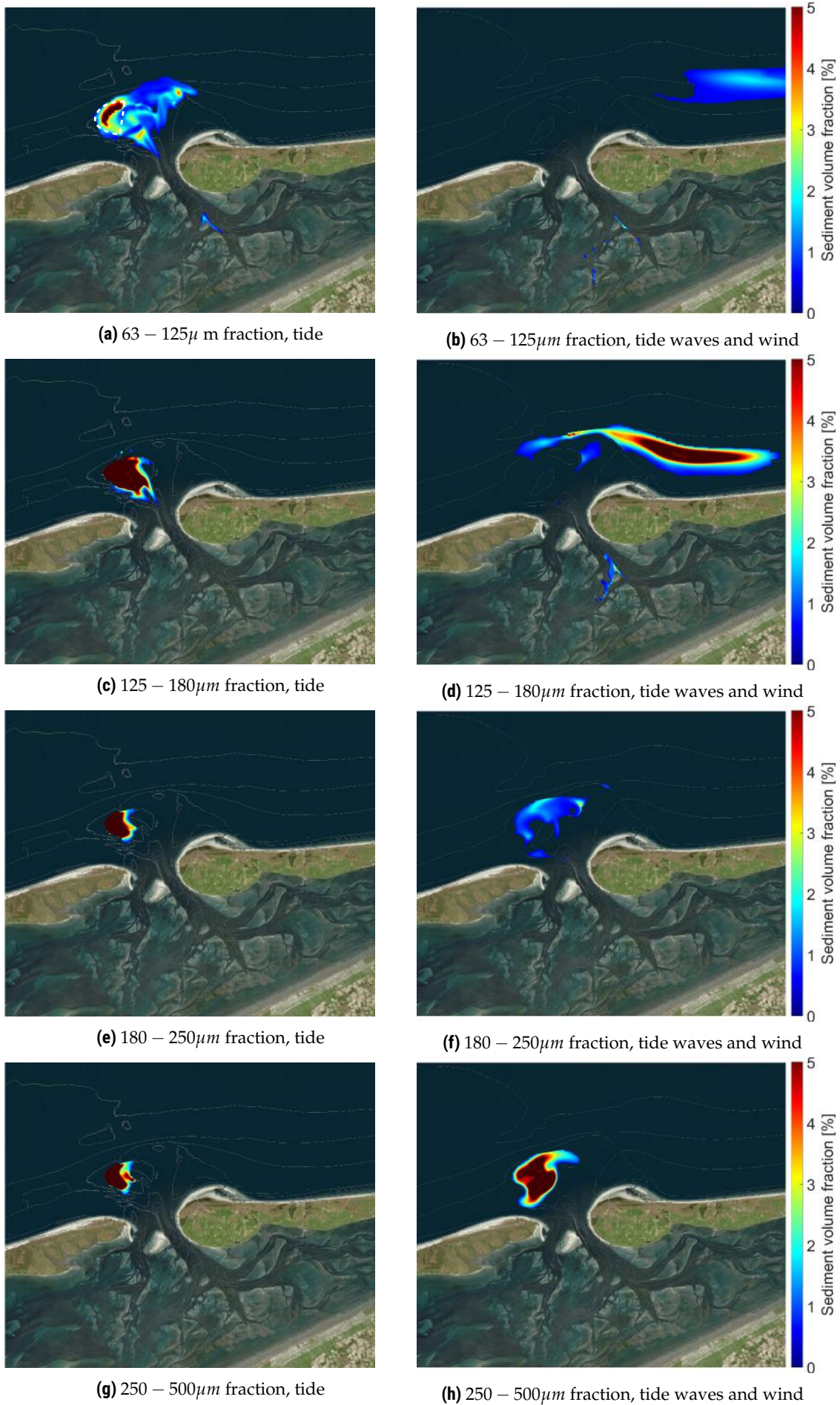


Figure 5.7: Nourishment location 3, pilot nourishment Kofmansbult: Percentage of nourishment sediment in the transport layer (upper 0.5m), per fraction. The dashed box in figure (a) indicates the outline of the initial nourishment location

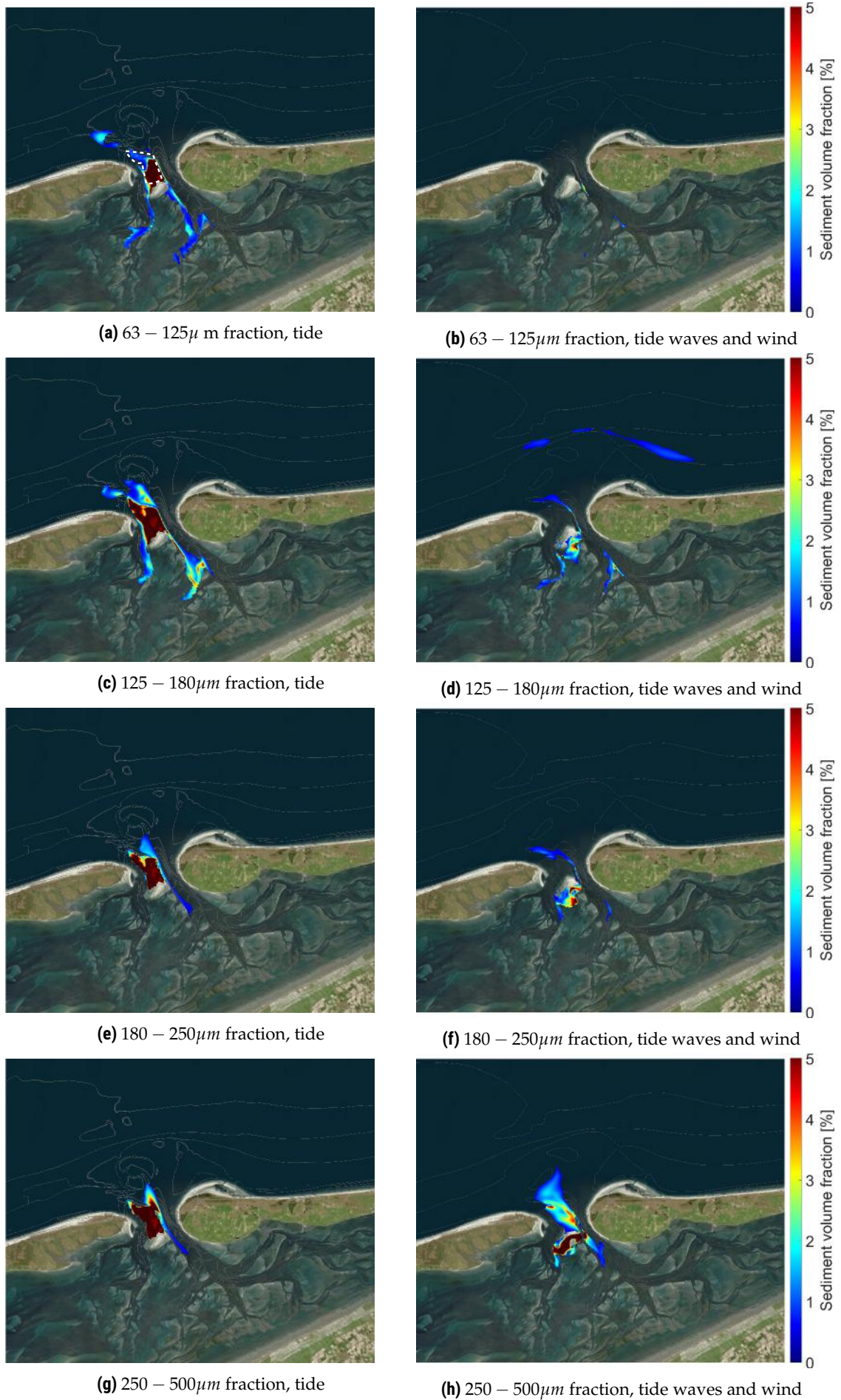


Figure 5.8: Nourishment location 4, nourishment between Boschgat and Borndiep: Percentage of nourishment sediment in the transport layer (upper 0.5m), per fraction. The dashed box in figure (a) indicates the outline of the initial nourishment location

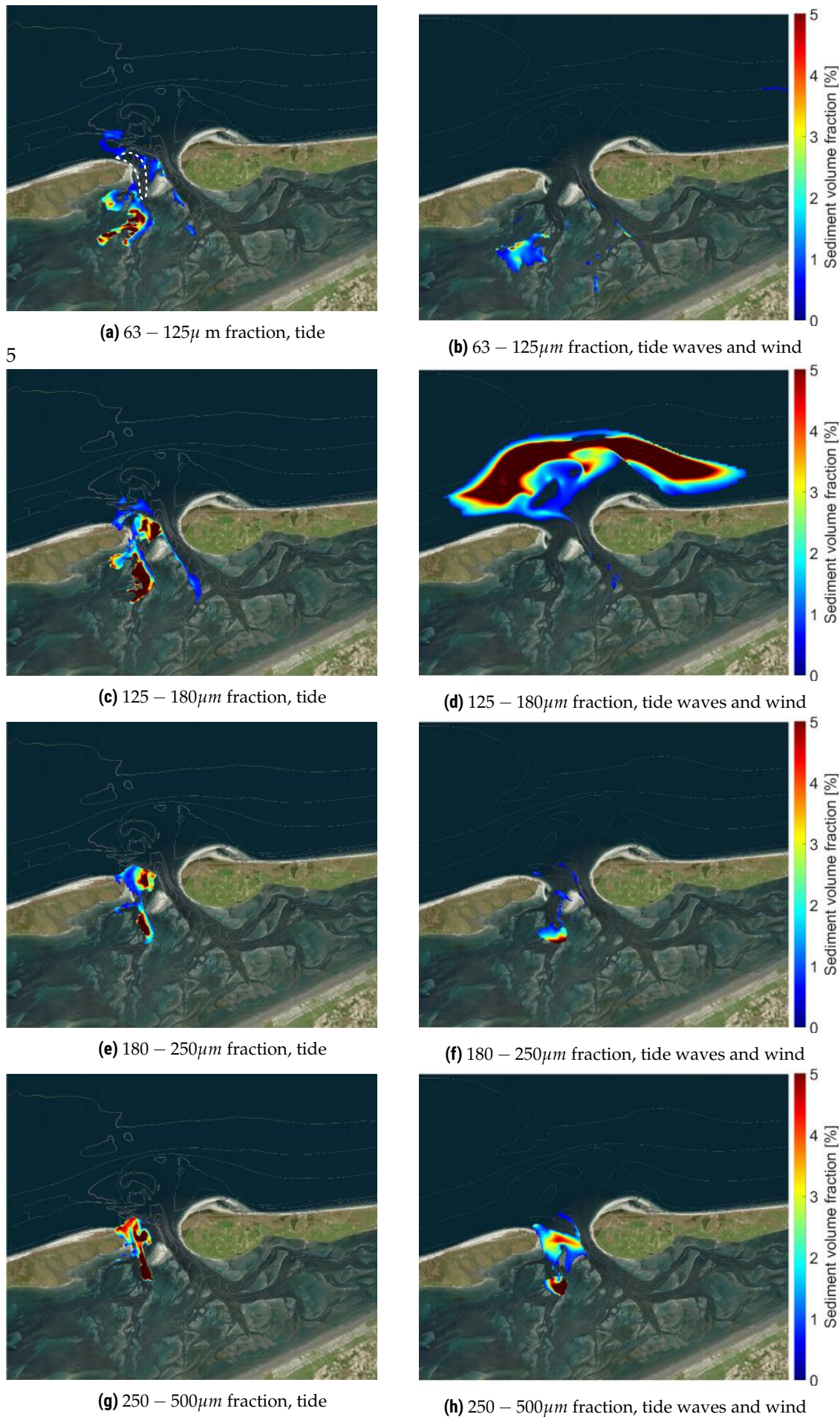


Figure 5.9: Nourishment location 5, nourishment in Boschgat: Percentage of nourishment sediment in the transport layer (upper 0.5m), per fraction. The dashed box in figure (a) indicates the outline of the initial nourishment location

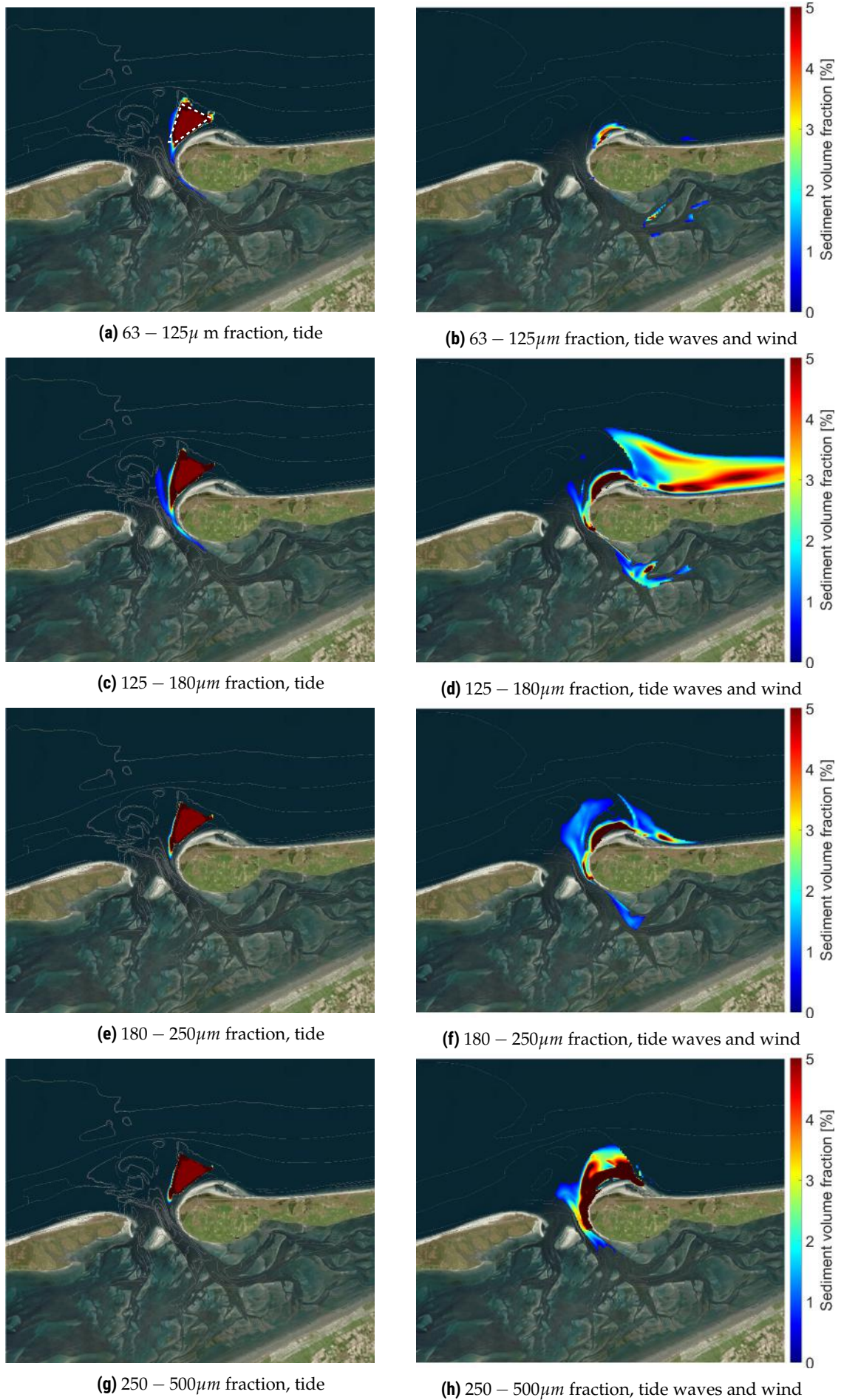


Figure 5.10: Nourishment location 6, mega nourishment at Bornrif: Percentage of nourishment sediment in the transport layer (upper 0.5m), per fraction. The dashed box in figure (a) indicates the outline of the initial nourishment location

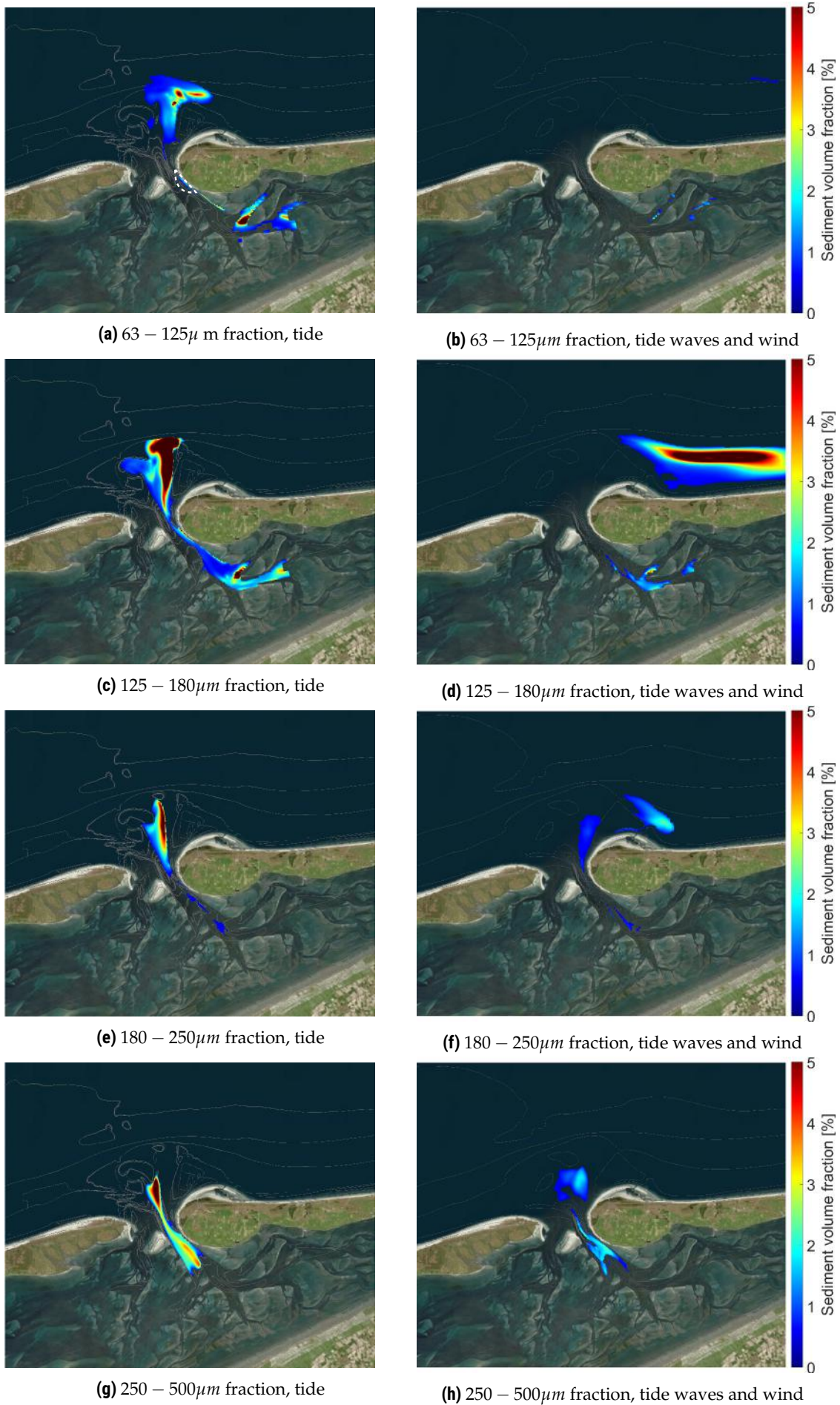


Figure 5.11: Nourishment location 7, channel wall nourishment Borndiep: Percentage of nourishment sediment in the transport layer (upper 0.5m), per fraction. The dashed box in figure (a) indicates the outline of the initial nourishment location

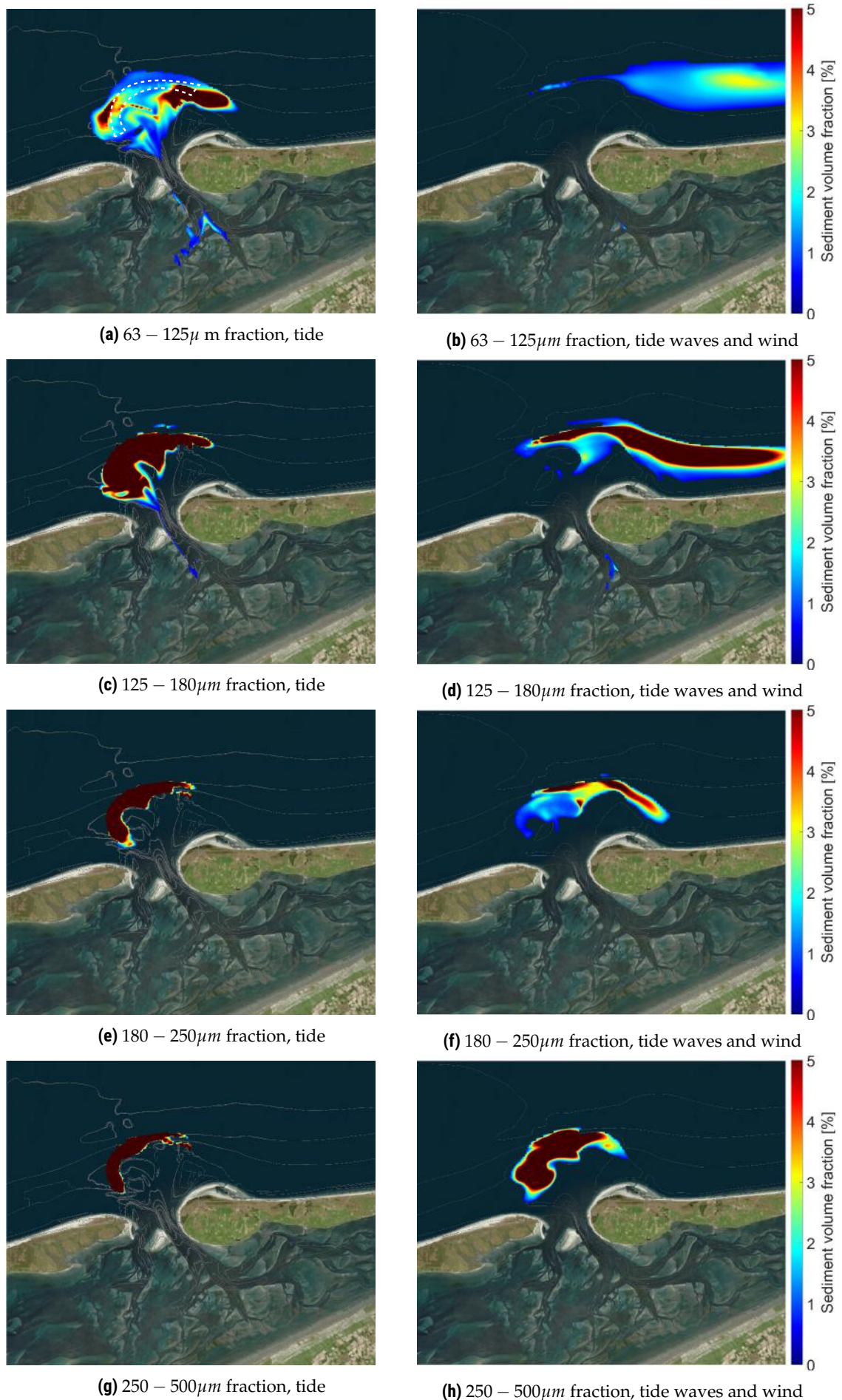


Figure 5.12: Nourishment location 8, mega ebb tidal delta nourishment: Percentage of nourishment sediment in the transport layer (upper 0.5m), per fraction. The dashed box in figure (a) indicates the outline of the initial nourishment location

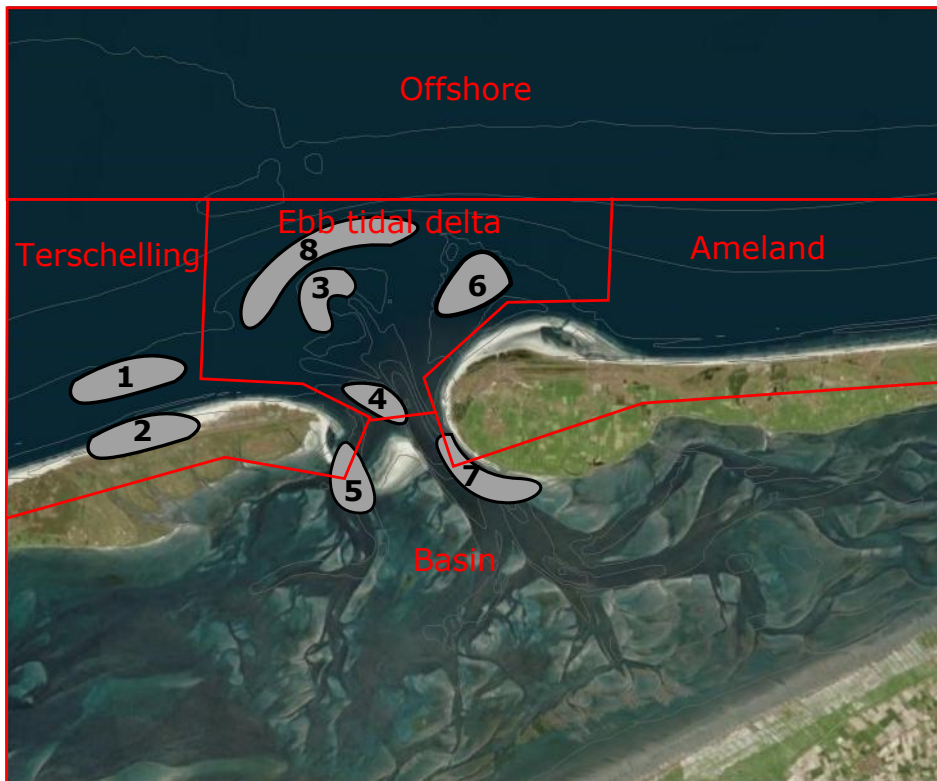


Figure 5.13: The five morphological units of the Ameland Inlet system and the nourishment locations

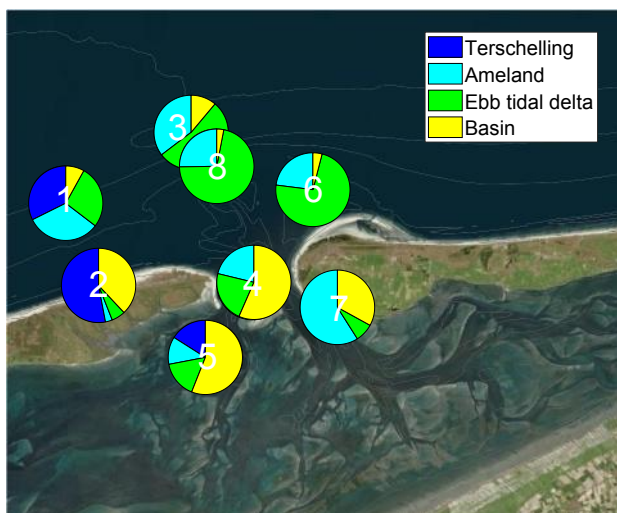


Figure 5.14: Pie charts showing the percentage of the 63 – 125 µm fraction found at the different morphological units after 10 years, for all 8 locations

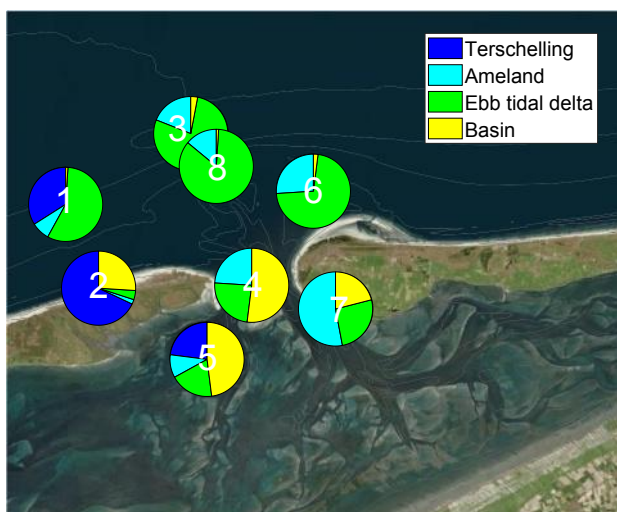


Figure 5.15: Pie charts showing the percentage of the 125 – 180 µm fraction found at the different morphological units after 10 years, for all 8 locations

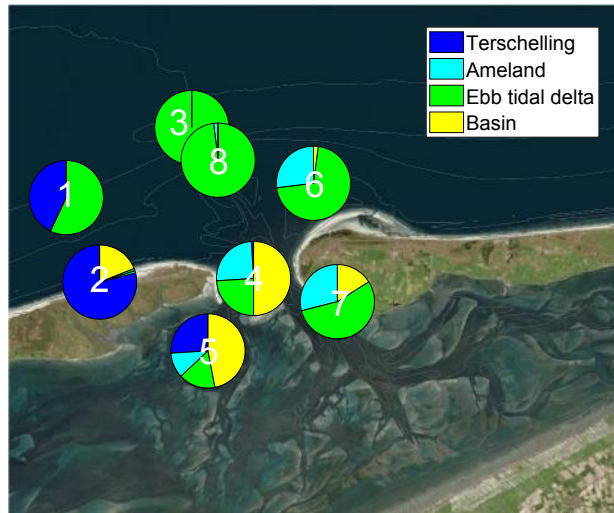


Figure 5.16: Pie charts showing the percentage of the 180 – 250 μm fraction found at the different morphological units after 10 years, for all 8 locations

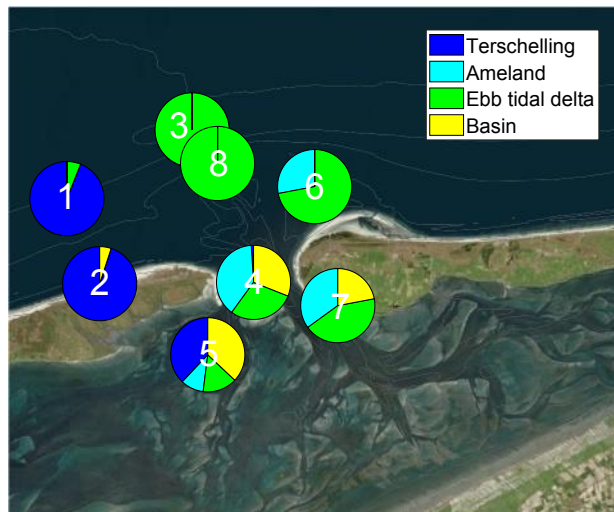


Figure 5.17: Pie charts showing the percentage of the 250 – 500 μm fraction found at the different morphological units after 10 years, for all 8 locations

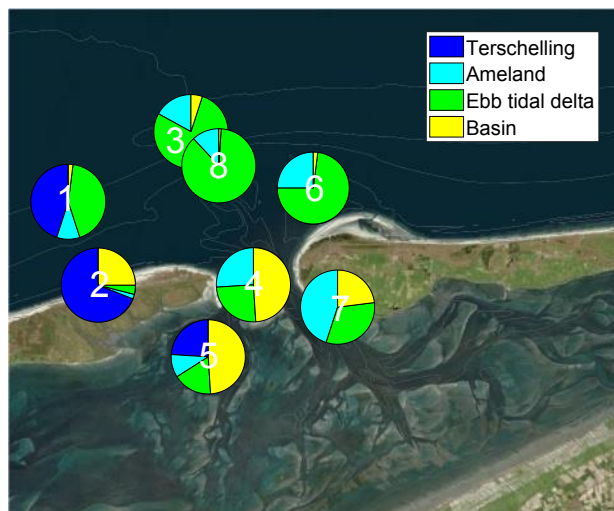
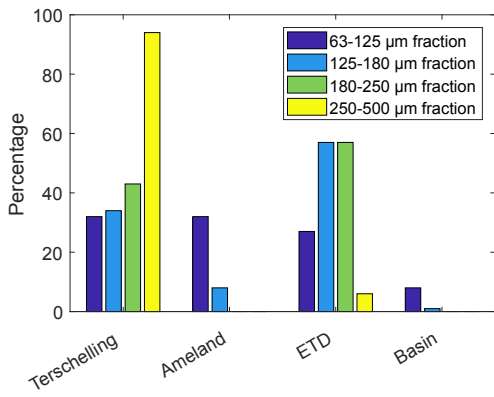


Figure 5.18: Pie charts showing the percentage of the total nourishment found at the different morphological units after 10 years, for all 8 locations

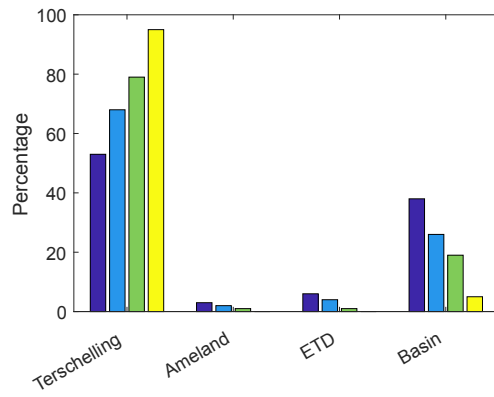
Table 5.1: Distribution of the nourishment sediment fractions over the model domain after 10 years

Sediment fraction [μm]	Percentage by volume of the nourishment fraction in the unit [%]				
	Terschelling	Ameland	ETD	Basin	Offshore
LOCATION 1 (FINE)					
63 - 125	32	32	27	8	2
125 - 180	34	8	57	1	0
180 - 250	43	0	57	0	0
250 - 500	94	0	6	0	0
Total	45	10	43	2	0
LOCATION 1 (COARSE)					
63 - 180	54	20	22	3	1
180 - 250	84	0	16	0	0
250 - 355	98	0	2	0	0
355 - 500	99	0	1	0	0
Total	92	3	5	0	0
LOCATION 2					
63 - 125	53	3	6	38	0
125 - 180	68	2	4	26	0
180 - 250	79	1	1	19	0
250 - 500	95	0	0	5	0
Total	69	2	4	25	0
LOCATION 3					
63 - 125	0	35	53	11	1
125 - 180	0	19	78	3	0
180 - 250	0	0	100	0	0
250 - 500	0	0	100	0	0
Total	0	17	78	5	0
LOCATION 4					
63 - 125	0	21	22	56	1
125 - 180	0	24	24	52	0
180 - 250	1	25	24	50	0
250 - 500	1	39	29	31	0
Total	0	26	25	49	0
LOCATION 5					
63 - 125	16	12	16	56	0
125 - 180	23	10	19	48	0
180 - 250	26	11	16	47	0
250 - 500	38	10	15	37	0
Total	24	10	17	49	0

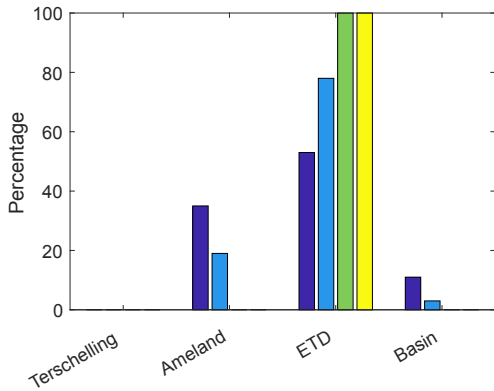
Sediment fraction [μm]	Percentage by volume of the nourishment fraction in the unit [%]				
	Terschelling	Ameland	ETD	Basin	Offshore
LOCATION 6					
63 - 125	0	23	73	4	0
125 - 180	0	26	72	2	0
180 - 250	0	27	71	2	0
250 - 500	0	28	72	0	0
Total	0	25	73	2	0
LOCATION 7					
63 - 125	0	59	8	33	0
125 - 180	0	53	26	21	0
180 - 250	0	29	55	16	0
250 - 500	0	35	43	22	0
Total	0	45	32	23	0
LOCATION 8					
63 - 125	0	25	71	3	1
125 - 180	0	14	85	1	0
180 - 250	0	2	98	0	0
250 - 500	0	0	100	0	0
Total	0	12	87	1	0



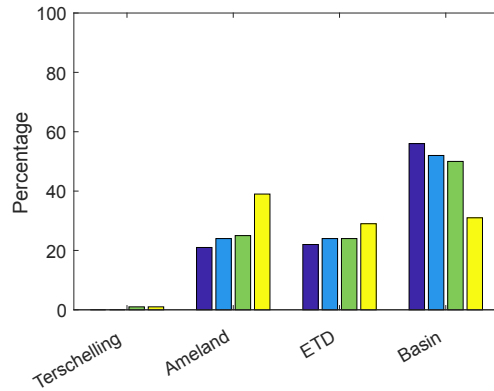
(a) Location 1



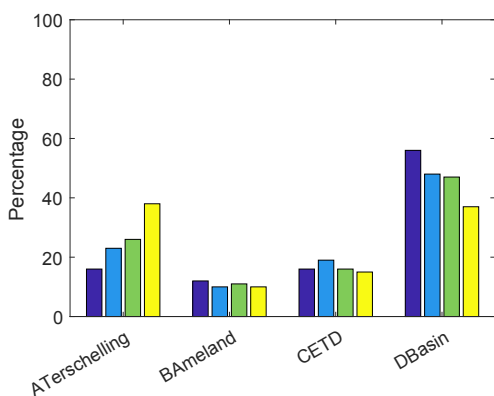
(b) Location 2



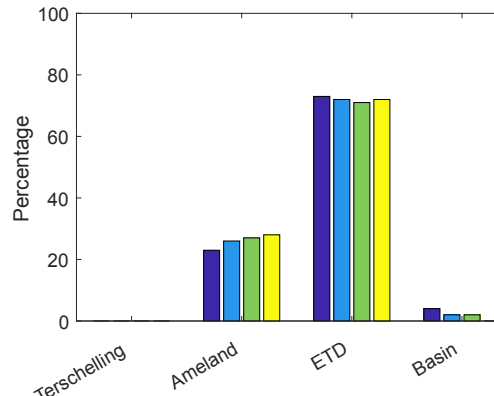
(c) Location 3



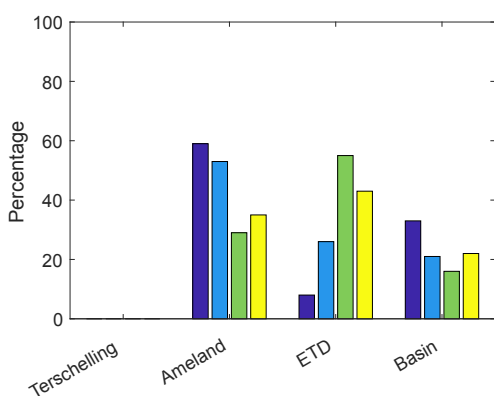
(d) Location 4



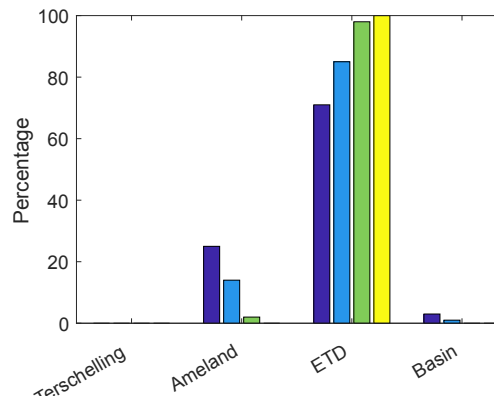
(e) Location 5



(f) Location 6



(g) Location 7



(h) Location 8

Figure 5.19: Percentage by volume of the nourishment fraction in the unit, for all nourishment locations

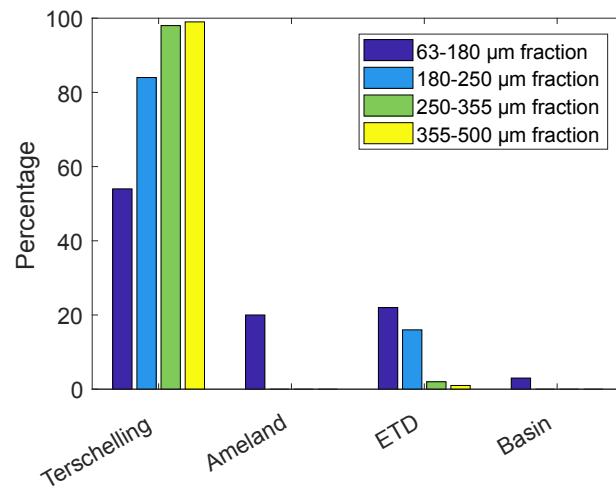


Figure 5.20: Percentage by volume of the nourishment fraction in the unit, for the coarse nourishment at Location 1

6.1 Nourishment evaluation for the Ameland Inlet

6.1.1 Evaluation criteria

As discussed in section 1.3 there are three main objectives for a nourishment at the Ameland Inlet: feeding the coastal foundation, feeding the basin and maintaining the wave shelter function of the ebb tidal delta. With regard to the objective of feeding the coastal foundation, we can distinguish between two sub-objectives. It concerns feeding the Ameland coastline including Bornrif, which is suffering from erosion or the Terschelling coast including the natural reserve Boschplaat, which is also shrinking. The results of the nourishment simulations are evaluated based on which objectives are met and to what extend.

Finally the location where the nourished sand ends up can have ecological consequences. On the one hand it can have undesired effects for instance when coarse sand is transported to the tidal flats, see Section 4.1.2. On the other hand it may create ecological value. For instance when it reinforces the Boschplaat, the natural reserve can be maintained. Residents and tourists may also be affected. However, no direct consequences are observed in this respect. The nourished sand does not results in the closure of a navigation channel, since for all nourishments the Boschgat navigation channel is at least $4mNAP$ deep. Residents and tourists may experience indirect consequences from the impact on ecology, for instance when nourishment sand contributes to the preservation of Robbeneiland.

6.1.2 Evaluation matrix

The results for the evaluation of the nourishment are shown in Table 6.1. The scores for feeding a morphological unit are based on the total sediment in the unit after 10 year, see Table 5.1. For locations 2, 4, 5 and 6 the sediment reinforces areas which have important ecological values. The nourishment at location 2 results in a significant reinforcement of the natural reserve Boschplaat. At location 4 it causes reinforcement of Robbeneiland and a relatively strong feeding of basin. At location 5 it results in less reinforcement of Robbeneiland however there is again a relatively strong feeding of the basin. A nourishment at location 6 feeds Bornrif, which is no natural reserve, however it can provide a resting area for animals. Therefore this nourishment is expected to have a positive impact on ecology, however to a lesser extent as locations 2, 4 and 5.

Table 6.1: Evaluation of the destination of the nourishment sediment

Nourishment scenario	Score for feeding morphological unit (1 - 5)				Ecological impact
	Terschelling	Ameland	ETD	Basin	
1 Terschelling foreshore (FINE)	2	1	2	0	0
1 Terschelling foreshore (COARSE)	5	0	0	0	0
2 Terschelling beach	4	0	0	3	++
3 Pilot Kofmansbult	0	2	4	1	0
4 Between Boschgat and Borndiep	0	3	1	5	++
5 Boschgat	1	1	1	5	++
6 Bornrif	0	3	4	0	+
7 Borndiep channel wall	0	5	2	2	0
8 Ebb tidal delta	0	1	5	0	0

As discussed before, residents and tourists may also benefit from a positive ecological impact, however these indirect social effects are not considered here.

6.1.3 Discussion

From the model results we now have a better picture of how sediment fractions of different nourishment designs behave in the Ameland tidal inlet system on medium term timescales. The composition of the modeled nourishments is based on the bottom investigation report of the borrow area, provided by Rijkswaterstaat [LABAN, 2014].

The model results indicate where the nourished sand will migrate. Furthermore, an analysis of the nourishment location gives an indication of the construction costs, the ecological and the social impact (Table 4.1). By comparing the results for the same composition at the different locations, we find that feeding the Terschelling coast is best achieved by placing the nourishment at location 2 (Beach nourishment Terschelling) (Table 6.1). This results in a reinforcement of Boschplaat and import into the basin, which is expected to have a positive ecological impact. However, since this concerns a beach nourishment the construction costs are high. Furthermore, during construction residents and tourists will be negatively effected due to the smell, noise and visual pollution on the beach.

Location 4, 6 and 7 score best at feeding the Ameland coast. A nourishment in Borndiep (location 7) or in between Borndiep and Boschgat (location 4) contributes to the development of the deeper parts of the Ameland coast. At Bornrif (location 6) the sand feeds the tip of Ameland. The sand traveling downdrift from this location reinforces the near shore part of the Ameland coast. At location 4 and 6 nourishments are relatively expensive since pumping is involved. At location 7 the construction is relatively cheap, however the sailing distance to the borrow pit is the largest. At location 4 and 6 there may be some initial disturbance of the local ecology. On the other hand they may create additional ecological value. The former reinforces Robbeneiland, the latter Bornrif. For location 7 the nuisance residents and tourists will experience during construction is larger than for the other locations.

The ebb tidal delta is maintained best by nourishments at locations 3, 6 and 8. At location 6 (Bornrif) this mainly concerns feeding Bornrif. The pilot nourishment (location 3) and the mega ebb tidal delta nourishment (location 6) contribute best to the maintenance of

the central part of the ebb tidal delta. The model predicts that the coarsest two fractions remain quite stable in the initial nourishment area. Sediment with a grain size larger than $180\ \mu\text{m}$ remains much longer in the ebb tidal delta region. The fine fractions are transported downdrift or remain armored under the coarse fractions. The construction costs are relatively low for these two nourishments since they are close to the borrow pit and most of the sand can be placed through dumping. Nonetheless the ecology is disturbed by placing it here, since birds hunt in this area and in the eastern part shellfish banks are present.

Nourishments at locations 2, 4 and 5 score best at feeding the basin. They predominantly supply sediment to the western part of the basin, via Boschgat. A beach nourishment at Terschelling (location 2) reinforces Boschplaat, but residents and tourists may experience nuisance during construction. In between Boschgat and Borndiep (location 4) and in Boschgat (location 5) they also contribute to the maintenance of ecologically valuable areas. However a nourishment in Boschgat may disturb the habitat of the Sand Eel and during construction pleasure navigation in Boschgat may experience some hindrance. The eastern part of the basin is best fed by placing a nourishment at location 7 (channel wall Borndiep). This again is expected to be an important habitat of the Sand Eel, furthermore inhabitants of Ameland and tourists will experience nuisance during construction. The $63 - 125\ \mu\text{m}$ and $125 - 180\ \mu\text{m}$ fractions are transported considerably deeper into the basin compared to the coarser fractions. Therefore if the objective is to feed the back of the basin, it seems beneficial to use more relatively fine sediment in the nourishment. If feeding the basin is undesired, relatively coarse sediment should be applied.

The model results for the two different nourishment compositions at location 1 provides us with information regarding the effect of the nourishment composition. When a coarser nourishment is applied, obviously less fine sand is available that can be carried away quickly by the flow. The coarser fractions are transported less easily. Additionally in a coarse composition more armoring of fine fractions under coarse sediments occurs. Consequently more sediment remains in the initial nourishment area. Dredging sediment from a coarser part of the borrow area has a major effect according to the model results. For a coarse nourishment 92% is predicted to remain near Terschelling, instead of 45% for a fine nourishment.

The main objective of this thesis is to find out how nourishment sand fractions are shared between the different morphological units of the Ameland Inlet system. Several important inferences can be drawn based on the model results. The most important transport pathways within the inlet system are displayed in Figure 6.1, they are discussed in detail in this section. First the system of channels is considered. The results suggest that the transport of sediment in and south of the inlet is mainly confined to the channels. Transport over the shallow areas of the system is limited here. Boschgat connects the Terschelling beach to the western part of the basin. This connection is only in one direction, from the Terschelling beach into the system. Moreover, Boschgat is connected to Borndiep via Westgat and the shallow area in between Boschgat and Borndiep. This is again in one direction, sand in Borndiep does not reach Boschgat. Boschgat also links the basin to the ebb tidal delta. Borndiep connects the eastern part of the basin to the ebb tidal delta. This is a two way connection. Sediment in Borndiep is recirculated for some time and is then either imported into the basin or exported to the ebb tidal delta. Borndiep also imports some of the nourishment sand when it is in the ebb tidal delta region. This effect is stronger for the smaller fractions.

Second, we look at the basin. The western part of the basin shows a strong connection with the Terschelling beach, but only in the direction of the basin. The connections of the basin to the rest of the system are much weaker. Except for the Ameland beach only sediment

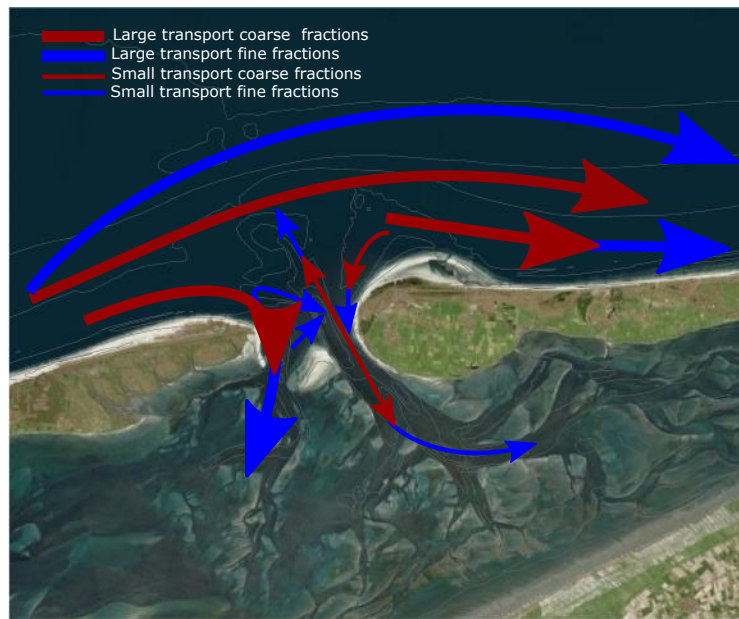


Figure 6.1: The main pathways of coarse and fine nourishment fractions, based on a qualitative interpretation of the model results

supplied in the basin significantly contributes to the sediment storage in the basin. The weaker connections from the basin to the ebb tidal delta and the Ameland coast are in two directions, resulting in a small import of sediment from outside the inlet. Looking at the tidal flats in particular, the connectivity between the tidal flats and the rest of the system appears to be low. In the Bed Composition Generation (BCG) of the model domain, different initial compositions are imposed at the tidal flats. Changes in composition are small and occur at long time scales for all scenarios. This is further supported by the nourishment results, which show that the transport of sediment fractions in the basin is mainly confined to the channels. Finer sediment fractions are transported deeper into the basin. Therefore the connectivity of the back part of the basin is higher for relatively fine sediment fractions.

Third, the connectivity of the ebb tidal delta is evaluated. The connection with the channels is previously discussed. There seems to be a strong connection of the Ameland shore to Terschelling via the ebb tidal delta. Nourishment fractions situated slightly offshore of the Terschelling beach are mainly transported downdrift via the ebb tidal delta. There is no connection in the other direction, nourishment fractions near Terschelling do not reach Ameland. The ebb tidal delta provides a two way connection between the Ameland coast and the basin. Nourishment sediment near Bornrif can end up in the basin via the ebb tidal delta. The other way around sediment fractions located in the basin may be exported over the ebb tidal delta towards the Ameland coast. When fine fractions are exported out of the system they are pushed away further offshore by the tidal currents. Therefore the subsequent downdrift transport with the wave driven flow occurs further offshore, compared to coarser fractions. The same holds for sediment that is bypassing the inlet via the ebb tidal delta.

Fourth, the Terschelling coast is considered. The connections with the rest of the system are discussed above. The most important observation is that nourishment sediment near

the beach of Terschelling is shared with the rest of the system in a much different way than when it is situated further offshore. Nourishments closer to the Terschelling beach are mainly imported via Boschgat. When a nourishment is placed further offshore, bypassing is dominant.

Finally, we look at the connections with Ameland. The part of Bornrif near the tip of Ameland is the only location with an westward connection with the system. From there all nourishment fractions show some transport to the west into the inlet. At the other locations there is no westbound transport. Therefore nourishments east of Terschelling do not contribute to the reinforcement of the Terschelling coastline. Most of the sediment supplied at this location is first transported as a bar and merges with Bornrif Strandhaak, after which it is transported eastward along the Ameland coast.

A nourishment will change the overall sediment composition of the inlet system. After analyzing Figure 3.12 and the model results in Chapter 5, it becomes clear that relatively fine nourishment fractions are often transported over coarser areas. In this way the local bed composition becomes temporarily finer. This is also the case inside the basin, where relatively fine fractions are transported through the coarser channels. On the other hand, relatively coarse fractions remain closer to the nourishment area. As a result the bed near the initial nourishment location becomes coarser. The fining effect caused by the fine fractions is limited, since after a period of 10 years the model predicts that the maximum concentration of the nourishment fraction in the upper layer (upper $0.5m$) of the model domain is about 5%. However, it extends over a considerable area. The coarsening effect of the relatively coarse fractions is larger, locally the concentration of the nourishment fraction in the upper layer can be up to about 50% after 10 years. However this effect is much more local, since the coarser fractions spread out more slowly. Based on this study no conclusions can be drawn regarding the effect of a nourishment on the composition of the tidal flats, since silt ($d < 63\mu m$) is not included in the models.

Based on the conclusions presented above a sand engine type of mega nourishment at the Terschelling coast seems to combine most of the different nourishment objectives. A part of the nourished sand may enter Boschgat, where the coarse sediment feeds Boschplaat and the finer fractions are imported into the basin. Sediment transported from Boschgat to Borndiep can reach the eastern part of the basin. Sand at the offshore end of the nourishment is expected to bypass the inlet and reinforce the ebb tidal delta. Finally when the sediment has bypassed the inlet, it ends up at the Ameland coast. Placing the nourishment at one of the islands further west of Terschelling is also an interesting strategy to consider, since this sediment will have to travel for a longer period before it leaves the Dutch coastal foundation.

6.1.4 Limitations

This study has several limitations. Previously studies have been carried out to validate and calibrate the model. Despite this the limitations are still mainly related to the modeling tools that are applied. First of all the formulations solved in the modeling software cause uncertainty. Advances have been made by implementing sophisticated sediment transport formulas, such as Van Rijn 1993 and Van Rijn 2007 [ELIAS *et al.*, 2015]. However still these formulas are approximations and differences between measurements and the formula outcomes are observed [VAN RIJN *et al.*, 2007].

An important uncertainty is the sediment bypassing mechanism predicted by the model. According to Bruun's r value for the Ameland Inlet (Section 2.3) bypassing will take place

predominantly via the inlet. However, the model predicts that it takes place mainly via the ebb tidal delta. If the model under predicts the import of sediment into the basin, more of the nourishment sediment supplied near Terschelling or at the ebb tidal delta, will end up in the basin.

Moreover, the model includes several factors for the sediment transport processes, which can be used to calibrate the model to transport or bathymetry data from the study area. However accurate data for this calibration is not yet available for the Ameland Inlet and therefore the settings are based on previous studies of other coastal systems. The transport patterns may therefore be different than predicted by the model. As a result this study may not provide the optimal dredging strategies for the different objectives. Additionally the input reduction techniques used for the tide and the wave climate will have some effect on the model results.

In this study the tidal watersheds are modeled as closed boundaries, since the connectivity to the other basins is expected to be limited [RIDDERINKHOF, 1988; DISSANAYAKE *et al.*, 2012b]. However the watersheds do allow for transport, especially by wind-driven flow [WANG *et al.*, 2012]. As a result, the finer nourishment fractions may be transported over the tidal watersheds. However, since the import of sediment into the basin is limited, the loss of nourishment fractions to the other basins is expected to be limited as well.

Furthermore, the data poses limitations on this study. The wave data for instance is obtained from measurement station Schiermonnikoog North (SON), which is located quite far from the Ameland Inlet. The model results show that waves are highly important for the sediment transport. Inaccuracies in the wave climate may effect the modeled sediment transport pathways and thereby the effectiveness of the different nourishment strategies. Setting up a new wave climate based on measured data near the study area may improve the model outcomes.

Finally, the assessment of the ecological impact of a nourishment is limited, since not much is yet known about the flora and fauna in the ebb tidal delta region of the Ameland Inlet. Therefore the ecological impact of the nourishments described in this thesis may differ from the actual impact.

Because of these limitations, it does not seem appropriate to use the model for accurate quantitative predictions. Despite this it is expected to give a good image of the transport pathways of nourishment sediment fractions, since many phenomena observed in the field are predicted by the model.

6.2 Other inlet systems

In this section an attempt is made to generalize the results and apply them to tidal inlet systems at other locations. First another mixed energy inlet in the Wadden Sea is considered. Hereafter the results are applied to a wave dominated system and finally a tide dominated system is treated. It concerns merely a qualitative analysis, no data analysis or model simulations have been performed for these sites. More research into these inlets is necessary to validate the recommendations below.

The Eierlandse Gat Inlet in between Vlieland and Terschelling, see Figure 1.1 is a mixed energy wave dominant environment, just like the Ameland Inlet [ELIAS *et al.*, 2012]. It is also a two channel system, however the main one lies west of the secondary channel. The wave driven bypassing and tide driven import and export are therefore expected to be similar as

indicated in Figure 6.1. Consequently similar nourishment strategies may be recommended as for the Ameland Inlet. This means that when the objective is to feed the Vlieland coast, it seems best to place the nourishment in this same area. The Terschelling coast can be nourished by placing sediment updrift, at the ebb tidal delta or in from of Vlieland. Coarser fractions will arrive closer to the Terschelling coast in this case. The ebb tidal delta can be reinforced in a similar way, at the ebb tidal delta or the Vlieland coast. When placed at the delta, a coarse nourishment is more beneficial, since the finer fractions experience a stronger bypassing. If the Vlieland coast is used as nourishment location, finer sand seems better, since the coarse fractions may not reach Terschelling within the foreseeable future. Finally, feeding the basin is probably best achieved by placing a relatively fine nourishment inside.

The Albufeira Lagoon, located on the west coast of Portugal (Figure 6.2) is classified as a wave dominated inlet [DODET *et al.*, 2013]. Waves cause a relatively small net littoral drift of $3 - 5 \cdot 10^3 m^3 / year$ in southern direction BAO *et al.* [1999]. The relative importance of the waves locally is clearly visible by the relatively straight coastline and the large amount of sediment in the throat of the inlet. The wave induced bypassing is expected to be relatively stronger at this location, compared to the Ameland Inlet. It is likely that there will be less exchange of sediment between the basin and the outside area. So again if the objective is to feed the basin, fine sediment should be placed in the basin. Due to the relatively high wave energy no clear ebb tidal delta is developed and therefore reinforcing it will not be an objective for a nourishment in this area. The coastline can be fed by placing a nourishment at a location in the North, wave induced currents will then transport the sediment in southern direction. Since the net littoral drift is relatively small, this will occur slowly. Therefore even for the fine nourishment fractions, transport distances will be small over time. Consequently if the objective is to feed the downdrift coastline, relatively fine sediment should be used.

The Boca Grande pass is an example of a tide dominated barrier inlet system. It is located on the west coast of Florida (Figure 6.3). The importance of the tide is evident from the main channel cutting through the extensive ebb tidal delta. In this case the in and export of sediment indicated in Figure 6.1 is expected to be much stronger. Bypassing via the ebb tidal delta is expected to be of minor importance. Therefore all nourishments placed on the updrift side of the inlet are expected to feed the basin. It is likely that even the coarse fractions will be imported by the strong tidal flow. The outflowing currents will feed the ebb tidal delta. However, since the wave energy is relatively low, reinforcing the ebb tidal delta does not seem important in this case, the wave sheltering function of it is limited. If the barrier coast needs to be nourished and import into the basin is undesired, the nourishment should be placed downdrift of the inlet. To feed the updrift coast, while limiting the import in the basin, a coarse and stable nourishment should be applied directly at the location that needs to be fed, since all fractions are likely to be imported into the basin when being transported downdrift.

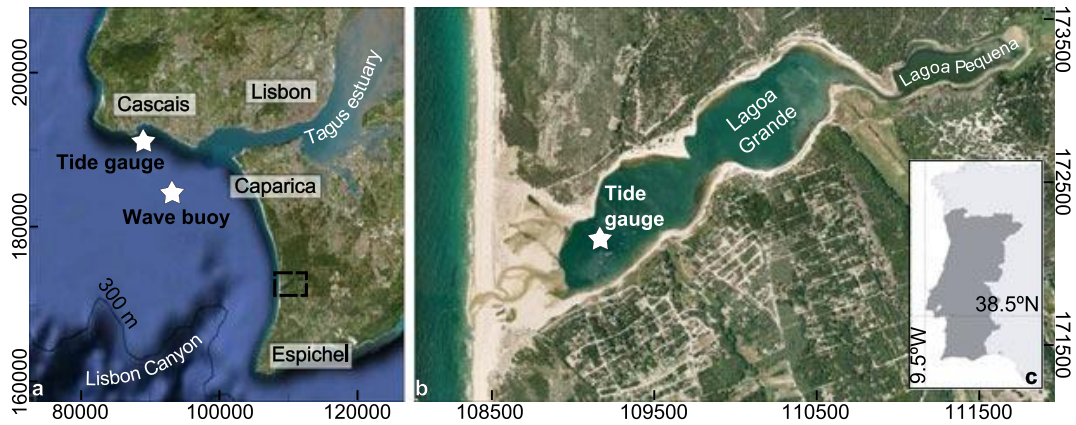
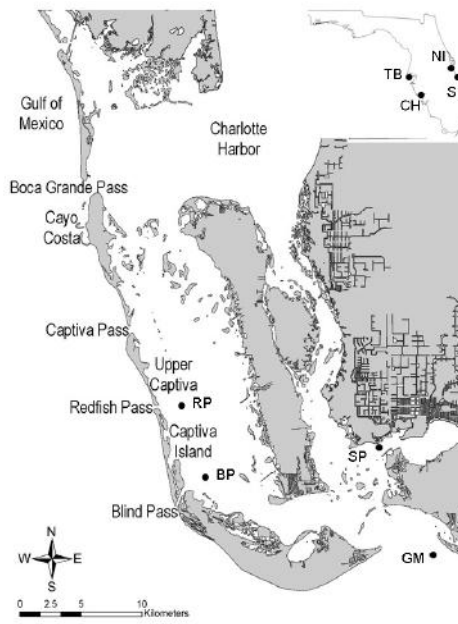
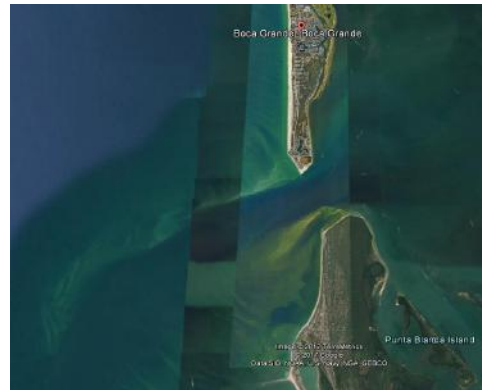


Figure 6.2: The Albufeira Lagoon, obtained from DODET *et al.* [2013]



(a) Map of southwestern Florida, obtained from ADAMS *et al.* [2012]



(b) Aerial view of the Boca Grande Pass, obtained from Google Earth

Figure 6.3: The Boca Grande Pass

7.1 Conclusions

The research presented in this thesis had improved our understanding of how nourishment sand fractions are shared between the different morphological units of the Ameland Inlet system. An existing Delft3D model of the system has been improved and adjusted to make predictions regarding the transport processes.

The first sub question is: What type of sediment is available for a nourishment? This question is answered by analyzing the bottom investigation report of the borrow area, provided by Rijkswaterstaat [LABAN, 2014]. It shows that the borrow area mainly consists of sand with a D_{50} of 140 – 180 μm , however there is a distinct area consisting of coarser sand with a D_{50} of 300 – 420 μm . The composition of the modeled nourishments is based on the particle size distribution of the sand in the borrow area.

The model results for the different nourishment locations provide an answer to the second research question: Depending on the goal of the nourishment, which locations are suitable? Nourishments in a complex system like the Ameland Inlet behave in a significantly different way when placed at a different location. Suitable nourishment strategies for the predefined objectives are discussed in depth in Section 6.1.3. In short, when the objective is to feed the near shore of Terschelling, including Boschplaat, it is recommended to place a nourishment on the beach of Terschelling or in Boschgat.

If the goal is to feed the northern and western part of the Ameland coast, it seems best to place the nourishment near Bornrif, from there Bornrif strandhaak is reinforced and the sediment transported downdrift remains relatively close to the beach. Especially coarse sediment reinforce Bornrif on the long run, finer sediment is moved downdrift quickly. At other locations in the system, the sediment will also eventually reach Ameland, if in those cases coarser sand is supplied, it arrives closer to the Ameland shoreline. The southwestern tip of Ameland, next to Bornrif is harder to reinforce efficiently. The model results suggest that the only way to get more sediment in this high velocity area is to place a nourishment at this location. In this case relatively fine fractions are ineffective, they are moved away within a short period of time. Coarse fractions remain longer at the initial location, however they still show a significant transport. Therefore it is recommended to apply a coarse nourishment at this location. However, if no additional 'hard' measures are taken, it is likely that nourishments have to be repeated every couple of years. Unless accretion of the coast

starts again in a future stage of the cycle (see Section 2.2 for cyclic behavior of the Ameland Inlet).

To reinforce the ebb tidal delta a nourishment can be placed directly at the ebb tidal delta, or updrift, offshore of the Terschelling coastline. In the latter case the bypassing fractions feed the delta. When it is placed more to the east, it is further in the stage of bypassing and therefore the sand will reach Terschelling faster. At the ebb tidal delta it is recommended to apply relatively coarse sediment, since the fine fractions are removed quickly. Updrift of the delta the nourishment should consist of finer material, since otherwise it takes long before the ebb tidal delta is reached.

If the objective of a nourishment is to feed the basin, it is recommended to place it on the Terschelling beach or in Boschgat. From there the western part of the basin is fed, mainly by applying relatively fine sediment. The eastern part should be fed by placing the nourishment in the system, since import from outside the inlet is limited for this area, according to the model results. On the other hand if feeding the basin is undesired, for instance due to the possible negative effects on the local ecology, it is recommended to supply a relatively coarse nourishment, since coarse fractions do not seem to penetrate deep into the basin.

The third sub question is: What is the effect of the composition on the fate of a nourishment? This question is answered based on the model results for the two different nourishment compositions. It is found that when coarser sand is used, the stability of a nourishment can be increased. The transport rates of the available sediment are in this way reduced and increased armoring of the fine fractions under coarser fractions takes place. The North Sea is not a warehouse from which sediment of all different grain sizes can be selected. Nonetheless the borrow area information shows us that distinct large areas with relatively coarse or fine sediment can be found. Since the grain size appears to have a large effect on the effectiveness of a nourishment, selecting the material based on the nourishment objectives may pay off.

Finally, the main research question can be answered: How is nourishment sand of different grain sizes shared between the different morphological units of the Ameland Inlet system? The model results predict that the tidal flow is mainly responsible for the import in and export out of the basin. When wave forcing is included the transport over shallow areas is increased and a strong bypassing mechanism is observed, through which sediment from the Terschelling coast is transported over the ebb tidal delta towards the Ameland coast. This is in line with the results of other studies [BRUUN AND GERRITSEN, 1960; CHEUNG *et al.*, 2007]. However, the bypassing mechanism predicted by the model is stronger than expected based on Bruun's r value, see Section 2.3. On the other hand the classification of the inlet as a mixed energy wave dominant environment [HAYES, 1979; DAVIS AND HAYES, 1984] seems to be appropriate, since there is exchange of sediment via the inlet, however bypassing via the ebb tidal delta is dominant. Finer fractions are imported further into the basin by the tidal flow. When bypassing the inlet, they are transported further offshore, since they are more influenced by the tidal currents flowing out of the inlet.

At the Ameland coast, strong differences in the nourishment sediment pathways are observed, depending on the cross shore location of the nourishment. Near the Terschelling beach import via Boschgat is dominant. Further offshore, most sediment bypasses the inlet rather than exchanging with the basin. Interaction between Boschgat, feeding the western part of the basin and Borndiep, feeding the eastern part, is limited. The model predicts some transport from Boschgat to Borndiep, via Westgat, or over the shallow area in between

Boschgat and Borndiep, for the relatively fine fractions. The connection via Westgat is tide driven, the transport over the shallow area is wave driven. There is no connection in the other direction: nourishment fractions in Borndiep do not reach Boschgat.

In general, finer nourishment sediments are moved away faster and further, also spreading out over a larger area over time, which is in line with the expectations. This is mainly the case in wave dominated areas such as the ebb tidal delta. In tide dominated areas with high flow velocities, such as Borndiep, even the coarsest nourishment sediment is transported over considerable distances.

Based on the model results, a mega nourishment comparable to the sand engine at the Terschelling coast seems to be a beneficial solution. This nourishment is expected to feed Boschplaat, the basin, and the bypassing sand reinforces the ebb tidal delta and the Ameland coast.

7.2 Recommendations

As stated in the introduction, the research presented in this thesis is part of the SEAWAD project. Based on the work performed for this thesis, several recommendations are provided for the further course of the project.

Delft3D is suitable for tracking different sediment particles, especially when large quantities of sand are considered, which is the case for the nourishments. By applying the Mormerge approach (parallel online approach) in combination with a phase shift in the tidal signal for each of the wave conditions, high *Morfac* values can be applied without resulting in instabilities. This approach makes long term modeling much more efficient.

Bed Composition Generation (BCG) in Delft3D can be applied to generate the bottom for the model domain. When the initial fractions for the BCG are selected carefully, a bottom can be generated that shows approximately the same distribution as the Wadden Sea Sediment Atlas.

It is recommended to base the composition of the nourishment on the particle size distributions found in the borrow area bottom investigation report. In Delft3D the nourishment fractions should be specified by the minimum and maximum sediment diameter, it then computes the associated D_{50} values itself. In this way overlap between the grain size distributions, which would occur if instead of minimum and maximum values, the D_{50} values for each fraction are specified (since Delft3D assumes a certain grain size distribution based on these D_{50} values, see DELTARES [2014a]), is prevented. Boundary issues in the model can be prevented by placing a layer on top of the nourishment layers with a thickness of 0 at the nourishment location and the desired thickness elsewhere.

However, the modeling software also poses limitations, discussed in Section 6.1.4. These are mainly related to the calibration and validation of the model. Previously different research projects have been carried out to improve the model and to make it suitable for medium term modeling [DE FOCKERT, 2008; JIAO, 2014; WANG, 2015; WANG *et al.*, 2016]. Yet not enough measurement data was available for a sound calibration and validation. Since there will be a extensive measurement campaign in September, it is recommended to gather data that can be used for the fine tuning and verification of the model. Discharge measurements can for instance be used to calibrate the hydrodynamic processes in the model.

Especially the transport calibration factors *Sus*, *Bed*, *SusW* and *BedW* seem to be important for the model calibration, see Section 3.6. By frequently measuring the bathymetry and

comparing the results over time, the model can be fine tuned by changing these factors. Alternatively sediment transport measurements can be used.

The sediment tracer study that is currently performed can also be used to calibrate these factors. In this tracer study a certain amount of tracer sediment is supplied on the ebb tidal delta, in the pilot nourishment area (location 3). Subsequently sediment samples are taken in order to find out where the tracer migrates. Another interesting application of the results of the tracer study is to validate the sediment bypassing as predicted by the model. The model predicts that bypassing via the ebb tidal delta is dominant. If much of the tracer material is found back further eastward on the ebb tidal delta, this may increase the confidence in the model. However, if most of the tracer is found on its way to the inlet, bypassing via the inlet may be underestimated and the model has to be adjusted.

The model can further be upgraded by including the transport over the tidal watersheds, which are now modeled as closed boundaries. For instance by nesting the Ameland Inlet model into a larger Wadden Sea model, the flow over the watersheds can be calculated and subsequently imposed as boundary conditions in the Ameland Inlet model. In this way the loss of nourishment sediment to other basins can be modeled as well.

Moreover, the model can be improved by updating the reduced wave climate. It is currently based on measurements of the measurement station SON (Schiermonnikoog North). However, this buoy is located quite far from the Ameland Inlet. Eight years of wave data, measured near the Ameland Inlet is now available at Rijkswaterstaat. The current Delft3D model can be improved by setting up a reduced wave climate based on this data.

Furthermore, it is recommended to do some more research into the sediment transport processes at other inlet systems, to gain more insight in how the results for the Ameland Inlet can be applied to these systems. For instance the relative impact of the tide and the waves can be varied in the model, in order to get an idea of how a different system will respond to the nourishments. If there is a wider application of the results of this study, it becomes much more valuable.

Finally it will be interesting to find out what the effect is of the cyclic behavior of the inlet on the long term evolution of the system. By applying different bathymetries in the model, knowledge regarding the future behavior of the system can be gained, so one can anticipate when a nourishment is designed.

Appendix A

Bottom Composition Generation

A.1 Tide only scenario

The graphs here show the evolution of the bottom composition over time at four locations in the model domain, for four different initial bottom compositions, see section A.

Figures A.11 and A.12 show the evolution of the D_{50} over time for bottom composition 1 and 2. From the envelopes of the graphs it can be inferred that most of the change in bottom composition occurs in the first ten years. Figures A.13 and A.14 show the results for the same model scenarios, but with an increased $MorFac$ of 100. Figures A.15 and A.16 show this development for scenarios 3 and 4.

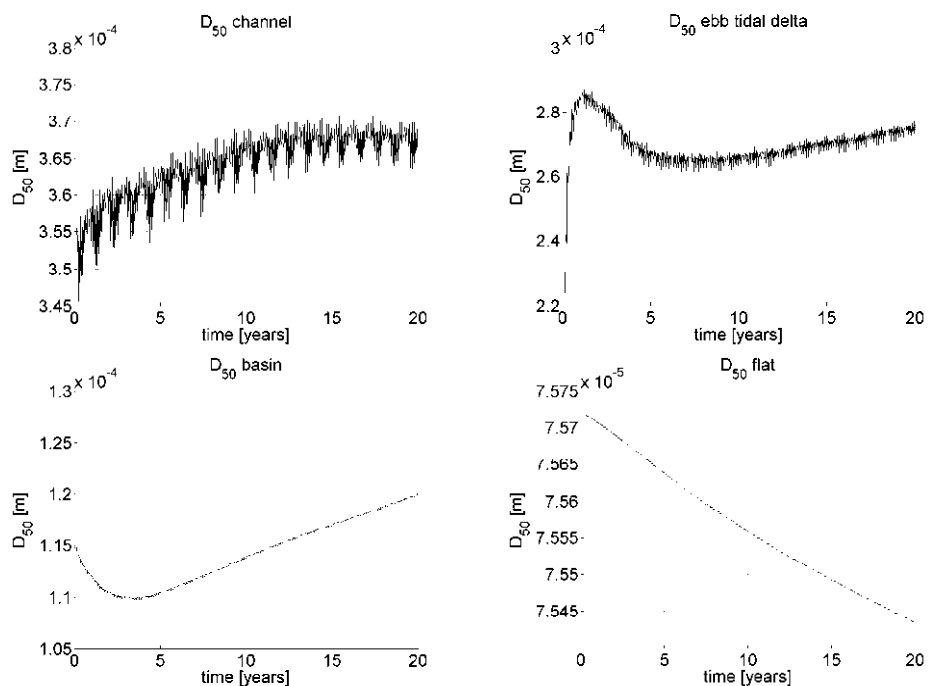


Figure A.11: Composition 1 with a $MorFac$ of 50, D_{50} evolution over time, tide only

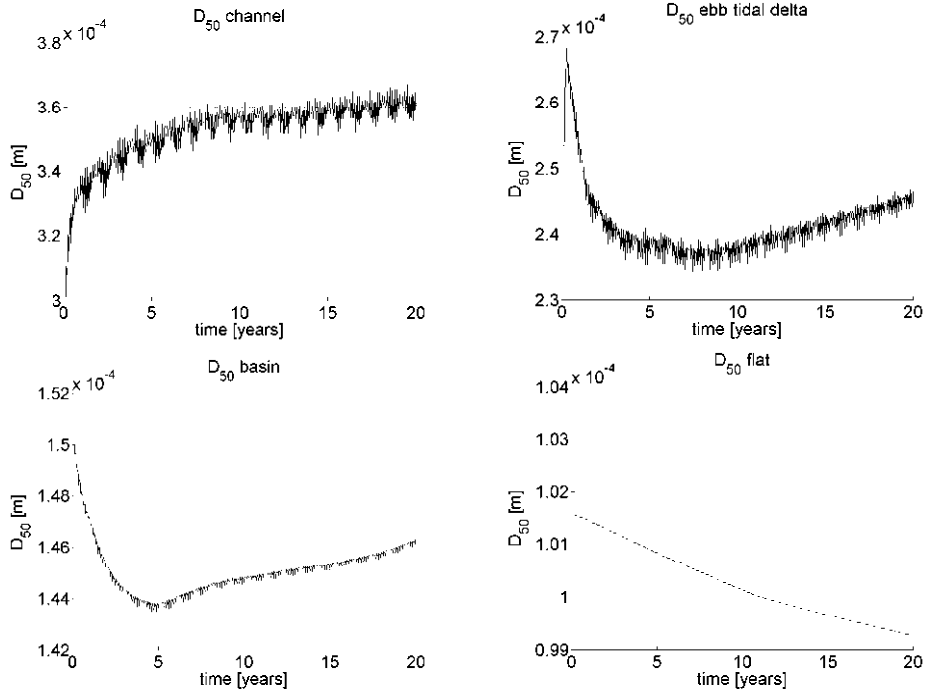


Figure A.12: Composition 2 with a $MorFac$ of 50, D_{50} evolution over time, tide only

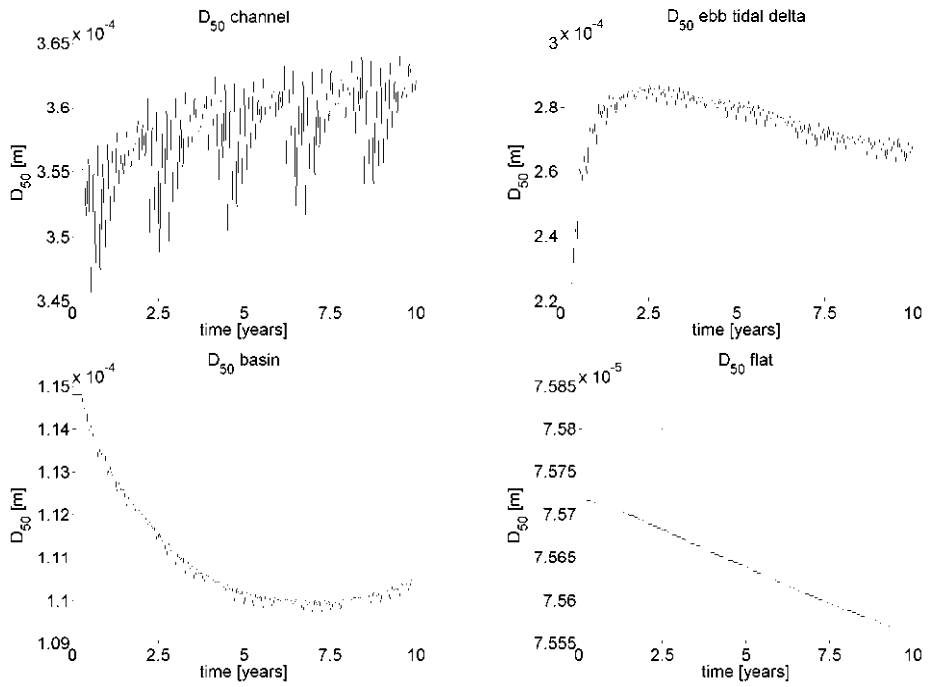


Figure A.13: Composition 1 with a $MorFac$ of 100, D_{50} evolution over time, tide only

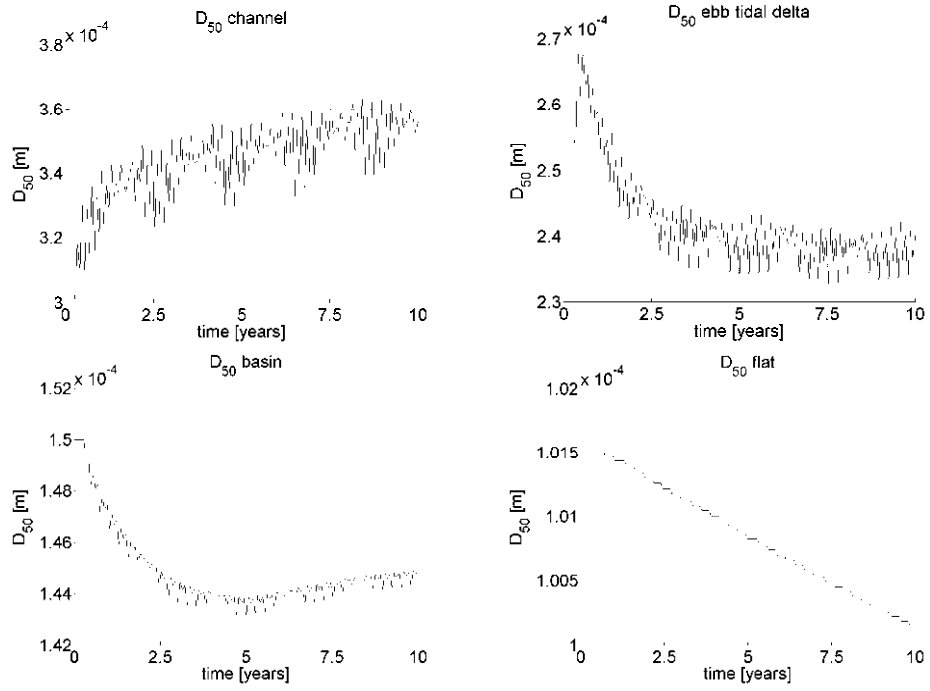


Figure A.14: Composition 2 with a *MorFac* of 100, D_{50} evolution over time, tide only

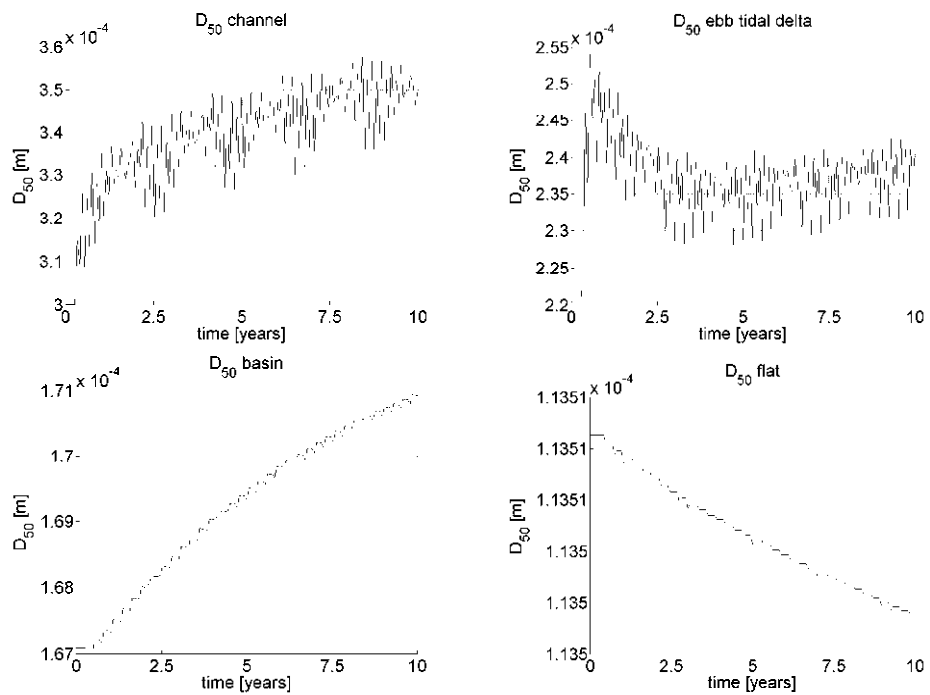


Figure A.15: Composition 3 with a *MorFac* of 100, D_{50} evolution over time, tide only

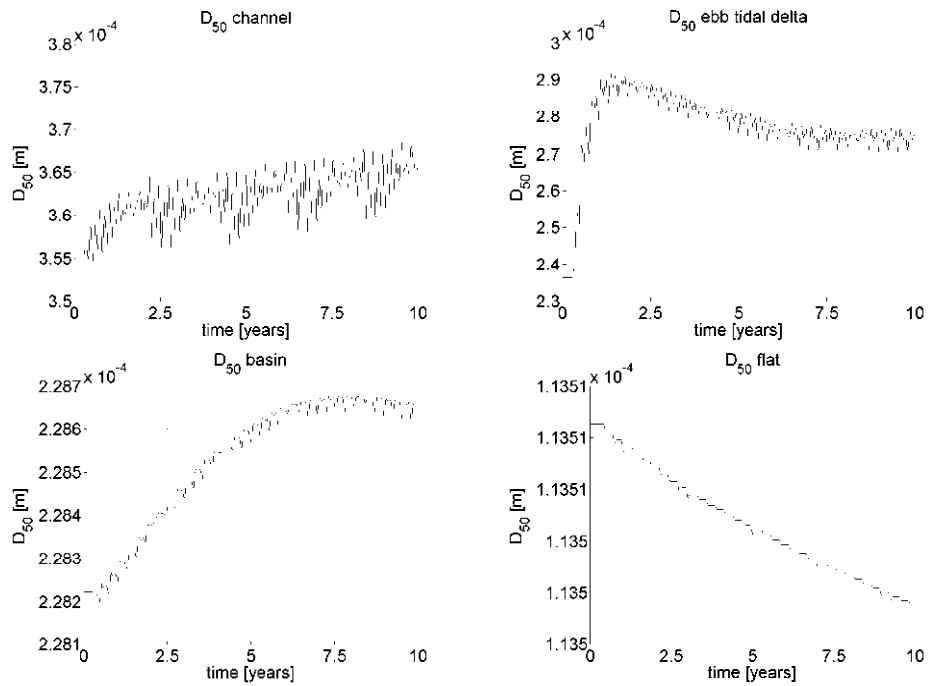


Figure A.16: Composition 4 with a *MorFac* of 100, D_{50} evolution over time, tide only

A.2 Tide, wind and waves

First the sensitivity regarding the *MorFac* setting is evaluated, by performing a BCG for composition 1 for *Morfac* values of 100 and 200, the value as suggested by JIAO [2014]. Both models show the same results, see figures A.27 and A.28. Furthermore it can be concluded again that most change in bottom composition occurs in the first ten years. Therefore the BCG runs will be performed with a *MorFac* of 200 and it will be limited to a period of ten years. The bottom evolution graphs for the simulations with initial composition 3 and 4 are shown in figures A.210 and A.211.

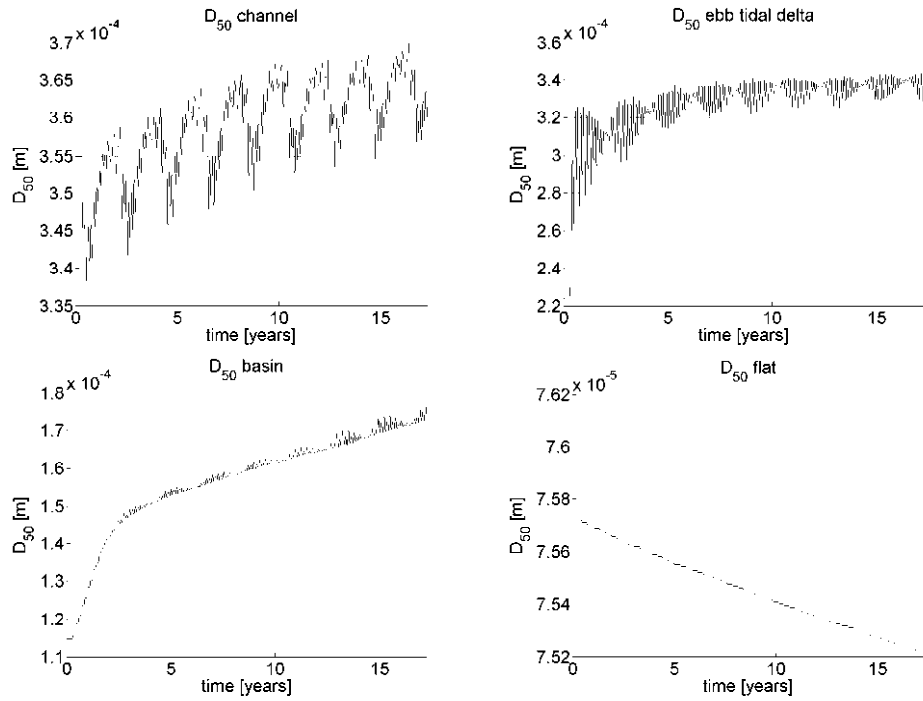


Figure A.27: Composition 1 with a $MorFac$ of 100, D_{50} evolution over time, tide wind and waves

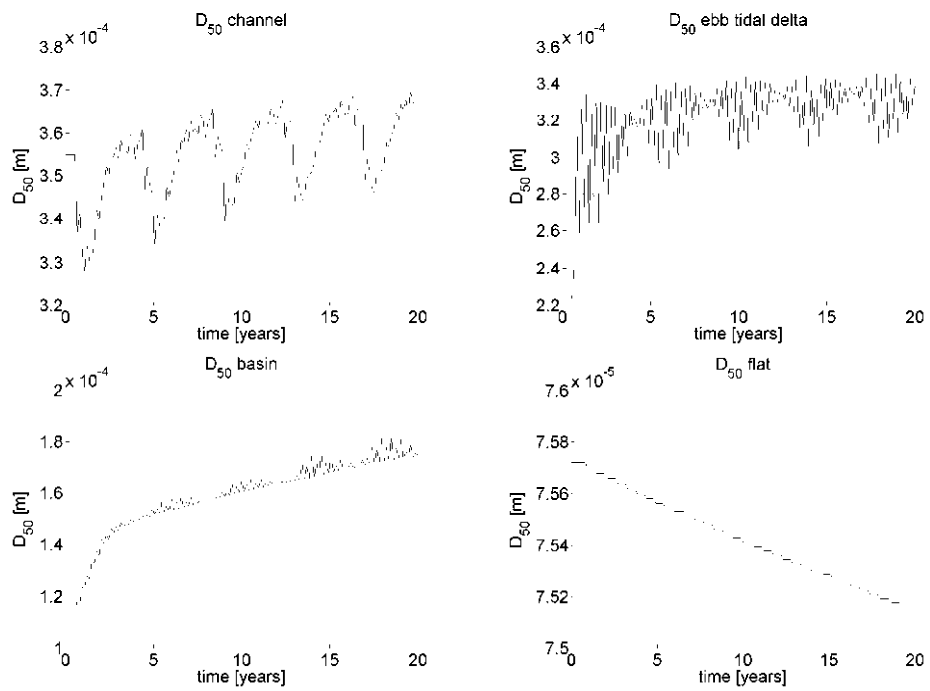


Figure A.28: Composition 1 with a $MorFac$ of 200, D_{50} evolution over time, tide wind and waves

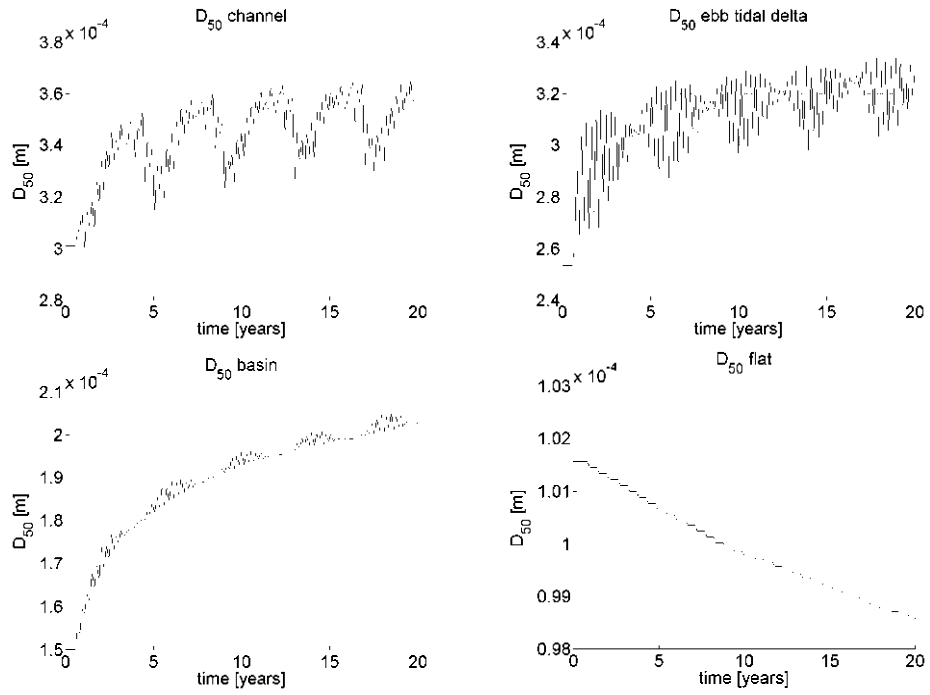


Figure A.29: Composition 2 with a $MorFac$ of 200, D_{50} evolution over time, tide wind and waves

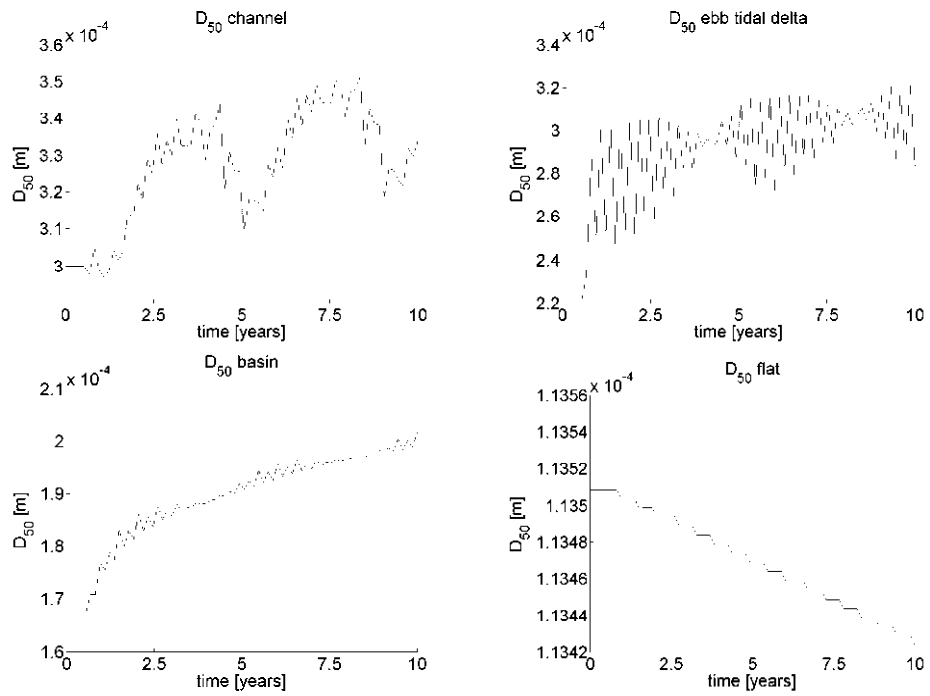


Figure A.210: Composition 3 with a $MorFac$ of 200, D_{50} evolution over time, tide wind and waves

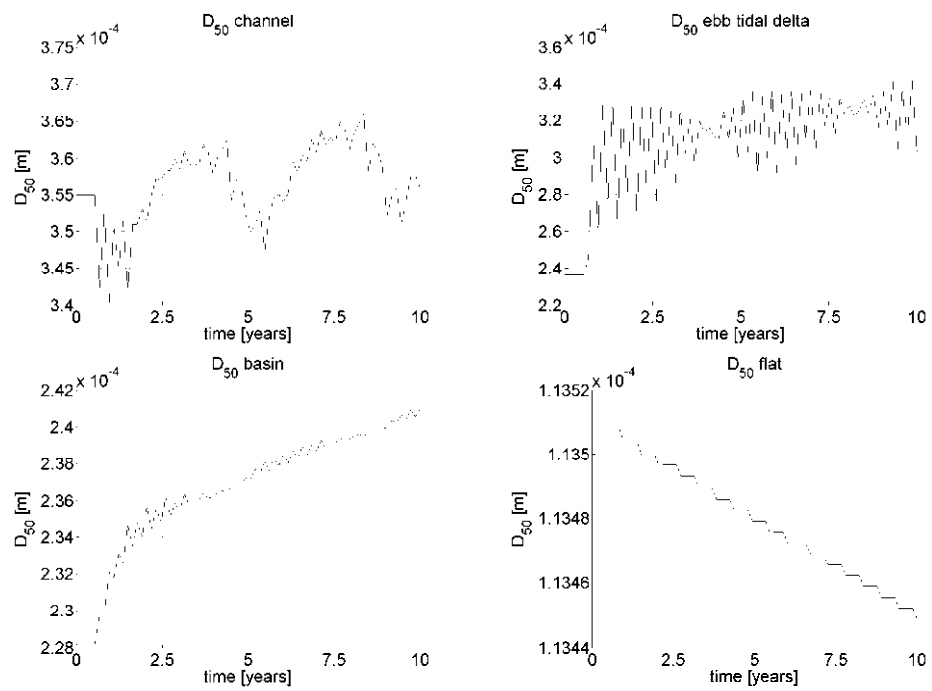


Figure A.211: Composition 4 with a *MorFac* of 200, D_{50} evolution over time, tide wind and waves

Appendix B

Map of the borrow areas

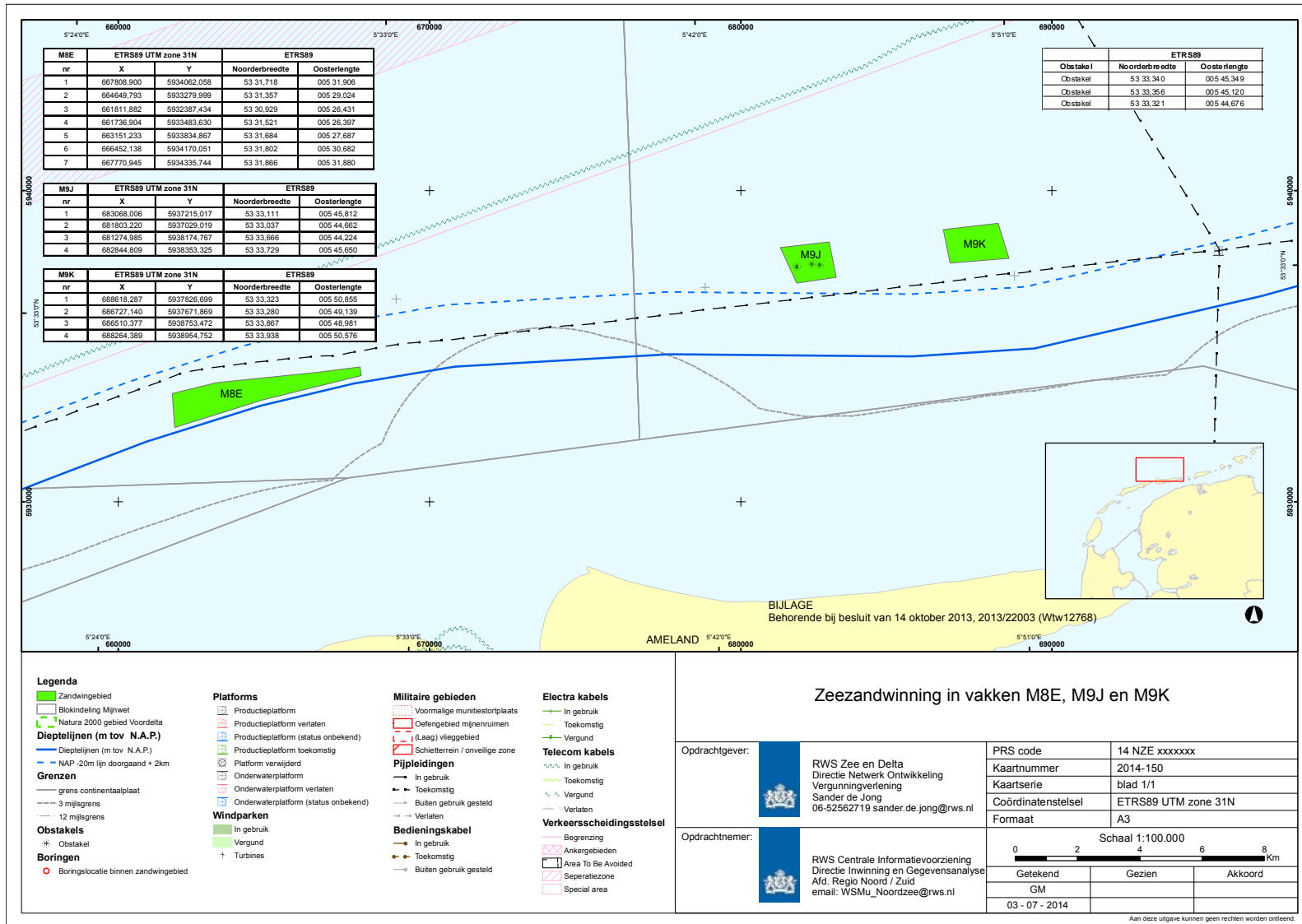


Figure B.01: Map showing the borrow areas M8E, M9J and M9K. Obtained from Rijkswaterstaat

Appendix C

Total transports

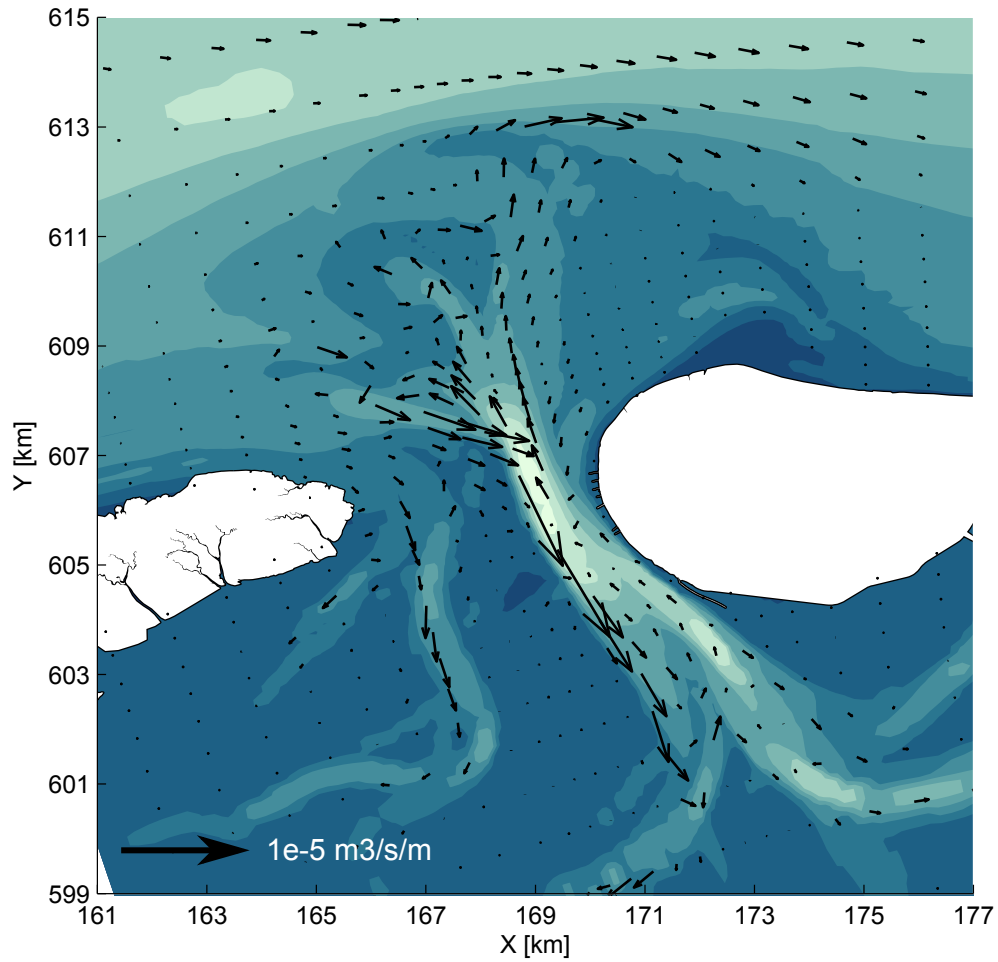


Figure C.01: Tide driven total transport of the $100\mu\text{m}$ fraction, tide only

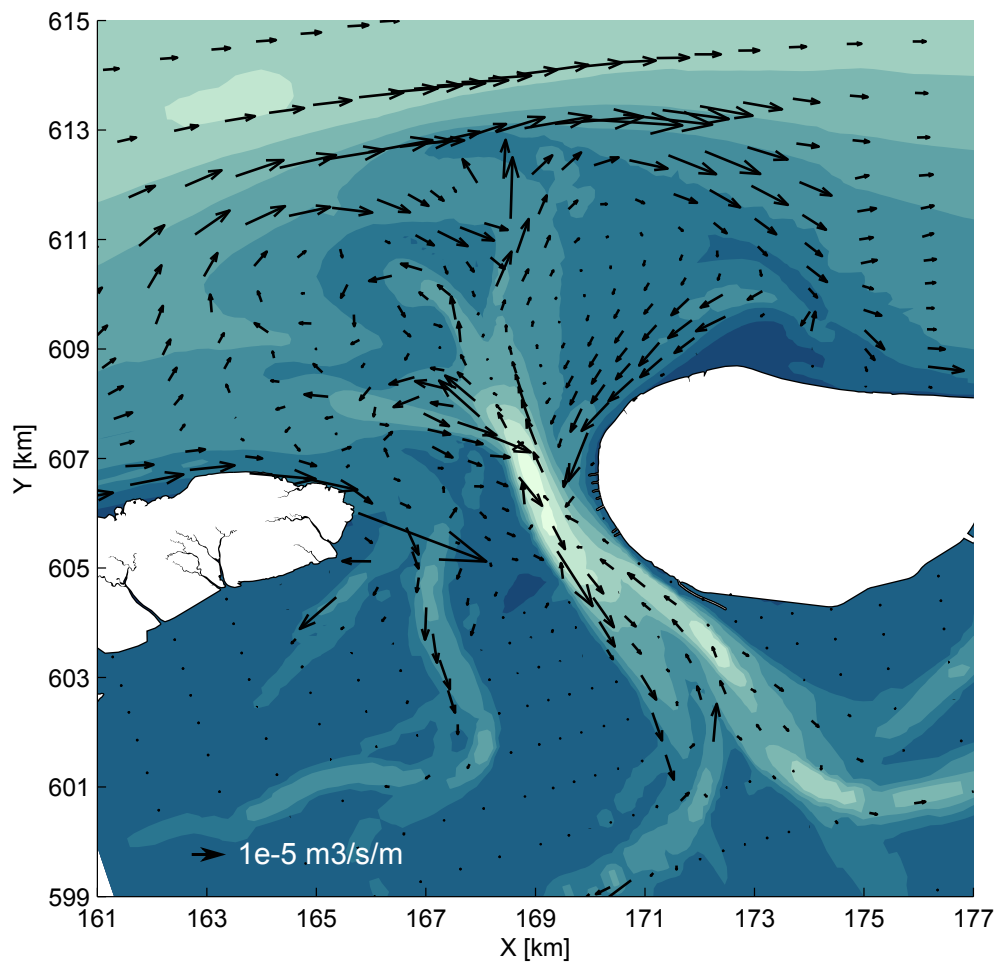


Figure C.02: Tide wave and wind driven total transport of the $100\mu\text{m}$ fraction

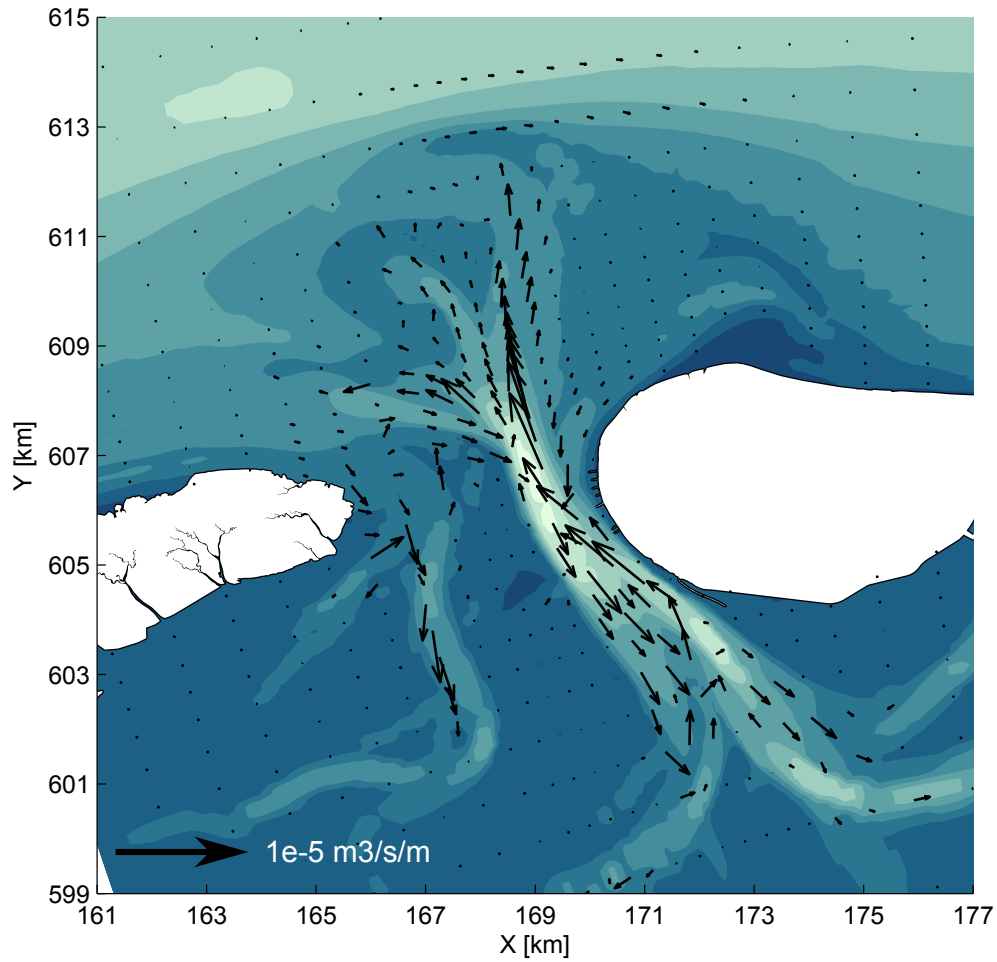


Figure C.03: Tide driven total transport of the $200\mu\text{m}$ fraction, tide only

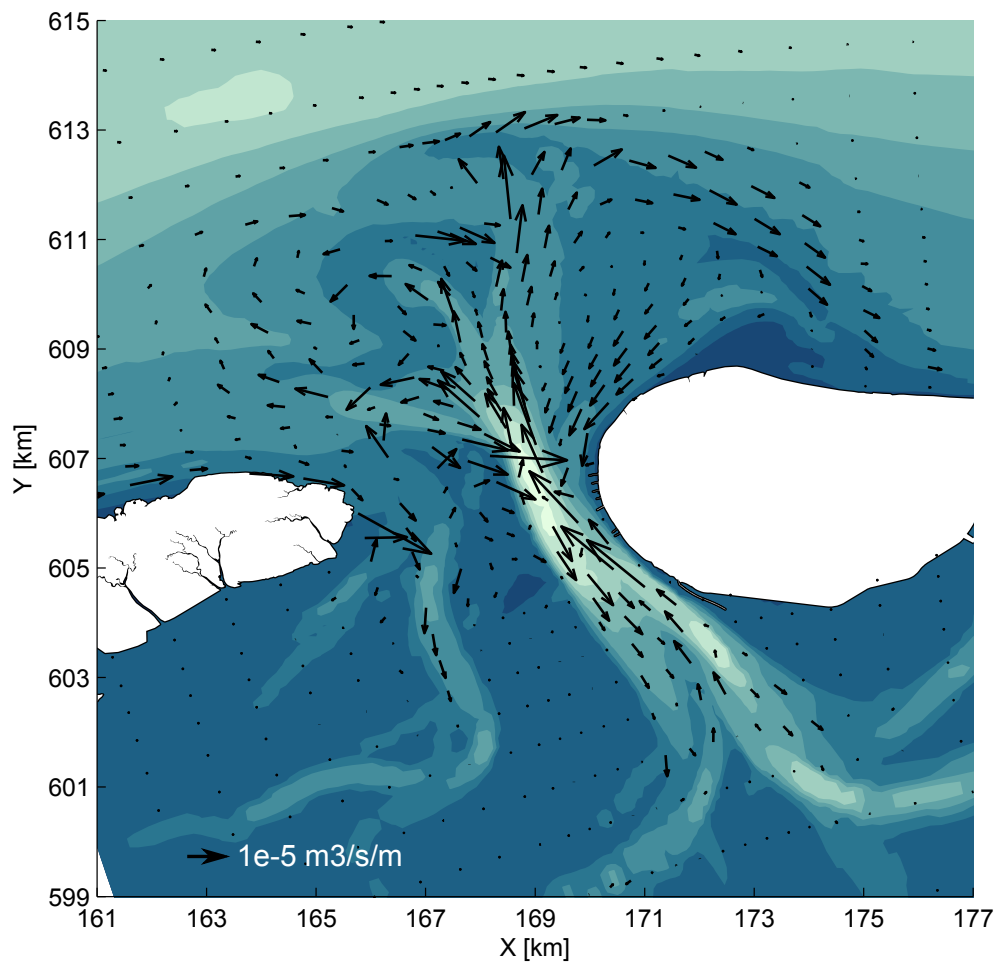


Figure C.04: Tide wave and wind driven total transport of the $200\mu\text{m}$ fraction

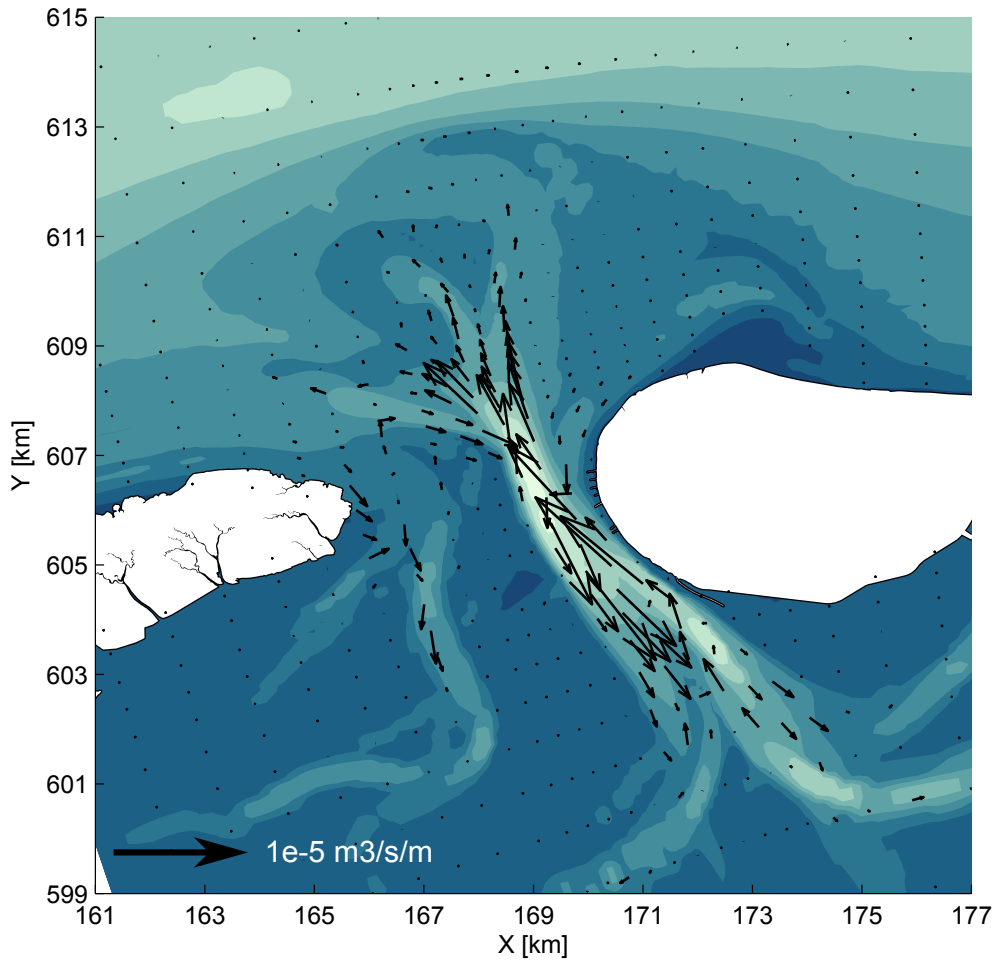


Figure C.05: Tide driven total transport of the 300 μm fraction, tide only

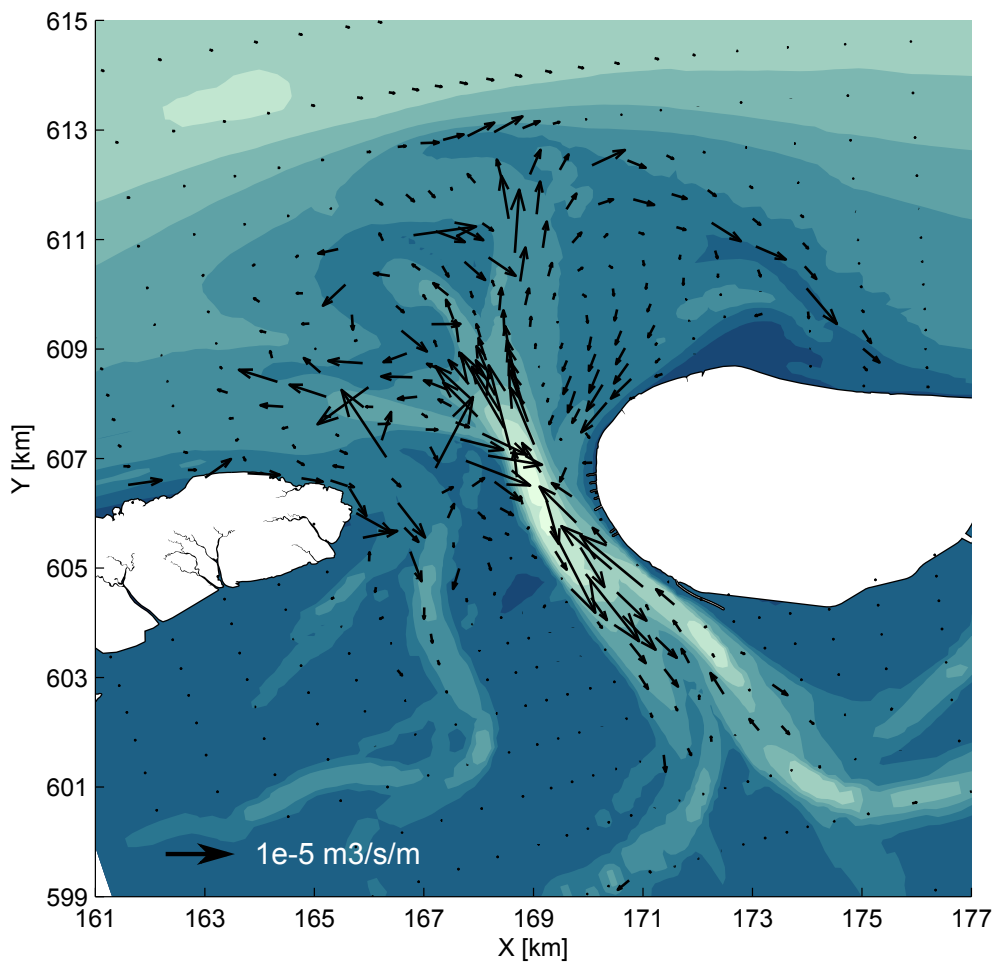


Figure C.06: Tide wave and wind driven total transport of the 300 μm fraction

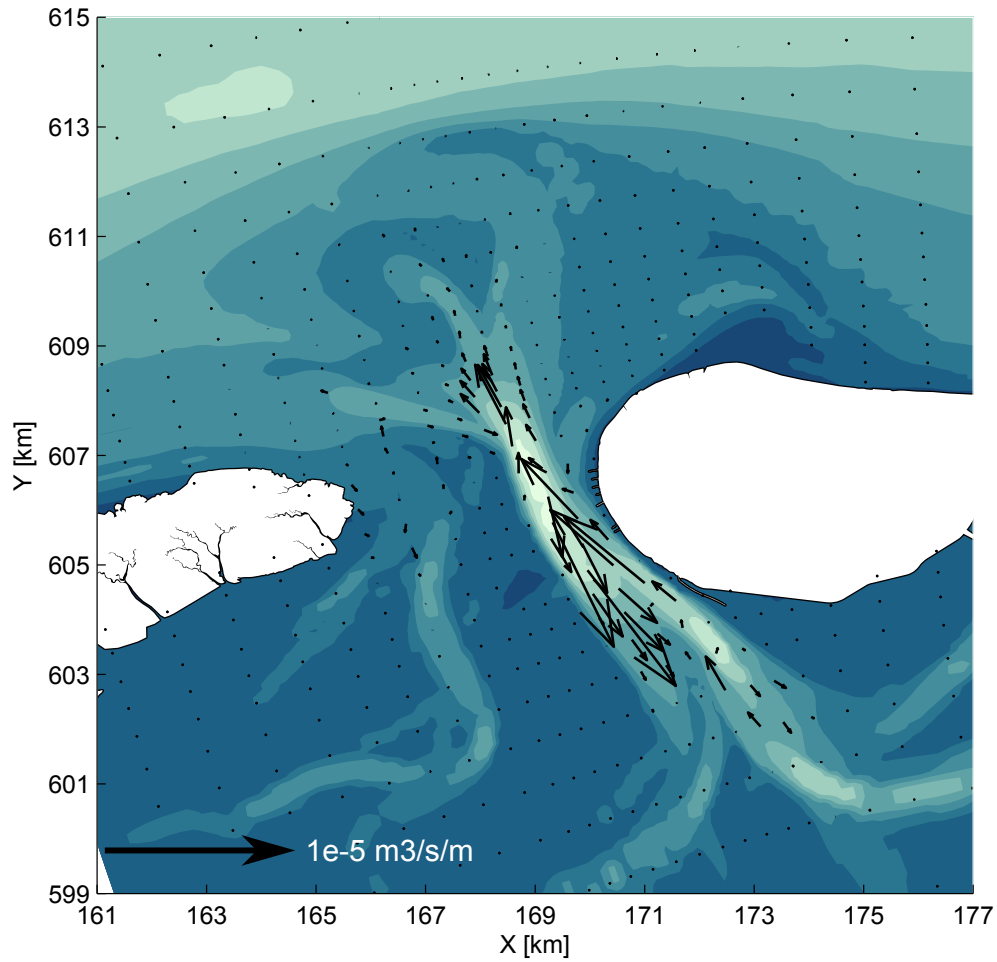


Figure C.07: Tide driven total transport of the $400\mu\text{m}$ fraction, tide only

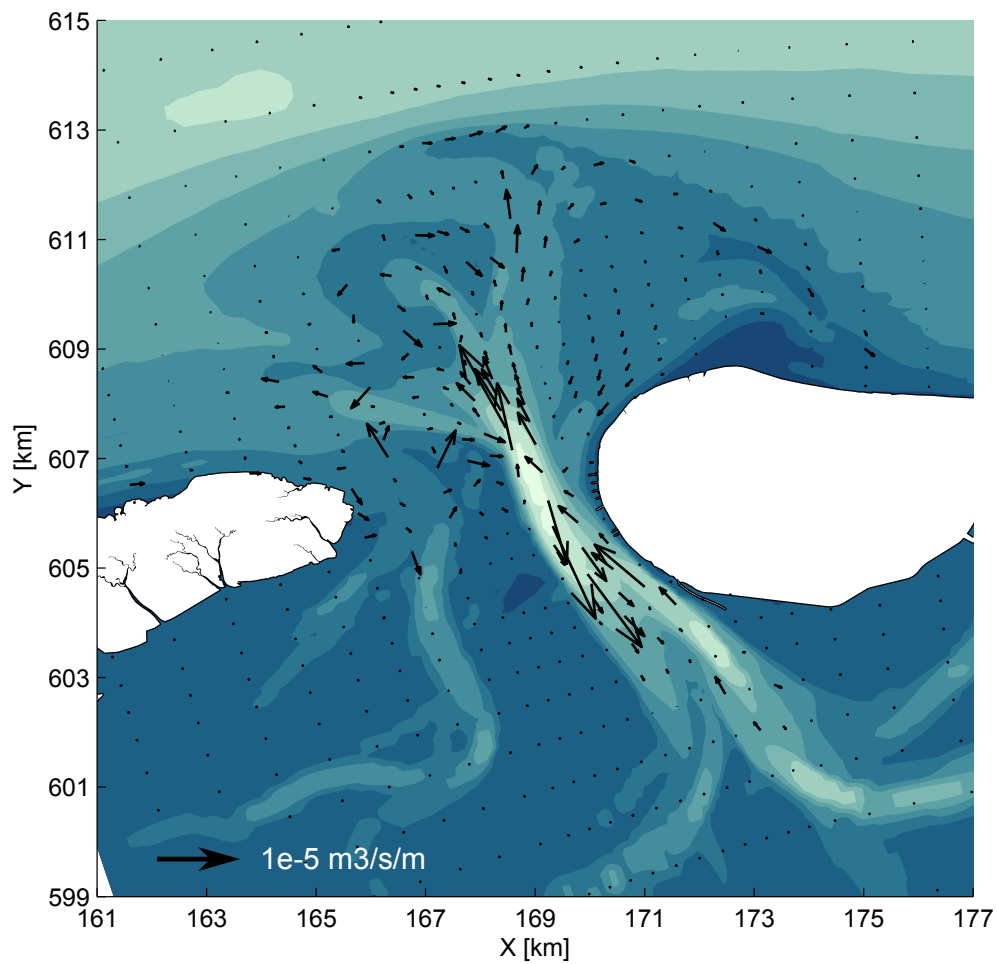


Figure C.08: Tide wave and wind driven total transport of the $400\mu\text{m}$ fraction

Appendix D

Vaklodingen 2014 and 2016

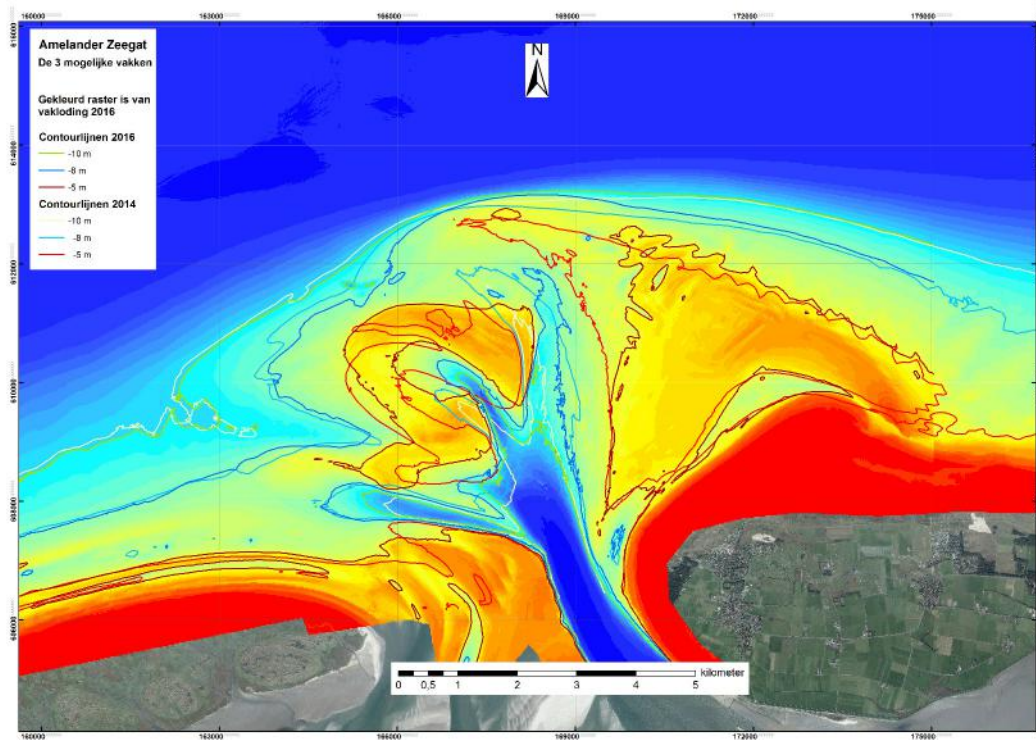


Figure D.01: Map showing the depth contours from the 2014 and 2016 Vaklodingen. Obtained from Rijkswaterstaat

- ACHETE, F.M. (2011) Morphodynamics of the Ameland Bornrif, 70
- ADAMS, A., HILL, J., KURTH, B. AND BARBOUR, A. (2012) Effects of a severe cold event on the subtropical, estuarine-dependent common snook, *Centropomus undecimalis*. *Gulf and Caribbean Research*, 24(Taylor 2000), 13–21
- AMELANDGANGER (2017) MS Zeehond
- BAO, R., DA CONCEICAO FREITAS, M. AND ANDRADE, C. (1999) Separating eustatic from local environmental effects: a late-Holocene record of coastal change in Albufeira Lagoon, Portugal. *The Holocene*, 9(3), 341–352. doi:10.1191/095968399675815073
- BAPTIST, A.M.J., WAL, J.T.V.D., GROOT, A.V.D. AND YSEBAERT, T.J.W. (2016) Eco-topenkaart Waddenzee volgens de ZES.1 typologie. *Tech. rep.*
- BHATTACHARYA, B., PRICE, R.K. AND SOLOMATINE, D.P. (2007) a Machine Learning Approach To Modeling Sediment Transport. 133(4), 440–450. doi:10.1061/(ASCE)0733-9429(2007)133
- BOSBOOM, J. AND STIVE, J. (2010) Coastal Dynamics 1. VSSD, Leeghwaterstraat 42 Delft, The Netherlands
- BOSKALIS (1999) Equipment Sheet
- BRUINS, R. (2016) Morphological behaviour of shoreface nourishments along the Dutch coast. *MSc thesis*
- BRUUN, P. (1978) Stability of tidal inlets, theory and engineering. *Developments in geotechnical engineering*, 23
- BRUUN, P. AND GERRITSEN, F. (1960) Stability of Coastal Inlets. *Coastal Engineering Proceedings*, 1(7), 23. doi:10.2307/1350422
- CBS (2017) Bevolkingsontwikkeling; regio per maand
- CHEUNG, K.F., GERRITSEN, F. AND CLEVERINGA, J. (2007) Morphodynamics and Sand Bypassing at Ameland Inlet, The Netherlands. *Journal of Coastal Research*, 231, 106–118. doi:10.2112/04-0403.1
- CLEVERINGA, J., ISRAËL, C.G. AND DUNSBERGEN, D.W. (2005) De westkust van Ameland. Resultaten van 10 jaar morfologisch onderzoek in het kader van de Rijkswaterstaat programma's KUST2000 en KUST2005. doi:Rapport RIKZ/2005.029

- CLEVERINGA, J., MULDER, S., OOST, A. AND KOSKAMP, G. (2004) Kustverdediging van de koppen van de Waddeneilanden: de dynamiek van de kust nabij buitendelta's en passende maatregelen voor het kustbeheer. doi:Rapport RIKZ/2004.017
- COOPER, N.J., COOPER, T. AND BURD, F. (2001) 25 years of salt marsh erosion in Essex: Implications for coastal defence and nature conservation. *Journal of Coastal Conservation*, 7(1), 31–40. doi:10.1007/BF02742465
- DANKER, N. AND ZUIDEMA, D.R. (1995) The Role of the Mussel (*Mytilus edulis* L.) and Mussel Culture in the Dutch Wadden Sea. *Estuaries*, 18(1A), 71–80
- DASTGHEIB, A. (2012) Long-term process-based morphological modeling of large tidal basins. UNESCO-IHE, Institute for Water Education
- DAVIS, R.A. AND DALRYMPLE, R.W. (2010) Principles of tidal sedimentology. *Principles of Tidal Sedimentology*, c, 1–621. doi:10.1007/978-94-007-0123-6
- DAVIS, R.A. AND HAYES, M.O. (1984) What is a Wave-Dominated Coast? *Developments in Sedimentology*, 39(C), 313–329. doi:10.1016/S0070-4571(08)70152-3
- DE FOCKERT, A. (2008) Impact of Relative Sea Level Rise on the Ameland Inlet Morphology. *MSc thesis*, 189
- DE VRIES, M. (2007) Morphological modeling of the Haringvlietmonding using Delft3D. *MSc-thesis University Twente*
- DELTARES (2014a) Delft3D-FLOW, User Manual, 1–684
- DELTARES (2014b) Delft3D WAVE User Manual, 226
- DISSANAYAKE, D.M.P.K., RANASINGHE, R. AND ROELVINK, J.A. (2012a) The morphological response of large tidal inlet/basin systems to relative sea level rise. *Climatic Change*, 113(2), 253–276. doi:10.1007/s10584-012-0402-z
- DISSANAYAKE, D.M.P.K., RANASINGHE, R. AND ROELVINK, J.A. (2012b) The morphological response of large tidal inlet/basin systems to relative sea level rise. *Climatic Change*, 113(2), 253–276. doi:10.1007/s10584-012-0402-z
- DODET, G., BERTIN, X., BRUNEAU, N., FORTUNATO, A.B., NAHON, A. AND ROLAND, A. (2013) Wave-current interactions in a wave-dominated tidal inlet. *Journal of Geophysical Research: Oceans*, 118(3), 1587–1605. doi:10.1002/jgrc.20146
- DUONG, T.M. (2015) Climate Change Impacts on the Stability of Small Tidal Inlets
- E. VAN DER ZEE, A. RIPPEN, J.L. (2017) Natuurwaarden sublitorale Waddenzee. *Programma naar een rijke Waddenzee*
- ELIAS, E.P.L. (2006) Morphodynamics of Texel Inlet
- ELIAS, E.P.L. (2017) Stroming en sedimenttransport langs de Boschplaat op Terschelling. *Deltares report*
- ELIAS, E.P.L., CLEVERINGA, J., BUIJSMAN, M.C., ROELVINK, J.A. AND STIVE, M.J.F. (2006) Field and model data analysis of sand transport patterns in Texel Tidal inlet (the Netherlands). *Coastal Engineering*, 53(5-6), 505–529. doi:10.1016/j.coastaleng.2005.11.006

- ELIAS, E.P.L., TESKE, R., VAN DER SPEK, A.J.F. AND LAZAR, M. (2015) Modelling Tidal-Inlet Morphodynamics on Medium Time Scales. *Coastal Sediments 2015*, 2012, 1–14. doi:10.1142/9789814689977
- ELIAS, E.P.L., VAN DER SPEK, A.J.F., WANG, Z.B. AND DE RONDE, J. (2012) Morphodynamic development and sediment budget of the Dutch Wadden Sea over the last century. *Geologie en Mijnbouw/Netherlands Journal of Geosciences*, 91(3), 293–310. doi:10.1017/S0016774600000457
- ENEMARK, J. (2005) The Wadden Sea protection and management schemes towards an integrated coastal management approach? *Ocean & Coastal Management*, 48(11-12), 996–1015. doi:10.1016/j.ocecoaman.2005.03.009
- FITZGERALD, D.M. (1984) Interactions between the ebb-tidal delta and landward shoreline; Price Inlet, South Carolina. *Journal of Sedimentary Research*, 54(4), 1303–1318. doi:10.1306/212F85C6-2B24-11D7-8648000102C1865D
- FITZGERALD, D.M., PENLAND, S. AND NUMMEDAL, D. (1984) Control of Barrier Island Shape by Inlet Sediment Bypassing: East Frisian Islands, West Germany. *Developments in Sedimentology*, 39(C), 355–376. doi:10.1016/S0070-4571(08)70154-7
- GRUNNET, N.M., RUESSINK, B.G. AND WALSTRA, D.J.R. (2005) The influence of tides, wind and waves on the redistribution of nourished sediment at Terschelling, The Netherlands. *Coastal Engineering*, 52(7), 617–631. doi:10.1016/j.coastaleng.2005.04.001
- H. MELTOFTE, J. BLEW, J. FRIKKE, H. U. ROSNER, C.J.S. (1994) Numbers and distribution of waterbirds in the Wadden Sea
- HANSON, H., BRAMPTON, A., CAPOBIANCO, M., DETTE, H.H. AND HAMM, L. (2002) Beach nourishment projects, practices, and objectives – a European overview. 47(0378), 81–111
- HAYES, M.O. (1979) Barrier Island Morphology as a Function of Wave and Tide Regime. (July), 1–29
- HAYES, M.O. (1980) General morphology and sediment patterns in tidal inlets. *Sedimentary Geology*, 26(1-3), 139–156. doi:10.1016/0037-0738(80)90009-3
- HERRLING, G. AND WINTER, C. (2014) Morphological and sedimentological response of a mixed-energy barrier island tidal inlet to storm and fair-weather conditions. *Earth Surface Dynamics*, 2(1), 363–382. doi:10.5194/esurf-2-363-2014
- HOEKSEMA, H., MULDER, H., ROMMEL, M., DE RONDE, J. AND DE VLAS, J. (2004) Bodemdalingstudie Waddenzee 2004
- HOFSTEDÉ, J.L.A., BECHERER, J. AND BURCHARD, H. (2016) Are Wadden Sea tidal systems with a higher tidal range more resilient against sea level rise? *Journal of Coastal Conservation*, 1–8. doi:10.1007/s11852-016-0469-1
- JAK, R., TAMIS, J. AND LAMMERS, H. (2011) Natura 2000-doelen in de Noordzeekustzone. *IMARES Wageningen*, (april)
- JIAO, J. (2014) Morphodynamics of Ameland - Inlet Medium-term Delft3D Modelling

- JOHNSON, J.C. (2006) Under new management: The obligation to protect cultural property during military occupation. *Military Law Review*, 190(1978), 111–152
- KABAT, P., BAZELMANS, J., VAN DIJK, J., HERMAN, P.M.J., VAN OIJEN, T., PEJRUP, M., REISE, K., SPEELMAN, H. AND WOLFF, W.J. (2012) The Wadden Sea Region: Towards a science for sustainable development. *Ocean and Coastal Management*, 68, 4–17. doi:10.1016/j.ocecoaman.2012.05.022
- KING, S.E. AND LESTERT, J.N. (1995) The Value of Salt Marsh as a Sea Defence. 30(3), 180–189
- KLEIN TANK, A., BEERSMA, J., BESSEMBINDER, J., VAN DEN HURK, B. AND LENDERINK, G. (2015) KNMI'14-klimaatscenario's voor Nederland; Leidraad voor professionals in klimaatadaptatie, 34
- KLUYVER, M. (2006) Smart Nourishment of the Frisian Inlet. *Master Thesis Report*
- KOFFIJBERG, K., DIJKSEN, L., HAELTERLEIN, B., LAURSEN, K., POTEL, P. AND SUEDBECK, P. (2006) Breeding birds in the Wadden Sea in 2001. Results of the total survey in 2001 and trends in numbers between 1991 and 2001. *Wadden Sea Ecosystem*, 22(22), 1–132
- LABAN, C. (2014) Onderzoek zandwingebieden Ameland West , Midden B , deel A en Midden B , deel B. *Marine Sampling Holland*
- LATTEUX, B. (1995) Techniques for long-term morphological simulation under tidal action. *Marine Geology*, 126(1-4), 129–141. doi:10.1016/0025-3227(95)00069-B
- LEOPOLD, M.F. AND BAPTIST, M.J. (2016) buitendelta 's van de Nederlandse Waddenzee De buitengewone biologie van de buitendelta 's van de Nederlandse Waddenzee. *IMARES Wageningen*
- LESSER, G.R., ROELVINK, J.A., VAN KESTER, J.A.T.M. AND STELLING, G.S. (2004) Development and validation of a three-dimensional morphological model. *Coastal Engineering*, 51(8-9), 883–915. doi:10.1016/j.coastaleng.2004.07.014
- LOTZE, H.K. (2005) Radical changes in the Wadden Sea fauna and flora over the last 2,000 years. *Helgoland Marine Research*, 59(1), 71–83. doi:10.1007/s10152-004-0208-0
- LUIJENDIJK, A.P., RANASINGHE, R., DE SCHIPPER, M.A., HUISMAN, B.A., SWINKELS, C.M., WALSTRA, D.J.R. AND STIVE, M.J.F. (2017) The initial morphological response of the Sand Engine: A process-based modelling study. *Coastal Engineering*, 119(July 2016), 1–14. doi:10.1016/j.coastaleng.2016.09.005
- MOLLER, I. (1999) Wave Transformation Over Salt Marshes: A Field and Numerical Modelling Study from North Norfolk, England. *Estuarine, Coastal and Shelf Science*, 49(3), 411–426. doi:10.1006/ecss.1999.0509
- MÖLLER, I., KUDELLA, M., RUPPRECHT, F., SPENCER, T., PAUL, M., VAN WESENBEECK, B.K., WOLTERS, G., JENSEN, K., BOUMA, T.J., MIRANDA-LANGE, M. AND SCHIMMELS, S. (2014) Wave attenuation over coastal salt marshes under storm surge conditions. *Nature Geoscience*, 7(September), 727–731. doi:10.1038/ngeo2251

- MÖLLER, I., SPENCER, T., FRENCH, J.R., LEGGETT, D.J. AND DIXON, M. (2001) The Sea-Defence Value of Salt Marshes: Field Evidence from North Norfolk. *Journal of the Chartered Institution of Water and Environmental Management*, 15(2), 109–116. doi:DOI: 10.1111/j.1747-6593.2001.tb00315.x
- NICHOLLS, R.J. AND CAZENAVE, A. (2010) Sea Level Rise and Its Impact on Coastal Zones. *Science*, 328(2010), 1517–1520. doi:10.1126/science.1185782
- OERTEL, G.F. (1972) Sediment transport of estuary entrance shoals and the formation of swash platforms. *Journal of Sedimentary Research*, 42(4), 858–863. doi:10.1306/74D72658-2B21-11D7-8648000102C1865D
- REISE, K., BAPTIST, M., BURBRIDGE, P., DANKERS, N., FISCHER, L., FLEMMING, B., OOST, A.P. AND SMIT, C. (2010) The Wadden Sea A Universally Outstanding Tidal Wetland. *Wadden Sea Ecosystem*, 29(29), 7–24
- RIDDERINKHOF, H. (1988) Tidal and residual flows in the Western Dutch Wadden Sea 1 numerical model results. *Netherlands Journal of Sea Research*, 22(1), 1–21
- RIJKSWATERSTAAT (2017) Meer zand voor geul voor kust Ameland Zuidwest
- RIJN, L.C.V. AND WALSTRA, D.J.R. (2003) Modelling of Sand Transport in DELFT3D. *Report*, (November), 1–154
- ROELSE, P. (2002) Water en zand in balans. *Rapport RIKZ*
- ROELVINK, J.A. (2006) Coastal morphodynamic evolution techniques. *Coastal Engineering*, 53(2-3), 277–287. doi:10.1016/j.coastaleng.2005.10.015
- SCHIERECK, G. AND VERHAGEN, H. (2012) Introduction to bed, bank and shore protection. VSSD, Leegwaterstraat 42 Delft, The Netherlands
- SHA, L.P. (1989) Variation in ebb-delta morphologies along the West and East Frisian Islands, The Netherlands and Germany. *Marine Geology*, 89(1-2), 11–28. doi:10.1016/0025-3227(89)90025-X
- SON, C.S., FLEMMING, B.W. AND BARTHOLOM, A. (2011) Evidence for sediment recirculation on an ebb-tidal delta of the East Frisian barrier-island system, southern North Sea. *Geo-Marine Letters*, 31(2), 87–100. doi:10.1007/s00367-010-0217-8
- SPEYBROECK, J., BONTE, D., COURTENS, W., GHESKIERE, T., GROOTAERT, P., MAELFAIT, J.P., MATHYS, M., PROVOOST, S., SABBE, K., STIENEN, E.W.M., VAN LANCKER, V., VINCX, M. AND DEGRAER, S. (2006) Beach nourishment: An ecologically sound coastal defence alternative? A review. *Aquatic Conservation: Marine and Freshwater Ecosystems*, 16(4), 419–435. doi:10.1002/aqc.733
- STEIJN, R. AND ROELVINK, J. (1999) Morfodynamische berekeningen voor het zeegat van Ameland. *Rapport A505/Z2731*
- STIVE, M., DE SCHIPPER, M., LUIJENDIJK, A., RANASINGHE, R., VAN THIEL DE VRIES, J., AARNINKHOF, S., VAN GELDER-MAAS, C., DE VRIES, S., HENRIQUEZ, M. AND MARX, S. (2013) The Sand Engine: a solution for vulnerable deltas in the 21st century. *Coastal Dynamics*, 1537–1546

- STIVE, M.J.F. AND EYSINK, W.D. (1989) Voorspelling Ontwikkeling Kustlijn 1990-2090, fase 3. Deelrapport 3.1: Dynamisch model van het Nederlandse Kuststelsysteem
- SWINKELS, C.M. AND BIJLSMA, A.C. (2012) Understanding the hydrodynamics of a North Sea tidal inlet by numerical simulation and radar current measurements. *Proceedings of 3rd International Symposium on Shallow Flows, Iowa City, USA*
- TONNON, P.K., VAN DER WERF, J. AND MULDER, J.P. (2009) Morphological simulations, Environmental Impact Assessment Sand Engine (in Dutch). (November), 138
- TUDELFT (2016) SEAWAD: research into a sand engine for the Wadden Islands
- VAN DER SPEK, A., ELIAS, E.P.L., LODDER, Q. AND HOOGLAND, R. (2015) Toekomstige suppletievolumes: eindrapport. doi:1208140-005-ZKS
- VAN DER SPEK, A.J.F. AND BEETS, D.J. (1992) Mid-Holocene evolution of a tidal basin in the western Netherlands: a model for future changes in the northern Netherlands under conditions of accelerated sea-level rise? *Sedimentary Geology*, 80(3-4), 185–197. doi:10.1016/0037-0738(92)90040-X
- VAN DER WEGEN, M., DASTGHEIB, A., JAFFE, B.E. AND ROELVINK, D. (2011) Bed composition generation for morphodynamic modeling: Case study of San Pablo Bay in California, USA. *Ocean Dynamics*, 61(2-3), 173–186. doi:10.1007/s10236-010-0314-2
- VAN DER ZWAAG, J. (2014) Modelling sediment sorting near the large scale nourishment 'The Sand Motor': Understanding cause and impact of sediment sorting processes. *MSc thesis*
- VAN GOOR, M.A., ZITMAN, T.J., WANG, Z.B. AND STIVE, M.J.F. (2003) Impact of sea-level rise on the morphological equilibrium state of tidal inlets. *Marine Geology*, 202(3-4), 211–227. doi:10.1016/S0025-3227(03)00262-7
- VAN HEUVEL, T. (1999) Evaluatie van zeewaartse kustverdediging. *RIKZ*
- VAN LEEUWEN, A., POSTMA, T.A.C., LEOPOLD, M.F. AND BERGMAN, M.J.N. (1994) De ecologie van de kustzone van Ameland tot Borkum. *NIOZ Rapport*
- VAN RIJN, L.C., WALSTRA, D.J.R. AND VAN ORMONDT, M. (2007) Unified View of Sediment Transport by Currents and Waves. IV: Application of Morphodynamic Model. *Journal of Hydraulic Engineering*, 133(7), 776–793. doi:10.1061/(ASCE)0733-9429(2007)133:7(776)
- VAN STRAATEN, L.M.J.U. AND KUENEN, P.H. (1958) Tidal action as a cause of clay accumulation. *Journal of Sedimentary Research*, (4), 406–413
- VAN WIJNEN, H. AND BAKKER, J. (2001) Long-term Surface Elevation Change in Salt Marshes: a Prediction of Marsh Response to Future Sea-Level Rise. *Estuarine, Coastal and Shelf Science*, 52(3), 381–390. doi:10.1006/ecss.2000.0744
- VERSCHUREN, E. (2016) Wadden verkozen tot mooiste Nederlandse natuurgebied. *NRC*
- VOS, P.C. AND KNOL, E. (2015) Holocene landscape reconstruction of the Wadden Sea area between Marsdiep and Weser. *Netherlands Journal of Geosciences*, 94(02), 157–183. doi:10.1017/njg.2015.4

- WANG, Y. (2015) Coupling bedform roughness with decadal morphodynamics of Ameland Inlet Yunwei Wang. *MSc thesis*
- WANG, Y., YU, Q., JIAO, J., TONNON, P.K., WANG, Z.B. AND GAO, S. (2016) Coupling bedform roughness and sediment grain-size sorting in modelling of tidal inlet incision. *Marine Geology*, 381, 128–141. doi:10.1016/j.margeo.2016.09.004
- WANG, Z.B., HOEKSTRA, P., BURCHARD, H., RIDDERINKHOF, H., DE SWART, H.E. AND STIVE, M.J.F. (2012) Morphodynamics of the Wadden Sea and its barrier island system. *Ocean and Coastal Management*, 68, 39–57. doi:10.1016/j.ocecoaman.2011.12.022